Draft version May 9, 2016
Preprint typeset using LaTeX style emulateapj v. 5/2/11

IMAGING EXTRASOLAR GIANT PLANETS

Brendan P. Bowler[1,2]

Draft version May 9, 2016

ABSTRACT

High-contrast adaptive optics imaging is a powerful technique to probe the architectures of planetary systems from the outside-in and survey the atmospheres of self-luminous giant planets. Direct imaging has rapidly matured over the past decade and especially the last few years with the advent of high-order adaptive optics systems, dedicated planet-finding instruments with specialized coronagraphs, and innovative observing and post-processing strategies to suppress speckle noise. This review summarizes recent progress in high-contrast imaging with particular emphasis on observational results, discoveries near and below the deuterium-burning limit, and a practical overview of large-scale surveys and dedicated instruments. I conclude with a statistical meta-analysis of deep imaging surveys in the literature. Based on observations of 384 unique and single young (≈5–300 Myr) stars spanning stellar masses between 0.1–3.0 $M_{\odot}$, the overall occurrence rate of 5–13 $M_{\rm Jup}$ companions at orbital distances of 30–300 AU is $0.6^{+0.7}_{-0.5}$% assuming hot-start evolutionary models. The most massive giant planets regularly accessible to direct imaging are about as rare as hot Jupiters are around Sun-like stars. Dividing this sample into individual stellar mass bins does not reveal any statistically-significant trend in planet frequency with host mass: giant planets are found around $2.8^{+3.7}_{-2.3}$% of BA stars, <4.1% of FGK stars, and <3.9% of M dwarfs. Looking forward, extreme adaptive optics systems and the next generation of ground- and space-based telescopes with smaller inner working angles and deeper detection limits will increase the pace of discovery to ultimately map the demographics, composition, evolution, and origin of planets spanning a broad range of masses and ages.

Subject headings: planets and satellites: detection — planets and satellites: gaseous planets

1. INTRODUCTION

Over the past two decades the orbital architecture of giant planets has expanded from a single order of magnitude in the Solar System (5–30 AU) to over five orders of magnitude among extrasolar planetary systems (0.01–5000 AU; Figure 1). High-contrast adaptive optics (AO) imaging has played a critical role in this advancement by probing separations beyond ∼10 AU and masses $\gtrsim$1 $M_{\rm Jup}$. Uncovering planetary-mass objects at hundreds and thousands of AU has fueled novel theories of planet formation and migration, inspiring a more complex framework for the origin of giant planets in which multiple mechanisms (core accretion, dynamical scattering, disk instability, and cloud fragmentation) operate on different timescales and orbital separations. In addition to probing unexplored orbital distances, imaging entails directly capturing photons that originated in planetary atmospheres, providing unparalleled information about the initial conditions, chemical composition, internal structure, atmospheric dynamics, photospheric condensates, and physical properties of extrasolar planets. These three science goals — the architecture, formation, and atmospheres of gas giants — represent the main motivations to directly image and spectroscopically characterize extrasolar giant planets.

This pedagogical review summarizes the field of direct imaging in the era leading up to and transitioning towards extreme adaptive optics systems, the *James Webb Space Telescope*, *WFIRST*, and the thirty meter-class telescopes. This "classical" period of high-contrast imaging spanning approximately 2000 to 2015 has set the stage and baseline expectations for the next generation of instruments and telescopes that will deliver ultra-high contrasts and reach unprecedented sensitivities. In addition to the first images of *bona fide* extrasolar planets, this early phase experienced a number of surprising discoveries including planetary-mass companions orbiting brown dwarfs; planets on ultra-wide orbits beyond 100 AU; enigmatic (and still poorly understood) objects like the optically-bright companion to Fomalhaut; and unexpectedly red, methane-free, and dust-rich atmospheres at low surface gravities. Among the most important results has been the gradual realization that massive planets are exceedingly rare on wide orbits; only a handful of discoveries have been made despite thousands of hours spent on hundreds of targets spanning over a dozen surveys. Although dismaying, these null detections provide valuable information about the efficiency of planet formation and the resulting demographics at wide separations. Making use of mostly general, non-optimized facility instruments and early adaptive optics systems has also led to creative observing strategies and post-processing solutions for PSF subtraction.

Distinguishing giant planets from low-mass brown dwarfs is a well-trodden intellectual exercise (e.g., Oppenheimer et al. 2000; Basri & Brown 2006; Chabrier et al. 2007; Chabrier et al. 2014). Except in the few rare cases where the architectures or abundance patterns of individual systems offer clues about a specific formation route, untangling the origin of imaged planetary-mass companions must necessarily

bpbowler@astro.as.utexas.edu
[1] McDonald Observatory and the University of Texas at Austin, Department of Astronomy, 2515 Speedway, Stop C1400, Austin, TX 78712
[2] McDonald Prize Fellow.

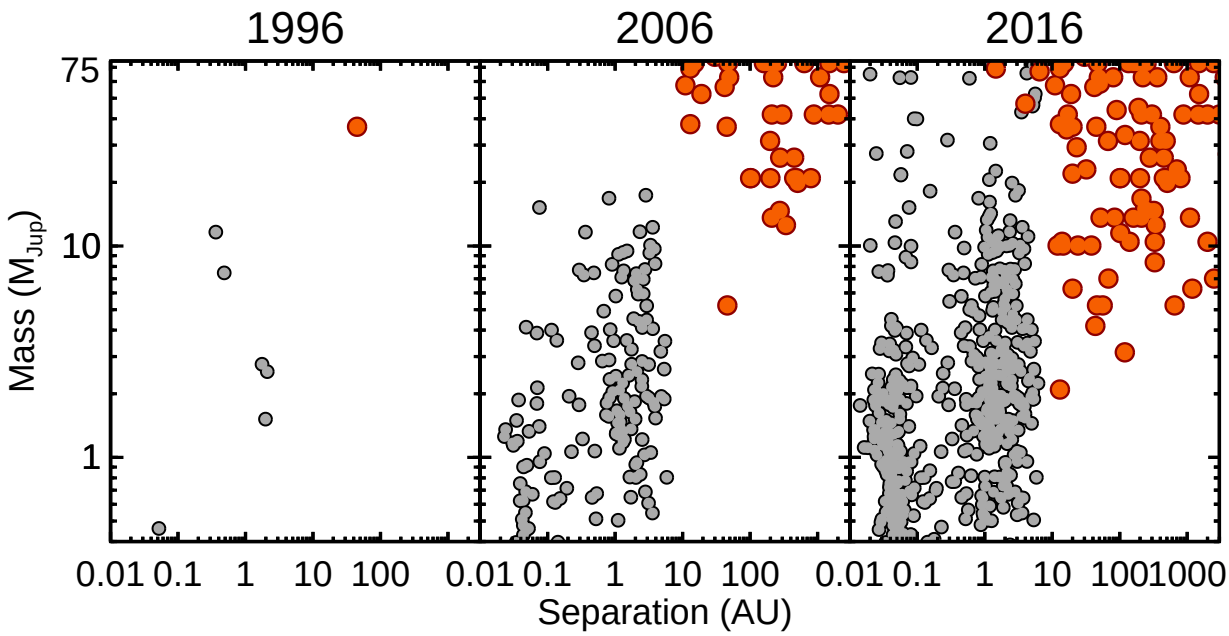

FIG. 1.— Substellar companions discovered via radial velocities (gray circles) and direct imaging (red circles) as of 1996, 2006, and 2016. Over this twenty year period the number of directly imaged companions below 10 $M_{\rm Jup}$ has steadily increased from one (2M1207–3932 b in 2004) to over a dozen. The surprising discovery of planetary companions at extremely wide separations of hundreds to thousands of AU has expanded the architecture of planetary systems to over five orders of magnitude. Note that the radial velocity planets are minimum masses ($m\sin i$) and the directly imaged companion masses are inferred from evolutionary models. RV-detected planets are from exoplanets.org (Wright et al. 2011; Han et al. 2014) and are supplemented with a compilation of RV-detected brown dwarfs from the literature. Imaged companions are from Deacon et al. (2014) together with other discoveries from the literature.

be addressed as a population and in a statistical manner. This review is limited in scope to self-luminous companions detected in thermal emission at near- and mid-infrared wavelengths (1–5 μm) with masses between $\approx$1–13 $M_{\rm Jup}$ with the understanding that multiple formation routes can probably produce objects in this "planetary" mass regime (see Section 5). Indeed, the separations regularly probed in high-contrast imaging surveys— typically tens to hundreds of AU— lie beyond the regions in protoplanetary disks containing the highest surface densities of solids where core accretion operates most efficiently (e.g., Andrews 2015). Direct imaging has therefore predominantly surveyed the wide orbital distances where alternative formation and migration channels like disk instability, cloud fragmentation, and planet-planet scattering are most likely to apply. In the future, the most efficient strategy to detect even smaller super-Earths and terrestrial worlds close to their host stars will be in reflected light from a dedicated space-based optical telescope.

By focusing on the optimal targets, early discoveries, largest surveys, and statistical results, this observationally-oriented overview aims to complement recent reviews on giant planet formation (Chabrier et al. 2007; Helled et al. 2013; Chabrier et al. 2014; Helling et al. 2014), atmospheric models (Marley et al. 2007a; Helling et al. 2008, Allard et al. 2012; Marley & Robinson 2015), evolutionary models, (Burrows et al. 2001; Fortney & Nettelmann 2009), observational results (Absil & Mawet 2009; Lagrange 2014; Bailey 2014; Helling & Casewell 2014; Madhusudhan et al. 2014; Quanz 2015; Crossfield 2015), and high contrast imaging instruments and speckle suppression techniques (Guyon et al. 2006; Beuzit et al. 2007; Oppenheimer & Hinkley 2009; Biller et al. 2008; Marois et al. 2010a; Traub & Oppenheimer 2010; Mawet et al. 2012b; Davies & Kasper 2012).

2. OPTIMAL TARGETS FOR HIGH-CONTRAST IMAGING

Planets radiatively cool over time by endlessly releasing the latent heat generated during their formation and gravitational contraction. Fundamental scaling relations for the evolution of brown dwarfs and giant planets can be derived analytically with basic assumptions of a polytropic equation of state and degenerate electron gas (Stevenson 1991; Burrows & Liebert 1993). Neglecting the influence of lithium burning, deuterium burning, and atmospheres, which act as partly opaque wavelength-dependent boundary conditions, substellar objects with different masses cool in a similar monotonic fashion over time:

$$L_{\rm bol} \propto t^{-5/4} M^{5/2}. \quad (1)$$

Here $L_{\rm bol}$ is the bolometric luminosity, t is the object's age, and M is its mass.

This steep mass-luminosity relationship means that luminosity tracks are compressed in the brown dwarf regime ($\approx$13–75 $M_{\rm Jup}$) and fan out in the planetary regime with significant consequences for high-contrast imaging. A small gain in contrast in the brown dwarf regime results in a large gain in the limiting detectable mass, whereas the same contrast gain in the planetary regime has a much smaller influence on limiting mass (Figure 2). It is much more difficult, for example, to improve sensitivity from 10 $M_{\rm Jup}$ to 1 $M_{\rm Jup}$ than from 80 $M_{\rm Jup}$ to 10 $M_{\rm Jup}$. Moreover, sensitivity to low masses and close separations is highly dependent on a star's youth and proximity. In terms of limiting detectable planet mass, observing younger and closer stars is equivalent to improving speckle suppression or integrating for

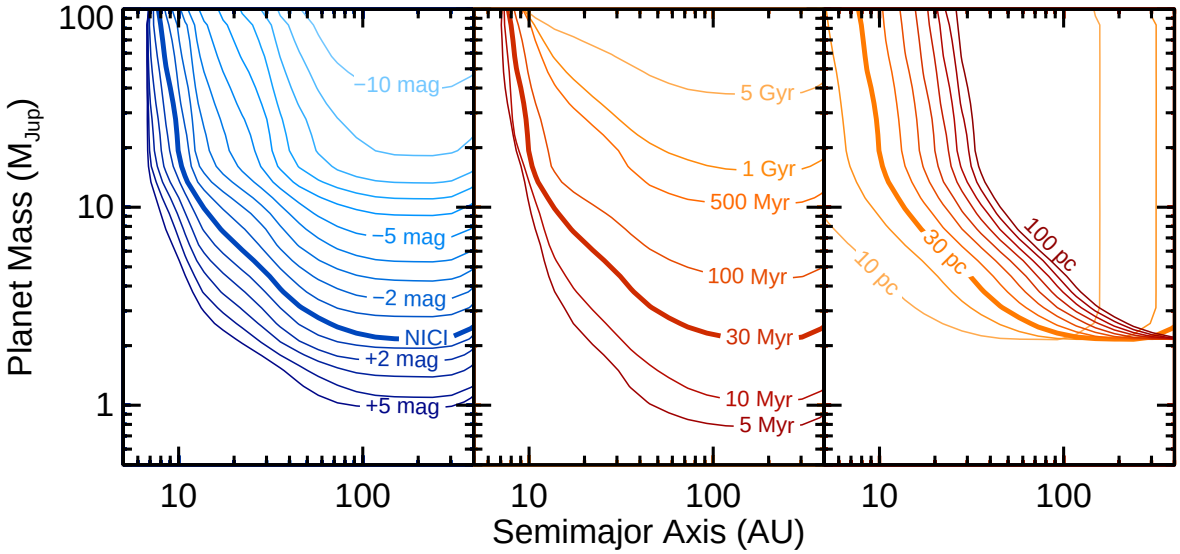

FIG. 2.— The influence of contrast (left), age (middle), and distance (right) on mass sensitivity to planets. The bold curve in each panel shows the 50% sensitivity contour based on the median NICI contrast from Biller et al. (2013) for a 30 Myr K1 star at 30 pc. The left panel shows the effect of increasing or decreasing the fiducial contrast curve between –10 magnitudes to +5 magnitudes. Similarly, the middle and right panels show changes to the fiducial age spanning 5 Myr to 5 Gyr and distances spanning 10 pc to 100 pc. Planet absolute magnitudes depend steeply on mass and age. As a result, a small gain in contrast in the brown dwarf regime corresponds to a large gain in limiting mass, but the same contrast gain in the planetary regime translates into a much smaller gain in mass. Mass sensitivity is particularly sensitive to stellar age, while closer distances mean smaller physical separations can be studied.

longer. Note that in a contrast-limited regime the absolute magnitude of the host star is also important. The same contrast around low-mass stars and brown dwarfs corresponds to lower limiting masses compared to higher-mass stars.

Young stars are therefore attractive targets for two principal reasons: planets are their most luminous at early ages, and the relative contrast between young giant planets and their host stars is lower than at older ages because stellar luminosities plateau on the main sequence while planets and brown dwarfs continue to cool, creating a luminosity bifurcation. For example, evolutionary models predict the H-band contrast between a 5 $M_{\rm Jup}$ planet orbiting a 1 $M_{\odot}$ star to be ≈25 mag at 5 Gyr but only ≈10 mag at 10 Myr (Baraffe et al. 2003; Baraffe et al. 2015). At old ages beyond ∼1 Gyr, 1–10 $M_{\rm Jup}$ planets are expected to have effective temperatures between 100–500 K and cool to the late-T and Y spectral classes with near-infrared absolute magnitudes $\gtrsim$18 mag (Dupuy & Kraus 2013).

Below are overviews of the most common classes of targets in direct imaging surveys highlighting the scientific context, strengths and drawbacks, and observational results for each category.

2.1. *Young Moving Group Members*

In principle, younger stars make better targets for imaging planets. In practice, the youngest T Tauri stars reside in star-forming regions beyond 100 pc. At these distances, the typical angular scales over which high-contrast imaging can probe planetary masses translate to wide physical separations beyond ∼20–50 AU (with some notable exceptions with non-redundant aperture masking and extreme AO systems). Moreover, these extremely young ages of ∼1–10 Myr correspond to timescales when giant planets may still be assembling through core accretion and therefore might have lower luminosities than at slightly later epochs (e.g., Marley et al. 2007b; Mollière & Mordasini 2012; Marleau & Cumming 2013). On the other hand, the closest stars to the Sun probe the smallest physical scales but their old ages of ∼1–10 Gyr mean that high contrast imaging only reaches brown dwarf masses.

Young moving groups— coeval, kinematically comoving associations young stars and brown dwarfs in the solar neighborhood— represent a compromise in age (≈10–150 Myr) and distance (≈10–100 pc) between the nearest star forming regions and field stars (Figure 3; see Zuckerman & Song 2004, Torres et al. 2008, and Mamajek 2016). One distinct advantage they hold is that their members span a wide range of masses and can be used to age date each cluster from lithium depletion boundaries and isochrone fitting (e.g., Bell et al. 2015; Herczeg & Hillenbrand 2015). As a result, the ages of these groups are generally much better constrained than those of isolated young stars. For these reasons young moving group members have emerged as the primary targets for high-contrast imaging planet searches over the past decade (e.g., Chauvin et al. 2010; Biller et al. 2013; Brandt et al. 2014c)

Identifying these nearby unbound associations of young stars is a difficult task. Each moving group's UVW space velocities cluster closely together with small velocity dispersions of ≈1–2 km s^{-1} but individual stars in the same group can be separated by tens of parsecs in space and tens of degrees across the sky. UVW kinematics can be precisely determined if the proper motion, radial velocity, and parallax to a star are known. Incomplete knowledge of one or more of these parameters (usually the radial velocity and/or distance) means the UVW kinematics are only partially constrained, making it challenging to unambiguously associate stars with

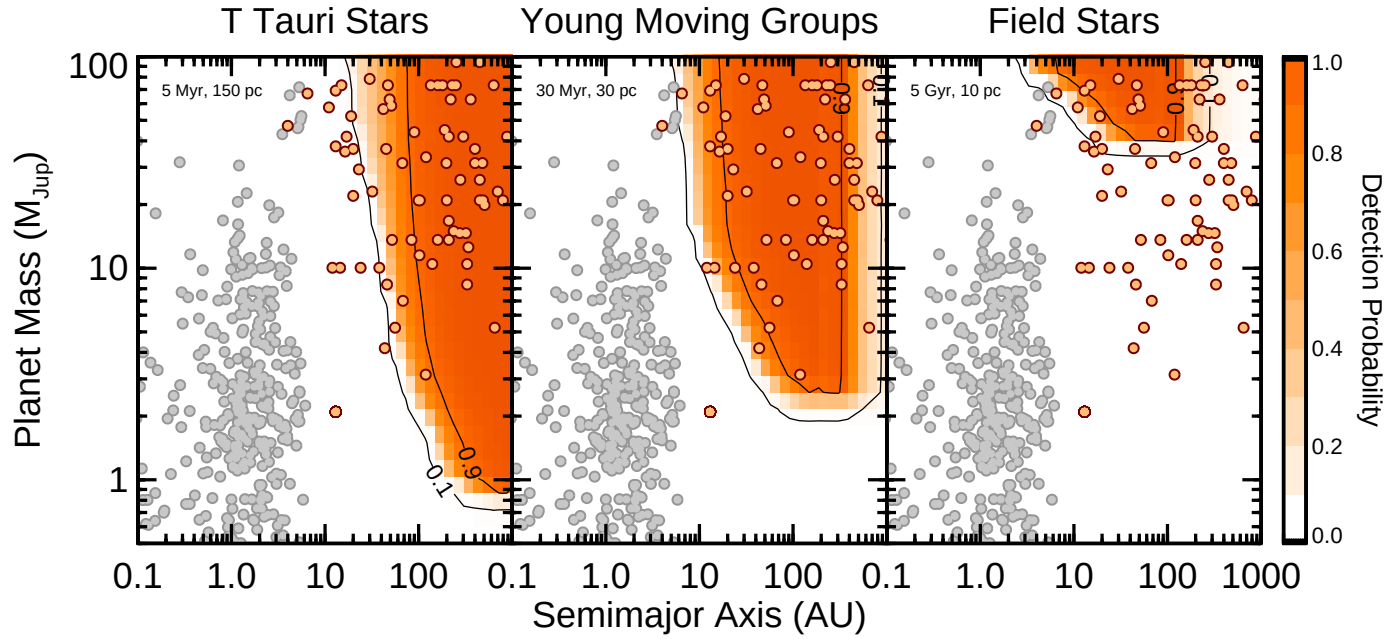

FIG. 3.— Typical sensitivity maps for high-contrast imaging observations of T Tauri stars (5 Myr at 150 pc), young moving group members (30 Myr at 30 pc), and field stars (5 Gyr at 10 pc). Young moving group members are "Golidlocks targets"— not too old, not too distant. Black curves denote 10% and 90% contour levels assuming circular orbits, Cond hot-start evolutionary models (Baraffe et al. 2003), and the median NICI contrast curve from Biller et al. (2013). Gray and orange circles are RV- and directly imaged companions, respectively (see Figure 1).

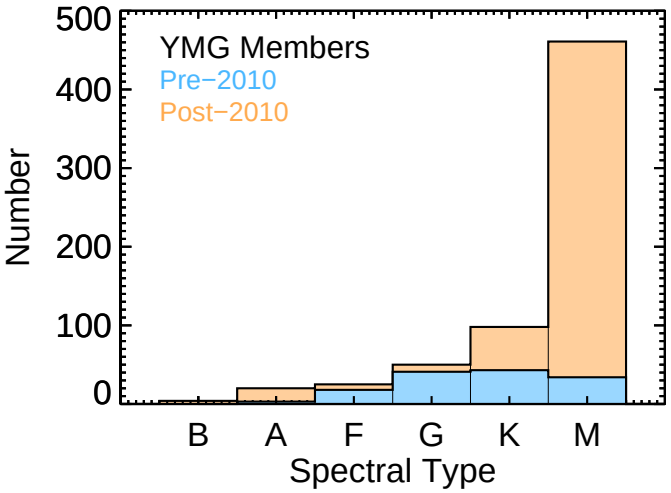

FIG. 4.— The census of members and candidates of young moving groups. Prior to 2010 the M dwarf members were largely missing owing to their faintness and lack of parallax measurements from *Hipparcos*. Concerted efforts to find low-mass members over the past few years have filled in this population and generated a wealth of targets for dedicated direct imaging planet searches.

known groups. Historically, most groups themselves and new members of these groups were found with the aid of the Tycho Catalog and *Hipparcos*, which provided complete space velocities for bright stars together with ancillary information pointing to youth such as infrared excess from IRAS; X-ray emission from the *Einstein* or *ROSAT* space observatories; strong Hα emission; and/or Li I λ6708 absorption. As a result, most of the faint low-mass stars and brown dwarfs have been neglected.

In recent years the population of "missing" low-mass stars and brown dwarfs in young moving groups has been increasingly uncovered as a result of large all-sky dedicated searches (Figure 4; Shkolnik et al. 2009; Lépine & Simon 2009; Schlieder et al. 2010; Kiss et al. 2010; Rodriguez et al. 2011a; Schlieder et al. 2012a; Schlieder et al. 2012b; Shkolnik et al. 2012; Malo et al. 2013; Moor et al. 2013; Rodriguez et al. 2013; Malo et al. 2014; Gagné et al. 2014; Riedel et al. 2014; Kraus et al. 2014b; Gagné et al. 2015b; Gagné et al. 2015c; Binks et al. 2015). Parallaxes and radial velocities are generally not available for these otherwise anonymous objects, but by adopting the UVW kinematics of known groups, it is possible to invert the problem and predict a distance, radial velocity, and membership probability. Radial velocities are observationally cheaper to acquire en masse compared to parallaxes, so membership confirmation has typically been accomplished with high-resolution spectroscopy. The exceptions are for spectroscopic binaries, which require multiple epochs to measure a systemic velocity, and rapidly rotating stars with high projected rotational velocities ($v \sin i$), which produce large uncertainties in radial velocity measurements. The abundance of low-mass stars in the field means that some old interlopers will inevitably share similar space velocities with young moving groups. These must be distilled from bona fide membership lists on a case-by-case basis (Barenfeld et al. 2013; Wöllert et al. 2014; Janson et al. 2014; Mccarthy & Wilhelm 2014; Bowler et al. 2015c).

The current census of directly imaged planets and companions near the deuterium-burning limit are listed in Table 1. Many of these host stars are members of young moving groups. β Pic, 51 Eri, and possibly TYC 9486-927-1 are members of the β Pic moving group (Zuckerman et al. 2001; Feigelson et al. 2006; Deacon et al. 2016). HR 8799 and possibly κ And are thought to be members of Columba (Zuckerman et al. 2011). 2M1207–3932 is in the TW Hydrae Association (Gizis 2002). GU Psc and 2M0122–2439 are likely members of the AB Dor moving group (Malo et al. 2013;

Naud et al. 2014; Bowler et al. 2013). AB Pic, 2M0103–5515, and 2M0219–3925 are in Tuc-Hor (Song et al. 2003; Delorme et al. 2013; Gagné et al. 2015b), though the masses of their companions are somewhat uncertain and may not reside in the planetary regime. In addition, the space motion of VHS 1256–1257 is well-aligned with the β Pic or possibly AB Dor moving groups (Gauza et al. 2015; Stone et al. 2016), but the lack of lithium in the host indicates the system is older and may be a kinematic interloper.

The number of moving groups in the solar neighborhood is still under debate, but at least five are generally considered to be well-established: the TW Hydrae Association, β Pic, Tuc-Hor, Carina, and AB Dor. Other associations have been proposed and may constitute real groups which formed together and are useful for age-dating purposes, but may require more scrutiny to better understand their size, structure, physical nature, and relationship to other groups. Mamajek (2016) provide a concise up-to-date census of their status and certitude. Soon, micro-arcsecond astrometry and parallaxes from *Gaia* will dramatically change the landscape of nearby young moving groups by readily identifying overlooked groups, missing members, and even massive planets on moderate orbits.

2.2. *T Tauri Stars, Herbig Ae/Be Stars, and Transition Disks*

Despite their greater distances (≈120–150 pc), the extreme youth (≈1–10 Myr) of T Tauri stars and their massive counterparts, Herbig Ae/Be stars, in nearby star-forming regions like Taurus, the Sco-Cen complex, and ρ Oph have made them attractive targets to search for planets with direct imaging and probe the earliest stages of planet formation when gas giants are still assembling (Itoh et al. 2008; Ireland et al. 2011; Mawet et al. 2012a; Janson et al. 2013a; Lafrenière et al. 2014; Daemgen et al. 2015; Quanz 2015; Hinkley et al. 2015b).

One of the most surprising results from these efforts has been the unexpected discovery of planetary-mass companions on ultra-wide orbits at several hundred AU from their host stars (Table 1). These wide companions pose challenges to canonical theories of planet formation via core accretion and disk instability and may instead represent the tail end of brown dwarf companion formation, perhaps as opacity-limited fragments of turbulent, collapsing molecular cloud cores (e.g., Low & Lynden-Bell 1976; Silk 1977; Boss 2001; Bate 2009).

Many (and perhaps most) of these young planetary-mass companions harbor accreting circum-planetary disks, which provide valuable information about mass accretion rates, circum-planetary disk structure, formation route, and the moon-forming capabilities of young planets. Accretion luminosity is partially radiated in line emission, making Hα a potentially valuable tracer to find and characterize protoplanets (Sallum et al. 2015a). For example, Zhou et al. (2014) find that up to 50% of the accretion luminosity in the ≈15 $M_{\rm Jup}$ companion GSC 6214-210 B is emitted at Hα. Searching for these nascent protoplanets has become a leading motivation to achieve AO correction in the optical and is actively being carried out with MagAO (Close et al. 2014). Deep sub-mm observations with ALMA have opened the possibility of measuring the masses of these subdisks (Bowler et al. 2015a) and possibly even indirect identification via gas kinematics (Perez et al. 2015). Larger disks may be able to be spatially resolved and a dynamical mass for the planet may be measured from Keplerian motion.

The relationship between protoplanetary disks and young planets is also being explored in detail at these extremely young ages. In particular, transition disks—young stars whose spectral energy distributions indicate they host disks with large optically thin cavities generally depleted of dust (e.g., see reviews by Williams & Cieza 2011, Espaillat et al. 2014, Andrews 2015, and Owen 2016)— have been used as signposts to search for embedded protoplanets. This approach has been quite fruitful, resulting in the discovery of companions within these gaps spanning the stellar (CoKu Tau 4: Ireland & Kraus 2008; HD 142527: Biller et al. 2012, Close et al. 2014, Rodigas et al. 2014, Lacour et al. 2015), brown dwarf (HD 169142: Biller et al. 2014, Reggiani et al. 2014), and planetary (LkCa 15: Kraus & Ireland 2012, Ireland & Kraus 2014, Sallum et al. 2015a; HD 100546: Quanz et al. 2013, Currie et al. 2014d, Quanz et al. 2015; Currie et al. 2015, Garufi et al. 2016) mass regimes using a variety of techniques.

However, environmental factors can severely complicate the interpretation of these detections. Extinction and reddening, accretion onto and from circum-planetary disks, extended emission from accretion streams, and circumstellar disk sub-structures seen in scattered light can result in false alarms, degenerate interpretations, and large uncertainties in the mass estimates of actual companions. T Cha offers a cautionary example; Huélamo et al. (2011) discovered a candidate substellar companion a mere 62 mas from the transition-disk host star with aperture masking interferometry, but additional observations did not show orbital motion as expected for a real companion. Additional modeling indicates that the signal may instead be a result of scattering by grains in the outer disk or possibly even noise in the data (Olofsson et al. 2013; Sallum et al. 2015b; Cheetham et al. 2015). This highlights an additional complication with aperture masking: because model fits to closure phases usually consist of binary models with two or more point sources, it can difficult to discern actual planets from other false positives. In these situations the astrometric detection of orbital motion is essential to confirm young protoplanets embedded in disks.

Other notable examples of ambiguous candidate protoplanets at wider separations include FW Tau b, an accreting low-mass companion to the Taurus binary FW Tau AB orbiting at a projected separation of 330 AU (White & Ghez 2001; Kraus et al. 2014a), and TMR-1C, a faint, heavily extincted protoplanet candidate located ≈1400 AU from the Taurus protostellar binary host TMR-1AB showing large-amplitude photometric variability and circumstantial evidence of a dynamical ejection (Terebey et al. 1998; Terebey et al. 2000; Riaz & Martín 2011; Riaz et al. 2013). Follow-up observations of both companions suggest they may instead be low-mass stars or brown dwarfs with edge-on disks (Petr-Gotzens et al. 2010; Bowler et al. 2014; Kraus et al. 2015; Caceres et al. 2015), underscoring a few of the difficulties that arise when interpreting candi-

date protoplanets at extremely young ages.

Altogether the statistics of planets orbiting the youngest T Tauri stars from direct imaging are still fairly poorly constrained. Quantifying this occurrence rate is important because it can be compared with the same values at older ages to determine the *evolution* of this population. Planet-planet scattering, for example, implies an increase in the frequency of planets on ultra-wide orbits over time. Ireland et al. (2011) found the frequency of 6–20 $M_{\rm Jup}$ companions from ≈200–500 AU to be $\sim 4^{+5}_{-1}$% in Upper Scorpius. Combining these results with those from Kraus et al. (2008) and their own shallow imaging survey, Lafrenière et al. (2014) find that the frequency of 5–40 $M_{\rm Jup}$ companions between 50–250 AU is <1.8% and between 250–1000 AU is $4.0^{+3.0}_{-1.2}$% assuming hot-start evolutionary models. In future surveys it will be just as important to report nondetections together with new discoveries so this frequency can be measured with greater precision.

2.3. *Brown Dwarfs*

Young brown dwarfs (≈13–75 $M_{\rm Jup}$) have low circum-substellar disk masses (Mohanty et al. 2013; Andrews et al. 2013) and are not expected to host giant planets as frequently as stars. Nevertheless, their low luminosities make them especially advantageous for high-contrast imaging because lower masses can be probed with contrast-limited observations.

Several deep imaging surveys with ground-based AO or *HST* have included brown dwarfs in their samples (Kraus et al. 2005; Ahmic et al. 2007; Stumpf et al. 2010; Biller et al. 2011; Todorov et al. 2014; Garcia et al. 2015). A handful of companions in the 5–15 $M_{\rm Jup}$ range have been discovered with direct imaging: 2M1207–3932 b (Chauvin et al. 2004; Chauvin et al. 2005a), 2M0441+2301 b (Todorov et al. 2010), and possibly both FU Tau B (Luhman et al. 2009b) and VHS 1256–1257 (Gauza et al. 2015) depending on their ages. A few other low-mass companions (and in some cases the primaries themselves) to late-T and early-Y field brown dwarfs may also reside in the planetary regime depending on the system ages: CFBDSIR J1458+1013 B (Liu et al. 2011), WISE J1217+1626 B (Liu et al. 2012), and WISE J0146+4234 B (Dupuy et al. 2015a).

The low mass ratios of these systems (q≈0.2–0.5) bear a closer resemblance to binary stars than canonical planetary systems ($q \lesssim 0.001$), and the formation route of these very low-mass binaries is probably quite different than around stars (Lodato et al. 2005). High-order multiple systems with low total masses like 2M0441+2301 AabBab and VHS 1256–1257 ABb suggest that cloud fragmentation can form objects in the planetary-mass domain (Chauvin et al. 2005a; Todorov et al. 2010; Bowler & Hillenbrand 2015; Stone et al. 2016). Continued astrometric monitoring of ultracool binaries will eventually yield orbital elements and dynamical masses for these intriguing systems to test formation mechanisms (Dupuy & Liu 2011) and giant planet evolutionary models.

2.4. *Binary Stars*

Close stellar binaries (≈0.1–5″) are generally avoided in direct imaging surveys. Multiple similarly-bright stars can confuse wavefront sensors, which are optimized for single point sources, and deep coronagraphic imaging generally saturates nearby stellar companions. Physically, binaries carve out large dynamically-unstable regions that are inhospitable to planets and there is strong evidence that they inhibit planet formation by rapidly clearing or truncating protoplanetary disks (e.g., Cieza et al. 2009; Duchêne 2010; Kraus et al. 2012). Nevertheless, many planets have been found in binary systems in both S-type orbital configurations (a planet orbiting a single star; e.g., Ngo et al. 2015) and P-type orbits (circumbinary planets; see Winn & Fabrycky 2015 for a recent summary). Binaries are common products of star formation, so understanding how stellar multiplicity influences the initial conditions (protoplanetary disk mass and structure), secular evolution (Kozai-Lidov interactions) and end products (dynamically relaxed planetary systems) of planet formation has important consequences for the galactic census of exoplanets (e.g., Wang et al. 2014; Kraus et al. 2016).

Several planetary-mass companions have been imaged around binary stars on wide circumbinary orbits: ROXs 42B b (Kraus et al. 2014a; Currie et al. 2014b), Ross 458 c (Goldman et al. 2010; Scholz 2010), SR 12 C (Kuzuhara et al. 2011), HD 106906 b (Bailey et al. 2014; Lagrange et al. 2016), and VHS 1256–1257 (Gauza et al. 2015; Stone et al. 2016). 2M0103–5515 b (Delorme et al. 2013) and FW Tau b (Kraus et al. 2014a) orbit close, near-equal mass stellar binaries, but the masses of the wide tertiaries are highly uncertain (Bowler et al. 2014).

On the other hand, few imaged planets orbiting single stars also have wide stellar companions. 51 Eri Ab is orbited by the pair of M dwarf binaries GJ 3305 AB (Feigelson et al. 2006; Kasper et al. 2007; Montet et al. 2015) at ∼2000 AU. Fomalhaut has two extremely distant stellar companions at ≈57 kAU and ≈158 kAU (Mamajek et al. 2013). 2M0441+2301 Bb orbits a low-mass brown dwarf and is part of a hierarchical quadruple system with a distant star-brown dwarf pair at a projected separation of 1800 AU (Todorov et al. 2010).

There has been little work comparing the occurrence rate of imaged planets in binaries and single stars. However, several surveys and post-processing techniques are now expressly focusing on binary systems and should clarify the statistical properties of planets in these dynamically complicated arrangements (Thalmann et al. 2014; Rodigas et al. 2015; Thomas et al. 2015).

2.5. *Debris Disks: Signposts of Planet Formation?*

Debris disks are extrasolar analogs of the asteroid and Kuiper belts in the Solar System. They are the continually-replenished outcomes of cascading planetesimal collisions that result in large quantities of transient dust heated by the host star. Observationally, debris disks are identified from unresolved infrared or sub-mm excesses over stellar photospheric emission. Deep observations spanning the optical, IR, and sub-mm can spatially resolved the largest and most luminous disks in scattered light and thermal emission to investigate disk morphology and grain properties. Topical reviews by Zuckerman (2001), Moro-Martin et al. (2008), Wyatt (2008), Krivov (2010), and Matthews et al. (2014a) high-

light recent theoretical and observational progress on the formation, modeling, and evolution of debris disks.

Debris disks are intimately linked to planets, which can stir planetesimals, sculpt disk features, produce offsets between disks and their host stars, and carve gaps to form belts with spectral energy distributions showing multiple temperature components. The presence of debris disks, and especially those with features indicative of a massive perturber, may therefore act as signposts for planets. The four directly imaged planetary systems β Pic, HR 8799, 51 Eri, and HD 95086 all possess debris disks, the latter three having multiple belts interior and exterior to the imaged planet(s). This remarkably consistent configuration is analogous to the Solar System's architecture in which gas giants are flanked by (very low-level) zodiacal emission.

Anecdotal signs point to a possible correlation between disks and imaged planets but this relationship has not yet been statistically validated. There have been hints of a correlation between debris disks and low-mass planets detected via radial velocities (Wyatt et al. 2012; Marshall et al. 2014), but these were not confirmed in a recent analysis by Moro-Martin et al. (2015). Indeed, many stars hosting multi-component debris disks have now been targeted with high-contrast imaging and do not appear to harbor massive planets (Rameau et al. 2013a; Wahhaj et al. 2013b; Janson et al. 2013c; Meshkat et al. 2015a). Given the high incidence of debris disks around main-sequence stars ($\gtrsim$16–20%: Trilling et al. 2008; Eiroa et al. 2013), with even higher rates at younger ages (Rieke et al. 2005; Meyer et al. 2008), any correlation of imaged giant planets and debris disks will be difficult to discern because the overall occurrence rate of massive planets on wide orbits is extremely low ($\lesssim$1%; see Section 4.5). Perhaps more intriguing would be a subset of this sample with additional contextual clues, for example the probability of an imaged planet given a two-component debris disk compared to a diskless control sample.

The Fabulous Four— Vega, β Pic, Fomalhaut, and ϵ Eridani— host the brightest debris disks discovered by IRAS (Aumann et al. 1984; Aumann 1985) and have probably been targeted more than any other stars with high-contrast imaging over the past 15 years, except perhaps for HR 8799. Despite having similarly large and luminous disks, their planetary systems are quite different and demonstrate a wide diversity of evolutionary outcomes.

Fomalhaut's disk possesses a sharply truncated, offset, and eccentric ring about 140 AU in radius suggesting sculpting from a planet (Dent et al. 2000; Boley et al. 2012; Kalas et al. 2005). A comoving optical source ("Fomalhaut b") was discovered interior to the ring by Kalas et al. (2008a) and appears to be orbiting on a highly inclined and eccentric orbit not coincident with the ring structure (Kalas et al. 2013). The nature of this intriguing companion remains puzzling; it may be a low-mass planet with a large circum-planetary disk, a swarm of colliding irregular satellites, or perhaps a recent collision of protoplanets (e.g., Kalas et al. 2008b; Kennedy & Wyatt 2011; Kenyon et al. 2014). Massive planets have been ruled out from deep imaging down to about 20 AU (Kalas et al. 2008a; Kenworthy et al. 2009; Marengo et al. 2009; Absil et al. 2011; Janson et al. 2012; Nielsen et al. 2013; Kenworthy et al. 2013; Currie et al. 2012b; Currie et al. 2013; Janson et al. 2015).

Vega's nearly face-on debris disk is similar to Fomalhaut's in terms of its two-component structure comprised of warm and cold dust belts and wide gaps with orbital ratios $\gtrsim$10, possibly indicating the presence of multiple low-mass planets (e.g., Wilner et al. 2002; Su et al. 2005; Su et al. 2013). Deep imaging of Vega over the past 15 years has thus far failed to identify planets with detection limits down to a few Jupiter masses (Metchev et al. 2003; Macintosh et al. 2003; Itoh et al. 2006; Marois et al. 2006; Hinz et al. 2006; Hinkley et al. 2007; Heinze et al. 2008; Janson et al. 2011a; Mennesson et al. 2011; Janson et al. 2015).

β Pic hosts an extraordinarily large, nearly edge-on disk spanning almost 2000 AU in radius (Smith & Terrile 1984; Larwood & Kalas 2001). Its proximity, brightness, and spatial extent make it one of the best-studied debris disks, showing signs of multiple belts (e.g., Wahhaj et al. 2003), asymmetries (e.g., Kalas & Jewitt 1995), molecular gas clumps (Dent et al. 2014), and an inner warp (Heap et al. 2000) predicted to be caused by a close-in inclined planet (Mouillet et al. 1997). Lagrange et al. (2009a) uncovered a possible massive planet at $\sim$9 AU and, despite immediate follow-up (Fitzgerald et al. 2009; Lagrange et al. 2009b), it was not until it reemerged on the other side of the star that β Pic b was unambiguously confirmed (Lagrange et al. 2010).

ϵ Eridani is another particularly fascinating example of a nearby, relatively young K2 star hosting a bright debris disk with spatially resolved ring structure and a warm inner component (Greaves et al. 1998; Greaves et al. 2005; Backman et al. 2009). At 3.2 pc this star harbors the closest debris disk to the Sun, has a Jovian-mass planet detected by radial velocity and astrometric variations (Hatzes et al. 2000; Benedict et al. 2006), and possesses a long-term RV trend pointing to an additional long-period giant planet. Because of its favorable age and proximity, ϵ Eridani has been exhaustively imaged with adaptive optics on the largest ground-based telescopes in an effort to recover the known planets and search for others (Luhman & Jayawardhana 2002; Macintosh et al. 2003; Itoh et al. 2006; Marengo et al. 2006; Janson et al. 2007; Lafrenière et al. 2007b; Biller et al. 2007; Janson et al. 2008; Heinze et al. 2008; Marengo et al. 2009; Heinze et al. 2010b; Wahhaj et al. 2013b; Janson et al. 2015). Together with long-baseline radial velocity monitoring, these deep observations have ruled out planets >3 $M_{\rm Jup}$ anywhere in this system.

2.6. *Field Stars and Radial Velocity Trends*

At the old ages of field stars ($\sim$1–10 Gyr), giant planets have cooled to late spectral types and low luminosities where high-contrast imaging does not regularly reach the planetary-mass regime. Nevertheless, several surveys have focused on this population because their proximity means very close separations can be probed and their old ages provide information about potential dynamical evolution of substellar companions and giant planets over time (McCarthy & Zuckerman 2004; Carson et al. 2005; Carson et al. 2006; Heinze et al. 2010a; Heinze et al. 2010b; Tanner et al. 2010; Leconte et al. 2010).

Of particular interest are stars showing low-amplitude,

long-baseline radial velocity changes (Doppler "trends"). These accelerations are regularly revealed in planet searches and point to the existence of unseen stars, brown dwarfs, or giant planets on wide orbits. High-contrast imaging is a useful tool to diagnose the nature of these companions and, in the case of non-detections, rule out massive objects at wide projected separations (Kasper et al. 2007; Geißler et al. 2007; Luhman & Jayawardhana 2002; Chauvin et al. 2006; Janson et al. 2009; Jenkins et al. 2010; Kenworthy et al. 2009; Rodigas et al. 2011).

When a companion is detected, its minimum mass can be inferred from the host star's acceleration ($\dot{v}$), the distance to the system (d), and the angular separation of the companion (ρ) following Torres (1999) and Liu et al. (2002):

$$M_{\rm comp} > 1.388 \times 10^{-5} \left(\frac{d}{\rm pc} \, \frac{\rho}{''} \right)^2 \left| \frac{\dot{v}}{\rm m\ s^{-1}\ yr^{-1}} \right| M_\odot. \quad (2)$$

The coefficient is 0.0145 when expressed in $M_{\rm Jup}$. This equation assumes an instantaneous radial velocity slope, but longer baseline coverage or a change in the acceleration ("jerk") can provide better constraints on a companion's mass and period (Rodigas et al. 2016). If a significant fraction of the orbit is measured with both astrometry and radial velocities, simultaneous modeling of both data sets can yield a robust dynamical mass measurement. Perhaps the best example of this is from Crepp et al. (2012a), who measured the mass and three-dimensional orbit of the brown dwarf companion HR 7672 B, initially discovered by Liu et al. (2002) based on an acceleration from the host star.

Many stellar and white dwarf companions have been discovered in this fashion but only a few substellar companions have been found (Table 2). Figure 5 shows the population of known companions inducing shallow RV trends on their host stars and which have also been recovered with high resolution (and often high-contrast) imaging. Most of these are M dwarfs with masses between ∼0.1–0.5 $M_\odot$ at separations of ∼10–100 AU. This is primarily due to the two competing methods at play: at these old ages, direct imaging is insensitive to low masses and close separations, while small accelerations induced from wide-separation and low-mass companions are difficult to measure even for long-baseline, precision radial velocity planet searches. The TRENDS program (e.g., Crepp et al. 2012a; Crepp et al. 2014) is the largest survey to combine these two methods and demonstrates the importance of both detections and non-detections to infer the population of planets on moderate orbits out to ∼20 AU (Montet et al. 2014).

Dynamical masses of planets may eventually be measured by combing radial velocity monitoring of the host star and direct imaging, effectively treating the system like a spatially resolved single-lined spectroscopic binary. Stellar jitter is a limiting factor at very young ages and at older ages the low luminosities of planets generally preclude imaging. The intermediate ages of moving group members may provide an adequate solution, and at least one ambitious survey by Lagrange et al. (2013) is currently underway to search for planets and long-term radial velocity trends for this population. An-

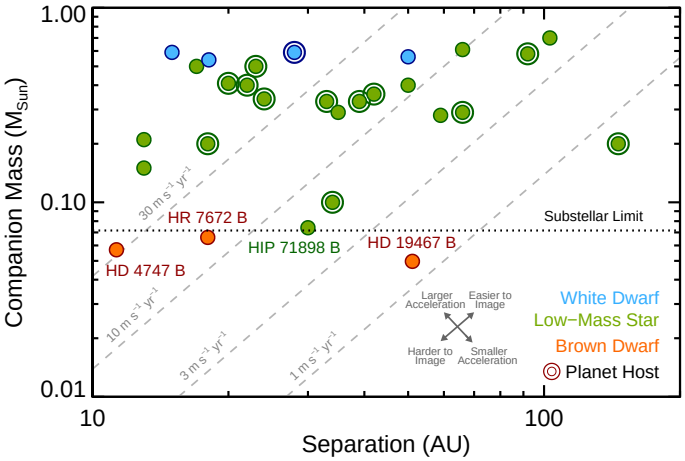

FIG. 5.— Imaged companions inducing shallow radial velocity trends on their host stars. Blue, orange, and red circles are white dwarf companions, low-mass stellar companions, and substellar companions, respectively. Concentric circles indicate the host star has a planetary system. Only three brown dwarf companions inducing shallow trends have been found: HR 7672 B (Liu et al. 2002), HD 19467 B (Crepp et al. 2014), and HD 4747 B (Crepp et al. 2016). Gray dashed lines show constant accelerations assuming circular orbits; the maximum host star acceleration is proportional to the companion mass and inversely proportional to the square of the projected physical separation, so a 1 $M_{\rm Jup}$ planet at 10 AU will produce the same maximum acceleration as a 100 $M_{\rm Jup}$ low-mass star at 100 AU (namely 0.7 m s^{-1} yr^{-1}). See Table 2 for details on these systems.

other solution is to image planets in reflected light at optical wavelengths, which requires a space-based telescope and coronagraph like *WFIRST* (Traub et al. 2014; Spergel et al. 2015; Brown 2015; Greco & Burrows 2015; Robinson et al. 2016). Similarly, astrometric accelerations can be used to identify and measure the masses of substellar companions when combined with high-contrast imaging. This will be particularly relevant in the near-future with *Gaia* as thousands of planets are expected to be found from the orbital reflex motion of their host stars (Sozzetti et al. 2013; Perryman et al. 2014).

Young stars in the field not necessarily associated with coherent moving groups have also been popular targets for high-contrast imaging planet searches. The advantage of this population is that they are numerous and often reside at closer distances than actual members of young moving groups, but their ages and metallicities are generally highly uncertain so substellar companions uncovered with deep imaging can have a wide range of possible masses (e.g., Mawet et al. 2015). GJ 504 and κ And are recent examples of young field stars with faint companions that were initially thought to have planetary masses (Kuzuhara et al. 2013; Carson et al. 2013) but which follow-up studies showed are probably older (Hinkley et al. 2013; Bonnefoy et al. 2014a; Fuhrmann & Chini 2015; Jones et al. 2016), implying the companions are likely more massive and reside in the brown dwarf regime. Sirius is another example of a young massive field star extensively targeted with high-contrast imaging (Kuchner & Brown 2000; Bonnet-Bidaud & Pantin 2008; Skemer & Close 2011; Thalmann et al. 2011; Vigan et al. 2015). This system is particularly noteworthy for possible periodic astrometric perturbations to the orbit of its white dwarf companion Sirius B that may be caused by an still-hidden

giant planet or brown dwarf (Benest & Duvent 1995).

3. THE MASSES OF IMAGED PLANETS

The masses of directly imaged planets are generally highly uncertain, heavily model-dependent, and difficult to independently measure. Yet mass is fundamentally important to test models of giant planet formation and empirically calibrate substellar evolutionary models. This Section describes how observables like bolometric luminosity, color, and absolute magnitude coupled with evolutionary models and semi-empirical quantities like age are used to infer the masses of planets. Although no imaged planet has yet had its mass directly measured, there are several promising routes to achieve this which will eventually enable rigorous tests of giant planet cooling models.

3.1. *Inferring Masses*

Like white dwarfs and brown dwarfs, giant planets cool over time so evolutionary models along with two physical parameters— luminosity, age, effective temperature, or radius— are needed to infer a planet's mass. Among these, luminosity and age are usually better constrained and less reliant on atmospheric models than effective temperature and radius, which can substantially vary with assumptions about cloud properties, chemical composition, and sources of opacity. Below are summaries of the major assumptions (in roughly descending order) involved in the inference of planet masses using atmospheric and evolutionary models along with notable advantages, drawbacks, and limitations of various techniques.

- **Initial conditions and formation pathway.** The most important assumption is the amount of initial energy and entropy a planet begins with following its formation. This defines its evolutionary pathway, which is embodied in three broad classes informed by formation mechanisms.

  Hot-start models begin with arbitrarily large radii and oversimplified, idealized initial conditions that generally ignore the effects of accretion and mass assembly. As such, they represent the most luminous outcome and correspond to the most optimistically (albeit unrealistically) low mass estimates. Ironically, hot-start grids are nearly unanimously adopted for estimating the masses of young brown dwarfs and giant planets even though the early evolution in these models is the least reliable. The most widely used hot-start models for imaged planets are the Cond and Dusty grids from Baraffe et al. (2003) and Chabrier (2001), Burrows et al. (1997), and Saumon & Marley (2008).

  Cold-start models were made prominent by Marley et al. (2007b) and Fortney et al. (2008) in the context of direct imaging as an attempt to emulate a more realistic formation scenario for giant planets through core accretion. In this model, accretion shocks radiate the gravitational potential energy of infalling gas as a giant planet grows. After formation, these planets begin cooling with much lower luminosities and initial entropies compared to the hot-start scenario, taking between $\sim 10^8$ and $\sim 10^9$ years to converge with hot-start cooling models depending on the planet mass. The observational implications of this are severe: planets formed from core accretion may be orders of magnitude less luminous than those produced from cloud fragmentation or disk instability. While this may offer a diagnostic for the formation route if the mass of a planet is independently measured, it also introduces considerable uncertainty in the more typical case when only an age and luminosity are known. For example, 51 Eri b may be as low as 2 $M_{\rm Jup}$ or as high as 12 $M_{\rm Jup}$ depending on which cooling model (hot or cold) is assumed (Macintosh et al. 2015).

  This picture is made even more complicated by large uncertainties in the details of cold-start models. The treatment of accretion shocks, circumplanetary disks, core mass, and even deuterium burning for the most massive planets can dramatically influence the initial entropy and luminosity evolution of planets (Mordasini et al. 2012; Bodenheimer et al. 2013; Mordasini 2013; Owen & Menou 2016). This motivated a class of warm-start models with intermediate initial entropies that probably better reflect dissipative accretion shocks that occur in nature (Spiegel & Burrows 2012; Marleau & Cumming 2013). Unfortunately, the relevant details of giant planet assembly are poorly constrained by observations. There is also likely to be intrinsic scatter in the initial conditions for a given planet which may result in large degeneracies in the planet mass, core mass, and accretion history for young gas giants with the same age and luminosity. It is quite possible, for instance, that the HR 8799 c, d, and e planets which all share the same age and nearly the same luminosity could have very different masses.

- **Stellar age.** After bolometric luminosity, which is generally uncomplicated to estimate for imaged planets, the age of the host star is the most sensitive parameter on which the mass of an imaged companion depends. It is also one of the most difficult quantities to accurately determine and usually relies on stellar evolutionary models or empirical calibrations. Recent reviews on this topic include Soderblom (2010), Jeffries (2014), and Soderblom et al. (2014). Figure 6 shows the current census of imaged companions near and below the deuterium-burning limit with both age and luminosity measurements (from Table 1). Apart from uncertainties in the formation history of these objects, age uncertainties dominate the error budget for inferring masses.

  Clusters of coeval stars spanning a wide range of masses provide some of the best age constraints but are still dominated by systematic errors. Several star-forming regions and young moving groups in particular have been systematically adjusted to older ages over the past few years, which has propagated to the ages and masses of planets in those

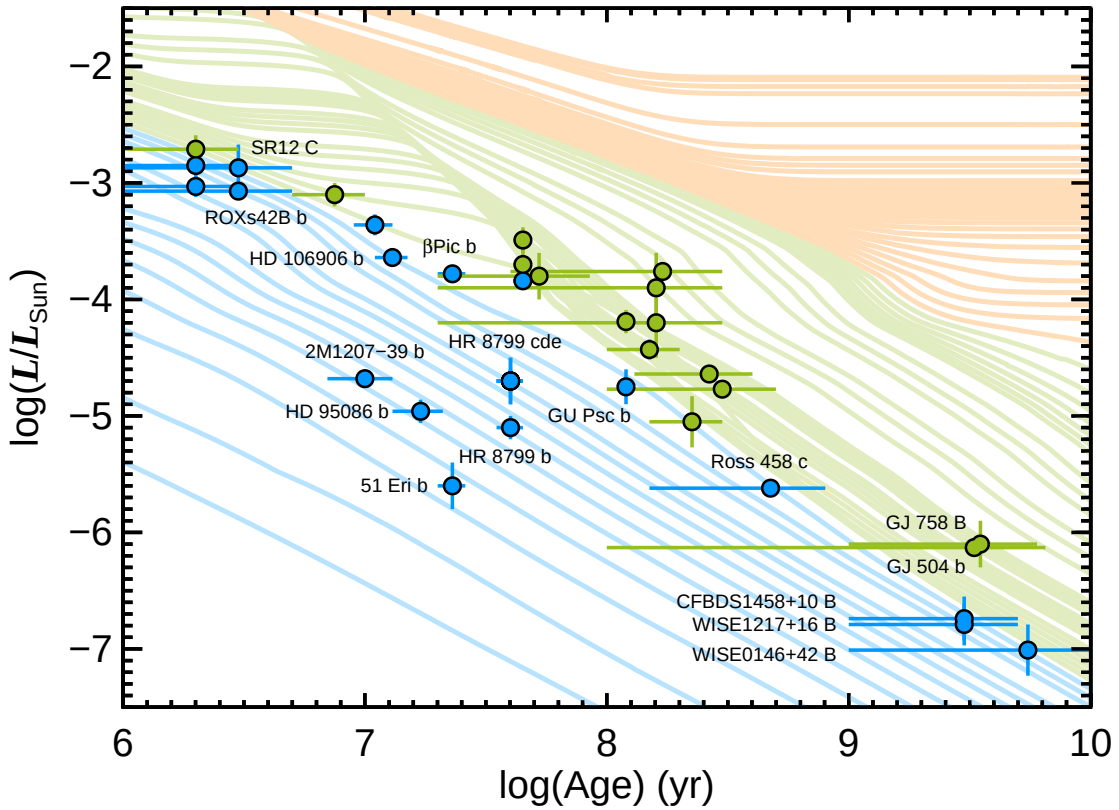

FIG. 6.— The current census of companions in the brown dwarf (green) and planetary (blue) mass regimes that have both age and bolometric luminosity measurements from the compilation in Table 1. Many companions lie near the deuterium-burning limit while only a handful of objects are unambiguously in the planetary-mass regime. Hot-start evolutionary models are from Burrows et al. (1997); orange, green, and blue tracks denote masses >80 $M_{\rm Jup}$, 14–80 $M_{\rm Jup}$, and <14 $M_{\rm Jup}$.

associations (Pecaut et al. 2012; Binks & Jeffries 2014; Kraus et al. 2014b; Bell et al. 2015). The implied hot-start mass for β Pic b, for example, increases by several Jupiter masses (corresponding to several tens of percent) assuming the planet's age is ≈23 Myr instead of ≈12 Myr (Mamajek & Bell 2014; although see the next bullet point).

For young field stars, distant stellar companions can help age-date the entire system. For example, the age of Fomalhaut was recently revised to ∼400 Myr from ∼200 Myr in part due to constraints from its wide M dwarf companions (Mamajek 2012; Mamajek et al. 2013). Ultimately, if the age of a host star is unknown, the significance and interpretation of a faint companion is limited if basic physical properties like its mass are poorly constrained.

- **Epoch of planet formation.** Planets take time to form so they are not exactly coeval with their host stars. Their ages may span the stellar age to the stellar age minus ∼10 Myr depending on the timescale for giant planets to assemble. Planets formed via cloud fragmentation or disk instability might be nearly coeval with their host star, but those formed by core accretion are expected to build mass over several Myr. While this difference is negligible at intermediate and old ages beyond a few tens of Myrs, it can have a large impact on the inferred masses of the youngest planets ($\lesssim$20 Myr). For example, if the age of the young planetary-mass companion 2M1207–3932 b is assumed to be coeval with the TW Hyrdae Association ($\tau = 10 \pm 3$ Myr) then its hot-start mass is ≈5 $M_{\rm Jup}$. On the other hand, if its formation was delayed by 8 Myr (τ = 2 Myr) then its mass is only ≈2.5 $M_{\rm Jup}$.

- **Atmospheric models.** Atmospheric models can influence the inferred masses of imaged exoplanets in several ways. They act as surface boundary conditions for evolutionary models and regulate radiative cooling through molecular and continuum opacity sources. This in turn impacts the luminosity evolution of giant planets, albeit minimally because of the weak dependence on mean opacity ($L(t) \propto \kappa^{0.35}$; Burrows & Liebert 1993; Burrows et al. 2001). Even the unrealistic cases of permanently dusty and perpetually condensate-free photospheres do not dramatically affect the luminosity evolution of cooling models or mass determinations using age and bolometric luminosity (Baraffe et al. 2002; Saumon & Marley 2008), although more realistic ("hybrid") models accounting for the evolution and dissipation of clouds at the L/T transition can influence the shape of cooling curves in slight but significant ways (Saumon & Marley 2008; Dupuy et al. 2015b).

  On the other hand, mass determinations in color-magnitude space are highly sensitive to atmospheric models and can result in changes of several tens of percent depending on the specific treatment of atmospheric condensates. Dust reddens spec-

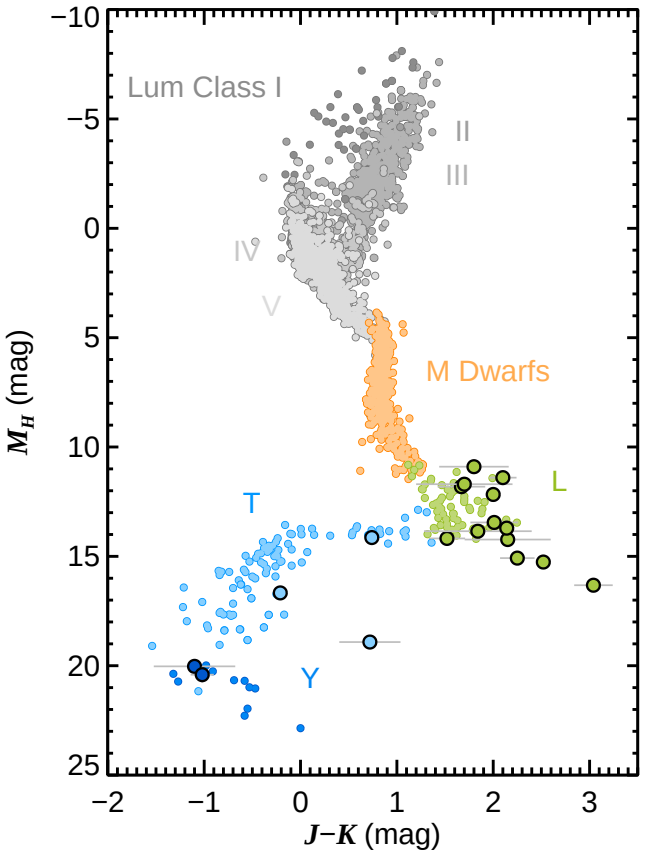

FIG. 7.— The modern color-magnitude diagram spans nearly 35 magnitudes in the near-infrared and 5 magnitudes in J–K color. The directly imaged planets (bold circles) extend the L dwarf sequence to redder colors and fainter absolute magnitudes owing to a delayed transition from cloudy atmospheres to condensate-free T dwarfs at low surface gravities. The details of this transition for giant planets remains elusive. OBAFGK stars (gray) are from the extended *Hipparcos* compilation XHIP (Anderson & Francis 2012); M dwarfs (orange) are from Winters et al. (2015); late-M dwarfs (orange), L dwarfs (green), and T dwarfs (light blue) are from Dupuy & Liu (2012); and Y dwarfs (blue) are compiled largely from Dupuy et al. (2014), Tinney et al. (2014), and Beichman et al. (2014) by T. Dupuy (2016, private communication). Directly imaged planets or planet candidates (bold circles) represent all companions from Table 1 with near-infrared photometry and parallactic distances.

tra and can modify the near-infrared colors and absolute magnitudes of ultracool objects by several magnitudes. This introduces another source of uncertainty if the spectral shape is poorly constrained, though the difference between dusty and cloud-free models is smaller at longer wavelengths and higher temperatures.

One of the most important and unexpected empirical results to emerge from direct imaging has been the realization that young brown dwarfs and massive planets retain photospheric clouds even at low effective temperatures where older, high-gravity brown dwarfs have already transitioned to T dwarfs (Metchev & Hillenbrand 2006; Chauvin et al. 2004; Marois et al. 2008; Patience et al. 2010; Bowler et al. 2010a; Faherty et al. 2012; Bowler et al. 2013; Liu et al. 2013; Filippazzo et al. 2015). This is demonstrated in Figure 7, which shows the location of imaged companions near and below the deuterium-burning limit on the near-infrared color-color diagram. At young ages, warm giant planets are significantly redder than the field population of brown dwarfs, and several of the most extreme examples have anomalously low absolute magnitudes. For old brown dwarfs, this evolution from dusty, CO-bearing L dwarfs to cloud-free, methane-dominated T dwarfs takes place over a narrow temperature range (∼1200–1400 K) but occurs at a lower (albeit still poorly constrained) temperature for young gas giants. The lack of methane is likely caused by disequilibrium carbon chemistry at low surface gravities as a result of vigorous vertical mixing (e.g., Barman et al. 2011a; Zahnle & Marley 2014; Ingraham et al. 2014; Skemer et al. 2014a), while the preservation of photospheric condensates can be explained by a dependency of cloud base pressure and particle size on surface gravity (Marley et al. 2012). Unfortunately, the dearth of known planets between ∼L5–T5 is the main limitation to understanding this transition in detail (Figure 8).

In principle, the mass of a planet can also be inferred by fitting synthetic spectra to the planet's observed spectrum or multi-band photometry. The mass can then be obtained from best-fitting model as follows:

$$M_p\ (M_{\rm Jup}) = 12.76 \times 10^{\log(g)-4.5\ \rm dex} \left(\frac{R}{R_{\rm Jup}}\right)^2. \quad (3)$$

Here $\log(g)$ is the surface gravity (in cm s^{-2}) and R is the planet's radius. The radius can either be taken from evolutionary models or alternatively from the multiplicative factor that scales the emergent model spectrum to the observed flux-calibrated spectrum (or photometry) of the planet. This scale factor corresponds to the planet's radius over its distance, squared (R^2/d^2; see Cushing et al. 2008 for details).

Clearly the inferred mass is very sensitive to both the surface gravity and the radius. In practice, gravity is usually poorly constrained for model fits to brown dwarf and giant planet spectra because its influence on the emergent spectrum is more subtle (e.g., Cushing et al. 2008; Bowler et al. 2011; Barman et al. 2011a; Macintosh et al. 2015). In addition, the scale factor strongly depends on the model effective temperature ($\propto T_{\rm eff}^{-4}$), which is typically not known to better than ∼100 K. Altogether, the current level of systematic imperfections present in atmospheric models and observed spectra of exoplanets (e.g., Greco & Brandt 2016) mean that masses cannot yet be reliably measured from fitting grids of synthetic spectra.

- **Deuterium burning history.** As brown dwarfs with masses between about 13 $M_{\rm Jup}$ and 75 $M_{\rm Jup}$ contract, their core temperatures become hot enough to burn deuterium, though not at sufficient rates to balance surface radiative losses (e.g.,

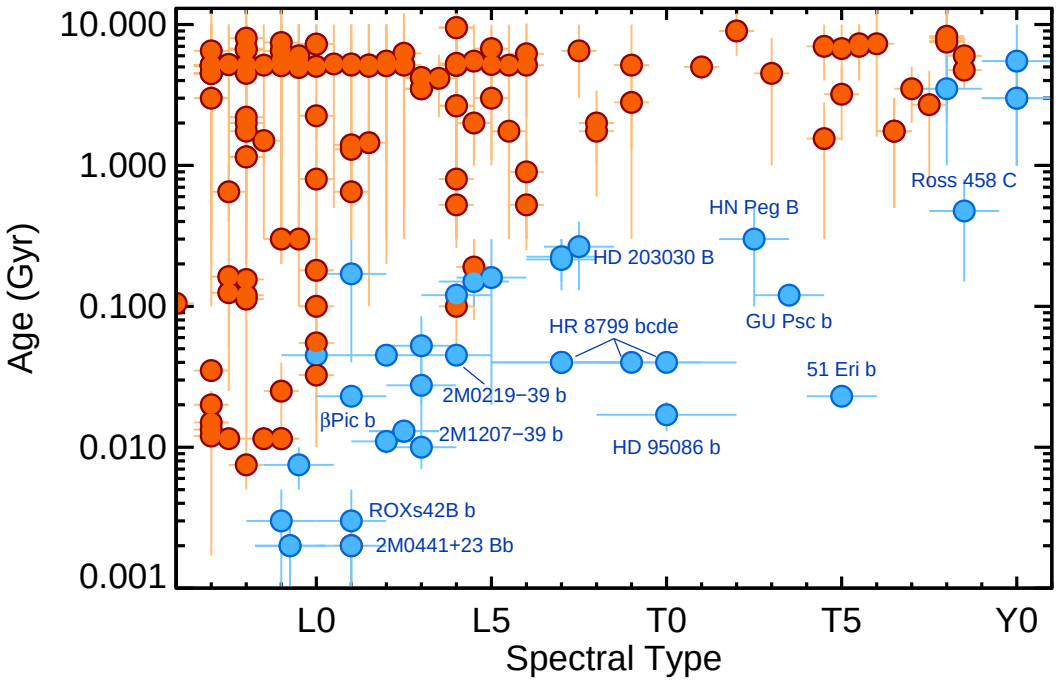

FIG. 8.— Ultracool substellar companions with well-constrained ages and spectroscopically-derived classifications. Red circles are low-mass stars and brown dwarfs (>13 $M_{\rm Jup}$) while blue circles show companions near and below the deuterium-burning limit. Companions are primarily from Deacon et al. (2014) together with additional discoveries from the literature.

Kumar 1963; Burrows & Liebert 1993).[3] The onset and timescale of deuterium burning varies primarily with mass but also with metallicity, helium fraction, and initial entropy (e.g., Spiegel et al. 2011); lower-mass brown dwarfs take longer to initiate deuterium burning than objects near the hydrogen-burning minimum mass. This additional transient energy source delays the otherwise invariable cooling and causes luminosity tracks to overlap. Thus, objects with the same luminosity and age can differ in mass depending on their deuterium-burning history. Many substellar companions fall in this ambiguous region, complicating mass determinations by up to a factor of ∼2 (Figure 6 and Table 1). With a large sample of objects in this region, spectroscopy may ultimately be able to distinguish higher- and lower-mass scenarios through relative surface gravity measurements (Bowler et al. 2013).

- **Planet composition.** The gas and ice giants in the Solar System are enriched in heavy elements compared to solar values. The specific mechanism for this enhancement is still under debate but exoplanets formed via core accretion are expected to show similar compositional and abundance ratio differences compared to their host stars, whereas planets formed through cloud fragmentation or disk instability are probably quite similar to the stars they orbit. The bulk composition of planets modifies their atmospheric opacities and influences both their emergent spectra and luminosity evolution (Fortney et al. 2008). A common practice when deriving masses for imaged planets is to assume solar abundances, which is largely dictated by the availability of published atmospheric and evolutionary models. Many of these assumptions can be removed with atmospheric retrieval methods by directly fitting for atomic and molecular abundances (Lee et al. 2013; Line et al. 2014; Todorov et al. 2015).

- **Additional sources of uncertainty.** A number of other factors and implicit assumptions can also introduce random and systematic uncertainties in mass derivations. Different methods of PSF subtraction can bias photometry if planet self-subtraction or speckle over-subtraction is not properly corrected (e.g., Marois et al. 2006; Lafrenière et al. 2007a; Soummer et al. 2012). Photometric variability from rapidly changing or rotationally-modulated surface features can introduce uncertainties in relative photometry (e.g., Radigan et al. 2014; Metchev et al. 2015; Zhou et al. 2016; Biller et al. 2015a). The host star can also be variable if it has unusually large starspot coverage or if it is very young and happens to have an edge-on disk (e.g., TWA 30A; Looper et al. 2010).

  Multiplicity can also bias luminosity measurements. Roughly 20% of brown dwarfs are close binaries with separation distributions peaking near 4.5 AU and mass ratios approaching unity (e.g., Burgasser et al. 2007; Kraus & Hillenbrand 2012; Duchêne & Kraus 2013). If some planetary-mass companions form in the same manner as brown dwarfs, and if the same trends in multiplicity continue into the planetary regime, then a small frac-

[3] Solar-metallicity brown dwarfs with masses above ≈63 $M_{\rm Jup}$ can also burn lithium. This limit changes slightly for non-solar values (Burrows et al. 2001).

tion of planetary-mass companions are probably close, unresolved, equal-mass binaries. These systems will appear twice as luminous.

If atmospheric chemistry or cloud structure varies latitudinally then orientation and viewing angle could be important. For the youngest protoplanets embedded in their host stars' circumstellar disks, accretion streams might dominate over thermal photospheric emission, complicating luminosity measurements and mass estimates (e.g., LkCa15 b and HD 100546 b; Kraus & Ireland 2012; Quanz et al. 2013). Approaches to applying bolometric corrections, measuring partly opaque coronagraphs and neutral density filters, finely interpolating atmospheric and evolutionary model grids, or converting models between filter systems (for example, CH_4S to K) may vary. Finally, additional energy sources like radioactivity or stellar insolation are assumed to be negligible but could impact the luminosity evolution of some exoplanets.

3.2. *Measuring Masses*

No imaged planet has yet had its mass measured. The most robust, model-independent way to do so is through dynamical interactions with other objects. Because planets follow mass-luminosity-age relationships, knowledge of all three parameters are needed to test cooling models. Once a mass is measured, its age (from the host star) and bolometric luminosity (from its distance and spectral energy distribution) enable precision model tests, although an assumption about energy losses from accretion via hot-, warm-, or cold-start must be made. Nevertheless, if all hot-start models overpredict the luminosities of giant planets, that would suggest that accretion history is indeed an important factor in both planet formation and realistic cooling models. Below is a summary of methods to measure substellar masses.

- **Dynamical masses.** Most close-in (<100 AU) planets have shown significant orbital motion since their discoveries (Table 1). This *relative* motion provides a measure of the total mass of the system ($M_{\rm star}$+$M_{\rm planet}$). If stationary background stars can simultaneously be observed with the planet-star pair then *absolute* astrometry is possible. This then gives individual masses for each component ($M_{\rm star}$ and $M_{\rm planet}$ separately). Unfortunately the long orbital periods and lack of nearby background stars for the present census of imaged planets means this method is currently impractical to measure masses.

  Relative astrometry can also be combined with radial velocities to measure a planet's mass. Assuming the visual orbit and total mass are well constrained from imaging, the mass of the companion can be measured by monitoring the line of sight reflex motion of the host star (e.g., Crepp et al. 2012a). This treats the system as a single-lined spectroscopic binary, giving the mass function $m_{\rm p}^3 \sin^3 i / M_{\rm tot}^2$, where $M_{\rm tot}$ is the measured total mass, i is the measured inclination, and $m_{\rm p}$ is the mass of the planet. If precise radial velocities are not possible for the host star because it has an early spectral type (with few absorption lines) or high levels of stellar activity (RV jitter) then RV monitoring of the planet can also yield its mass. This can be achieved by combining adaptive optics imaging and high-resolution near-infrared spectroscopy to spatially separate the star and planet, as has been demonstrated with β Pic b (Snellen et al. 2014). Soon *Gaia* will produce precise astrometric measurements of the host stars of imaged planets. Together with orbit monitoring though high-contrast imaging, this may offer another way to directly constrain the masses of imaged planets.

  Close substellar binaries offer another approach. Their orbital periods are typically faster and, in rare cases when such binaries themselves orbit a star, the age of the tertiary components can be adopted from the host star. Several brown dwarf-brown dwarf masses have been measured in this fashion: HD 130948 BC (Dupuy et al. 2009), Gl 417 BC (Dupuy et al. 2014), and preliminary masses for ϵ Indi Bab (Cardoso et al. 2009). Isolated substellar pairs are also useful for dynamical mass measurements but their ages are generally poorly constrained unless they are members of young clusters or moving groups. No binaries with both components unambiguously residing in the planetary-mass regime are known, but there is at least one candidate (WISE J014656.66+423410.0; Dupuy et al. 2015a).

- **Keplerian disk rotation.** Dynamical masses for young protoplanets may eventually be possible using ALMA through Keplerian rotation of circumplanetary disks. This requires resolving faint gas emission lines (e.g., CO J=3–2 or CO J=2–1) from the planet both spatially and spectrally, something that has yet to be achieved for known young planets harboring subdisks (e.g., Isella et al. 2014; Bowler et al. 2015a). Although challenging, this type of measurement can act as a detailed probe of the initial conditions of giant planet formation and evolution.

- **Stability analysis.** Numerical modeling of planets and their interactions with debris disks, protoplanetary disks, or additional planets offers another way to constrain the mass of an imaged planet. If their masses are too low, planets will not be able to gravitationally shape dust and planetesimals in a manner consistent with observations. Modeling of the disks and companions orbiting Fomalhaut and β Pic illustrate this approach; independent constraints on the orbit and masses of these companions can be made by combining spatially-resolved disk structures (a truncated, offset dust ring encircling Fomalhaut and a warped inner disk surrounding β Pic b) and observed orbital motion (e.g., Chiang et al. 2009; Dawson et al. 2011; Kalas et al. 2013; Beust et al. 2014; Millar-Blanchaer et al. 2015). Likewise, if a planet's mass is too high then it carves a larger disk gap or may destabilize other planets in the system through mutual interactions.

For example, detailed N-body simulations of HR 8799's planets have shown that they must have masses $\lesssim$10–20 $M_{\rm Jup}$ — consistent with giant planet evolutionary models — or they would have become dynamically unstable by the age of the host star (e.g., Goździewski & Migaszewski 2009; Fabrycky & Murray-Clay 2010; Currie et al. 2011b; Sudol & Haghighipour 2012; Goździewski & Migaszewski 2014).

- **Disk morphology.** Large-scale structures in disks — clumps, asymmetries, warps, gaps, rings, truncated edges, spiral arms, and geometric offsets — can also be used to indirectly infer the presence of unseen planets and predict their masses and locations (e.g., Wyatt et al. 1999; Ozernoy et al. 2000; Kenyon & Bromley 2004). This approach relies on assumptions about disk surface density profiles and grain properties, so it is not a completely model-free measurement, but it is potentially sensitive to planet masses as low as a few tens of Earth masses (Rosotti et al. 2016). It also enables an immediate mass evaluation without the need for long-term orbit monitoring. Recently, Dong et al. (2015) and Zhu et al. (2015) presented a novel approach along these lines to predict the locations and masses widely-separated companions inducing spiral arms on a circumstellar disk (see also Dong et al. 2016b, Dong et al. 2016a, and Jilkova & Zwart 2015). This may prove to be a valuable way to constrain masses of planetary companions at extremely wide orbital distances.

4. SURVEY OF SURVEYS

Myriad large high-contrast imaging surveys have been carried out over the past decade[4]. The most impactful programs are highly focused, carefully designed with well-understood biases, and have meticulously-selected target lists to address specific science questions. The advantages of large surveys include homogeneous observations, instrument setups, data reduction pipelines, and statistical treatments of the results.

Below are summaries of the most substantial high-contrast imaging surveys carried out to date with a focus on deep adaptive optics imaging programs that routinely reach planetary masses and employ modern observing and post-processing techniques to suppress speckle noise. These surveys produced the first wave of discoveries (Figure 9), opening the door to directly characterizing the atmospheres of exoplanets as well as their orbits through astrometric monitoring (Figure 10 and Appendix 4) This section follows an historical approach by outlining early ground- and space-based experiments, the first generation of planet-finding instruments and associated surveys, and the next generation of instruments characterized by extreme adaptive optics systems with exceptionally high Strehl ratios.

4.1. *Early Surveys*

[4] The basic properties for most of these programs until 2014 are summarized in Table 1 of Chauvin et al. (2015).

Early high-contrast imaging surveys in search of closely-separated brown dwarf companions and giant planets were conducted with speckle interferometry (Henry & McCarthy 1990), image stabilizers (Nakajima et al. 1994), *HST* (Sartoretti et al. 1998; Schroeder et al. 2000; Brandner et al. 2000; Lowrance et al. 2005; Luhman et al. 2005), speckle cameras (Neuhäuser et al. 2003), or newly-commissioned adaptive optics systems from the ground with facility instruments (Oppenheimer et al. 2001; Macintosh et al. 2001; Chauvin et al. 2003; McCarthy & Zuckerman 2004; Carson et al. 2005; Nakajima et al. 2005; Tanner et al. 2007). When PSF subtraction was performed, it usually entailed roll-subtraction (for *HST*; e.g., Liu 2004), self-subtraction with a rotated PSF, or reference star subtraction.

Some of these pioneering programs are especially noteworthy for their depth and emphasis on statistical results. Lowrance et al. (2005) targeted 45 single young A–M stars with NICMOS in the $F160W$ filter (1.6 μm) on board *HST*. Two brown dwarfs were uncovered, TWA 5 B (Lowrance et al. 1999) and HR 7372 B (Lowrance et al. 2000), as well as Gl 577 BC, a tight binary companion near the hydrogen-burning limit. Masciadri et al. (2005) used NaCo at the VLT to obtain deep adaptive optics imaging of 28 young nearby stars. No substellar companions were found, but the importance of thoroughly reporting survey results is highlighted, even for non-detections, a theme that continues today. Focusing exclusively on young moving group members in L'-band enabled Kasper et al. (2007) to reach exceptionally low limiting masses for a sample of 22 stars with NaCo. The Palomar and Keck adaptive optics survey by Metchev & Hillenbrand (2009) is another especially valuable contribution; they imaged 266 FGK stars and discovered two brown dwarf companions, HD 49197 B (Metchev & Hillenbrand 2004) and HD 203030 B (Metchev & Hillenbrand 2006), implying a substellar occurrence rate of $3.2^{+3.1}_{-2.7}$%. HD 203030 B was the first young brown dwarf for which signs of a discrepancy between the field spectral type-effective temperature sequence was recognized, now understood as a retention of clouds to lower effective temperatures at low surface gravities. These groundbreaking surveys helped define the scientific motivation, framework, and early expectations for the first generation planet-finding instruments and larger observing programs.

4.2. *The First Generation: Dedicated Instruments, Expansive Surveys, and Innovative Speckle Suppression Techniques*

High-contrast imaging is largely driven by advances in instrumentation and speckle suppression. The first wave of instruments specifically designed to image giant planets gave rise to large surveys (N≈50–500) targeting mostly young nearby stars. Deep observations in pupil-tracking mode (angular differential imaging) have become standardized as a way to distinguish quasi-static speckles from planets (Marois et al. 2006). This era is also characterized by the advent of advanced PSF subtraction techniques to optimally remove speckles during post-processing. Two especially important algorithms are the Locally Optimized Combination

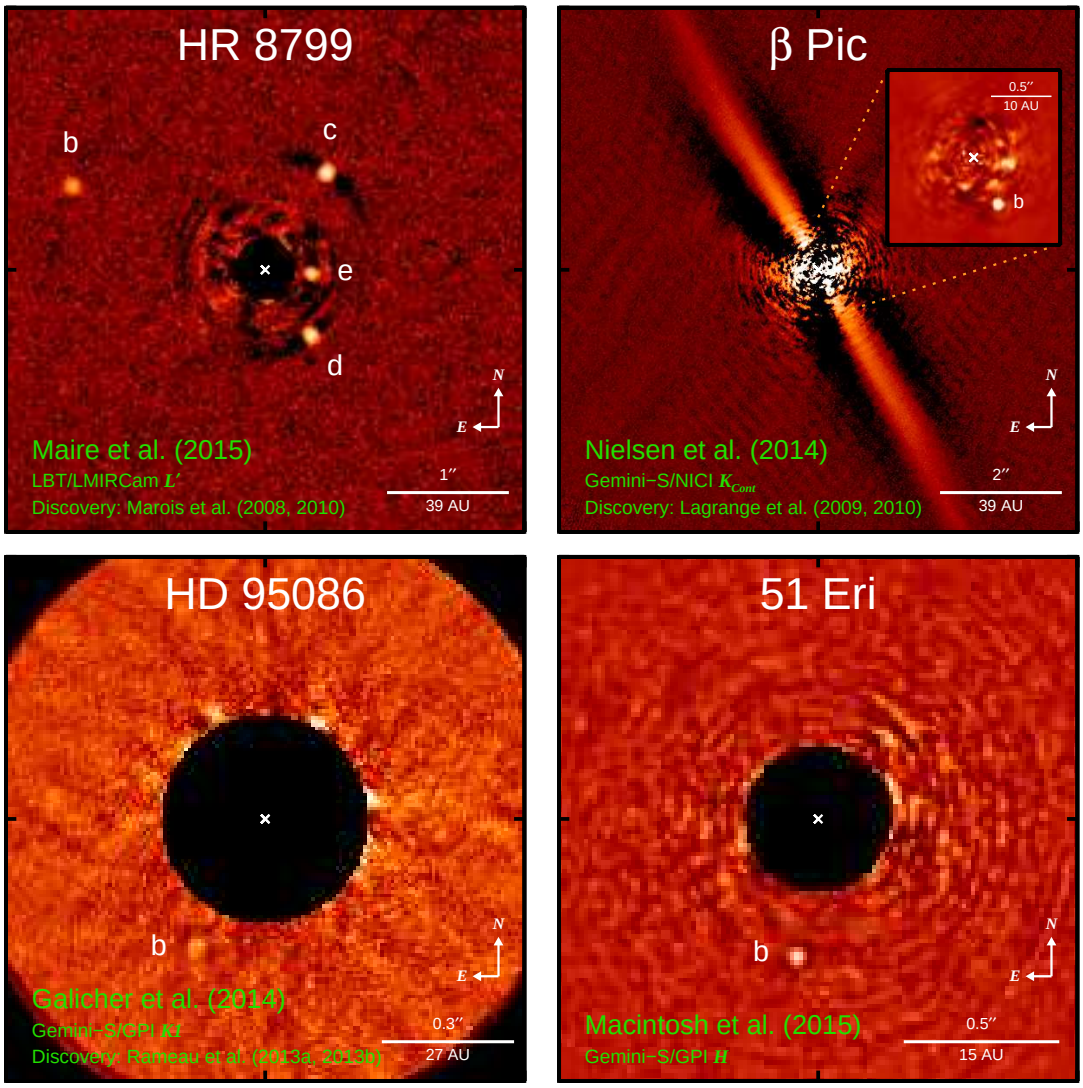

FIG. 9.— Gallery of imaged planets at small separations (<100 AU). HR 8799 harbors four massive planets (5–10 $M_{\rm Jup}$) at orbital distances of 15–70 AU (Marois et al. 2008; Marois et al. 2010b), β Pic hosts a nearly edge-on debris disk and a ≈13 $M_{\rm Jup}$ planet at 9 AU (Lagrange et al. 2009a; Lagrange et al. 2010), a ≈5 $M_{\rm Jup}$ planet orbits HD 95086 at 56 AU (Rameau et al. 2013c; Rameau et al. 2013b), and 51 Eri hosts a ∼2 $M_{\rm Jup}$ planet at 13 AU (Macintosh et al. 2015). Images are from Maire et al. (2015a), Nielsen et al. (2014), Galicher et al. (2014), and Macintosh et al. (2015).

of Images (LOCI; Lafrenière et al. 2007a), which is based on least-squares minimization of residual speckle noise, and Karhunen-Loève Image Projection (KLIP; Soummer et al. 2012), a computationally-fast method based on principal component analysis. The introduction of these new methods gave rise to an array of sophisticated data reduction pipelines with additional features aimed at minimizing biases and avoiding both self- and over-subtraction of planet flux in ADI and SDI datasets (Marois et al. 2010a; Amara & Quanz 2012; Pueyo et al. 2012; Meshkat et al. 2013a; Wahhaj et al. 2013a; Brandt et al. 2013; Fergus et al. 2014; Mawet et al. 2014; Marois et al. 2014; Currie et al. 2014c; Cantalloube et al. 2015; Rameau et al. 2015; Wahhaj et al. 2015; Savransky 2015; Dou et al. 2015; Hagelberg et al. 2016; Gonzalez et al. 2016).

The suite of instrumentation for high-contrast imaging has ballooned over the past 15 years and includes dual-channel imagers, infrared wavefront sensors, non-redundant aperture masking interferometry, adaptive secondary mirrors, integral field units, high-order adaptive optics systems, and specialized coronagraphs (e.g., apodized Lyot coronagraph, annular groove phase mask coronagraph, vector vortex coronagraph, apodizing phase plate, and four quadrant phase mask; Rouan et al. 2000; Guyon et al. 2005; Soummer 2005; Mawet et al. 2005; Kenworthy et al. 2007; Mawet et al. 2010). Many of these have been implemented in the first generation of instruments in part as testbeds for regular use in second-generation systems. These instruments are reviewed in detail in Guyon et al. (2006), Beuzit et al. (2007), Oppenheimer & Hinkley (2009), Perryman (2011), and Mawet et al. (2012b).

4.2.1. *VLT and MMT Simultaneous Differential Imager Survey*

This survey (PI: B Biller) targeted 45 young stars between 2003–2006 with ages $\lesssim$250 Myr and distances

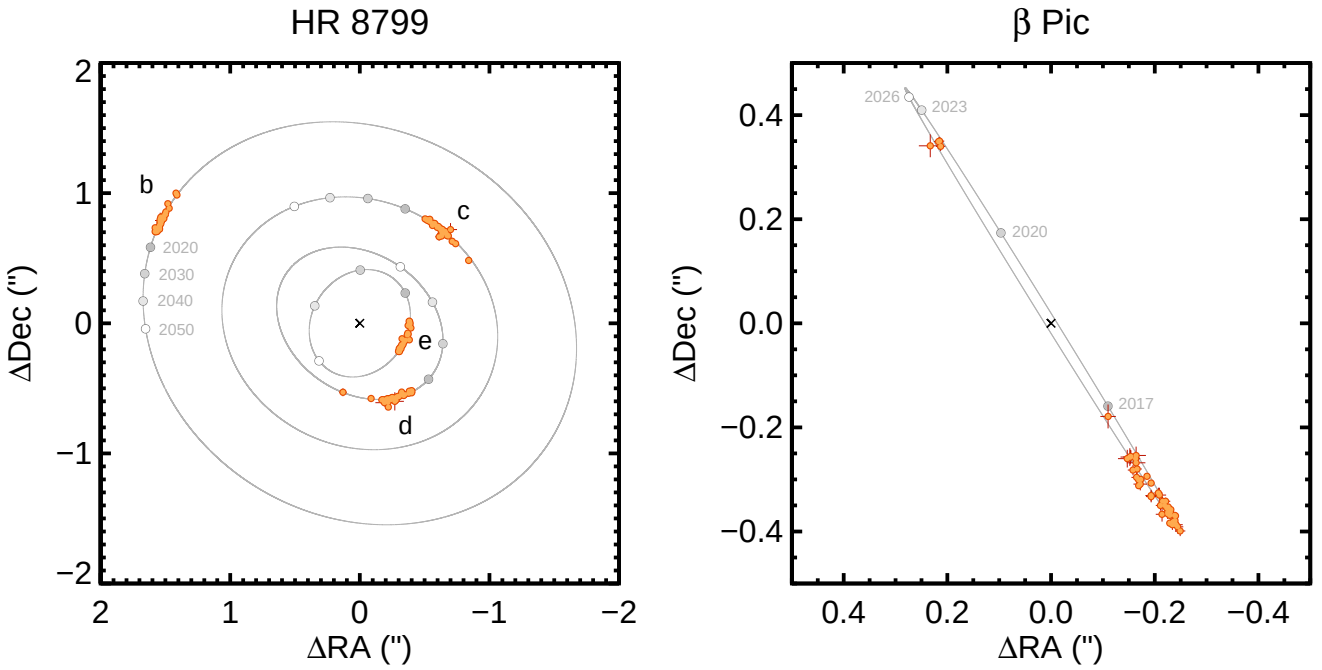

FIG. 10.— The orbits of HR 8799 bcde and β Pic b. Astrometric monitoring has revealed significant orbital motion over the past decade, enabling measurements of their Keplerian orbital parameters and offering clues about their dynamical history. The HR 8799 planets are on low-eccentricity orbits with some evidence that HR 8799 d may be mutually misaligned with the other planets, which otherwise appear to be coplanar (e.g., Pueyo et al. 2015). β Pic b follows a nearly edge-on orbit with a low eccentricity (e.g., Millar-Blanchaer et al. 2015). Astrometric measurements are compiled in Appendix 4. Orbits depicted here are from Zurlo et al. (2016) and Nielsen et al. (2014).

within 50 pc using Simultaneous Differential Imagers mounted on the VLT and MMT (Biller et al. 2007). It was among the first to utilize simultaneous differential imaging to search for cold planets around a large sample of young stars. The SDI method takes advantage of expected spectral differences between the star, which has a nearly flat continuum, and cool, methanated planets by simultaneously imaging in multiple narrow-band filters across this deep absorption feature at 1.6 μm. Because speckles radially scale with wavelength while real objects remain stationary, their observations also had some sensitivity to warmer planets without methane (though it is now clear that the onset of methane occurs at lower temperatures for giant planets than for brown dwarfs). No substellar companions were found, which ruled out a linearly-flat extension of close-in giant planets out to 45 AU with high confidence.

4.2.2. *GDPS: Gemini Deep Planet Survey*

GDPS (PI: D. Lafrenière) was a large high-contrast imaging program at the Gemini-North 8.1-m telescope with the NIRI camera and Altair AO system focusing on 85 stars, 16 of which were identified as close multiples (Lafrenière et al. 2007b). The sample contained a mix of nearby GKM stars within 35 pc comprising then-known or suspected nearby young moving group members, stars with statistically young ages, and several others harboring circumstellar disks. Altogether the ages span 10 Myr to ∼5 Gyr. The observations were taken in ADI mode with the CH_4S filter, and PSF subtraction was carried out with the LOCI algorithm (Lafrenière et al. 2007a). No substellar companions were discovered, implying an occurrence rate of <23% for >2 $M_{\rm Jup}$ planets between 25–420 AU and <12% for >2 $M_{\rm Jup}$ planets between 50–295 AU at the 95% confidence level.

4.2.3. *MMT L' and M-Band Survey of Nearby Sun-Like Stars*

Heinze et al. (2010b) carried out a deep L'- and M-band survey of 54 nearby FGK stars at the MMT with Clio. The MMT adaptive optics system uses a deformable secondary mirror which reduces the thermal background by minimizing the number of optical elements along the light path. Observations were carried out between 2006–2007 with angular differential imaging. The image processing pipeline is described in Heinze et al. (2008) and Heinze et al. (2010b). The target ages are generally older (∼0.1–2 Gyr) but the long wavelengths of the observations and proximity of the sample ($\lesssim$25 pc) enabled sensitivity to planetary masses for most of the targets. One new low-mass stellar companion was discovered and the binary brown dwarf HD 130948 BC was recovered in the survey. The statistical results are detailed in Heinze et al. (2010a); they find that no more than 50% of Sun-like stars host $\geq$5 $M_{\rm Jup}$ planets between 30–94 AU and no more than 15% host $\geq$10 $M_{\rm Jup}$ planets between 22–100 AU at the 90% confidence level.

4.2.4. *NaCo Survey of Young Nearby Austral Stars*

This program utilized NaCo at the VLT between 2002–2007 to target 88 young GKM stars within 100 pc (Chauvin et al. 2010). 17 new close multiple systems were uncovered and deep imaging was obtained for 65 single young stars. Observations were taken with a Lyot coronagraph in H and K_S bands and PSF subtraction was performed with azimuthally-averaged subtraction and high-pass filtering.

The most important discovery from this survey was 2M1207–3932 b, a remarkable 5 ± 2 $M_{\rm Jup}$ companion to a 25 $M_{\rm Jup}$ brown dwarf in the 10 Myr TWA moving group

(Chauvin et al. 2004; Chauvin et al. 2005a) enabled with infrared wavefront sensing. The unusually red colors and spectral shape of 2M1207–3932 b (Patience et al. 2010) have made it the prototype of young dusty L dwarfs, now understood as a cloudy extension of the L dwarf sequence to low temperatures (Barman et al. 2011b; Marley et al. 2012). This system is also unusual from the perspective of brown dwarf demographics; the mass ratio of ∼0.2 and separation of ∼41 AU make it an outlier compared to brown dwarf mass ratio and separation distributions in the field (Burgasser et al. 2007). Two other substellar companions were discovered in this survey: GSC 08047-00232 B (Chauvin et al. 2005c), also independently found by Neuhäuser et al. (2003), and AB Pic B (Chauvin et al. 2005b), which resides near the deuterium-burning limit.

4.2.5. *NaCo Survey of Young Nearby Dusty Stars*

This VLT/NaCo survey targeted 59 young nearby AFGK stars with ages $\lesssim$200 Myr and distances within 65 pc (Rameau et al. 2013a). Most of the sample are members of young moving groups and the majority (76%) were chosen to have mid-infrared excesses, preferentially selected for having debris disks. Observations were carried out in L'-band between 2009–2012 using angular differential imaging. Four targets in the sample had known substellar companions (HR 7329, AB Pic, HR 8799, and β Pic). No new substellar companions were discovered but eight new visual binaries were resolved. A statistical analysis of AF stars between 5–320 AU and 3–14 $M_{\rm Jup}$ implies a giant planet occurrence rate of $7.4^{+3.6}_{-2.4}$% (68% confidence level).

4.2.6. *SEEDS: Strategic Exploration of Exoplanets and Disks with Subaru*

The SEEDS survey (PI: M. Tamura) was a 125-night program on the 8.2-m Subaru Telescope targeting about 500 stars to search for giant planets and spatially resolve circumstellar disks (Tamura et al. 2009). Tamura (2016) provide an overview of the observing strategy, target samples, and main results. Observations were carried out with the HiCIAO camera behind Subaru's AO188 adaptive optics system over five years beginning in 2009. The sample contained a mixture of young stars in star-forming regions, moving groups, and open clusters; nearby stars and white dwarfs; and stars with protoplanetary disks and debris disks. Most of the observations were taken in H-band in angular differential imaging mode as well as polarimetric differential imaging for young disk-bearing stars. The ADI reduction pipeline is described in Brandt et al. (2013).

Three new substellar companions were found in SEEDS: GJ 758 B (Thalmann et al. 2009), κ And B (Carson et al. 2013), and GJ 504 b (Kuzuhara et al. 2013). The masses of GJ 504 b and κ And B may fall in the planetary regime depending on the ages and metallicities of the system, which are still under debate. Two brown dwarf companions found in the Pleiades (HD 23514 B and HII 1348 B; Yamamoto et al. 2013) had also independently been discovered by other groups. SEEDS resolved a remarkable number of protoplanetary and transition disks in polarized light— over two dozen in total — revealing previously unknown gaps, rings, and spiral structures down to 0.″1 with exceptional clarity (e.g., Thalmann et al. 2010; Hashimoto et al. 2011; Mayama et al. 2012; Muto et al. 2012).

The statistical results for debris disks are presented in Janson et al. (2013c). At the 95% confidence level, they find that <15–30% of stars host >10 $M_{\rm Jup}$ planets at the gap edge. Brandt et al. (2014a) inferred a frequency of 1.0–3.1% at the 68% confidence level for 5–70 $M_{\rm Jup}$ companions between 10–100 AU by combining results from the SEEDS moving group sample (Brandt et al. 2014c), the SEEDS disk sample (Janson et al. 2013c), the SEEDS Pleiades sample (Yamamoto et al. 2013), GDPS (Lafrenière et al. 2007b), and the NICI Campaign moving group sample (Biller et al. 2013).

4.2.7. *Gemini NICI Planet-Finding Campaign*

The Gemini NICI Planet-Finding Campaign (PI: M. Liu) was a 500-hour survey targeting about 230 young stars of all spectral classes with deep imaging using the Near-Infrared Coronagraphic Imager on the Gemini-South 8.1-m telescope (Liu et al. 2010). NICI is an imaging instrument encompassing an adaptive optics system, tapered and partly-translucent Lyot coronagraph, and dual-channel camera (Chun et al. 2008). Campaign observations spanned 2008–2012 and were carried out in two modes: single-channel H-band with angular differential imaging, and simultaneous dual-channel (CH_4S at 1.578 μm and CH_4L at 1.652 μm) angular and spectral differential imaging to maximize sensitivity to methane-dominated planets. The observing strategy and reduction pipeline are detailed in Biller et al. (2008) and Wahhaj et al. (2013a), and NICI astrometric calibration is discussed in Hayward et al. (2014).

One previously-known brown dwarf companion was resolved into a close binary, HIP 79797 Bab (Nielsen et al. 2013), and three new substellar companions were found: PZ Tel B, a highly eccentric brown dwarf companion in the β Pic moving group (Biller et al. 2010); CD-35 2722 B, a young mid-L dwarf in the AB Dor moving group (Wahhaj et al. 2011); and HD 1160 B, a substellar companion orbiting a young massive star (Nielsen et al. 2012). No new planets were discovered but β Pic b was recovered during the survey and its orbit was shown to be misaligned with the inner and outer disks (Nielsen et al. 2014; Males et al. 2014). Two debris disks surrounding HR 4796 A and HD 141569 were also resolved with unprecedented detail (Wahhaj et al. 2014; Biller et al. 2015b).

The statistical results are organized in several studies. From a sample of 80 members of young moving groups, Biller et al. (2013) measured the frequency of 1–20 $M_{\rm Jup}$ planets between 10–150 AU to be <6–18% at the 95.4% confidence level, depending on which hot-start evolutionary models are adopted. The high-mass sample of 70 B and A-type stars was described in Nielsen et al. (2013); they found that the frequency of >4 $M_{\rm Jup}$ planets between 59–460 AU is <20% at 95% confidence. Wahhaj et al. (2013b) found that <13% of debris disk stars have $\geq$5 $M_{\rm Jup}$ planets beyond 80 AU at 95% confidence from observations of 57 targets.

4.2.8. *IDPS: International Deep Planet Search*

IDPS is an expansive imaging survey carried out at the VLT with NaCo, Keck with NIRC2, Gemini-South

with NICI, and Gemini-North with NIRI targeting ≈300 young A–M stars (PI: C. Marois). This 14-year survey was mostly carried out in K band, though much of the survey comprised a mix of broad- and narrow-band near-infrared filters. Target ages were mostly $\lesssim$300 Myr and encompassed distances from ∼10–80 pc (Galicher et al. 2016, submitted).

The main result from this survey was the discovery of the HR 8799 planets (Marois et al. 2008; Marois et al. 2010b). Altogether over 1000 unique point sources were found, most of which were meticulously shown to be background stars from multi-epoch astrometry (Galicher et al. 2016, submitted). The preliminary analysis of a subset of high-mass A and F stars spanning ≈1.5–3.0 $M_{\odot}$ was presented in Vigan et al. (2012). 39 new observations in H, K, and $CH4_S$ filters were carried out in angular differential imaging mode between 2007–2012 and were combined with three high-mass targets from the literature. Stellar ages span 8–400 Myr with distances out to 90 pc and comprise a mix of young moving group members, young field stars, and debris disk hosts. The subsample of 42 massive stars includes three hosts of substellar companions: HR 8799, β Pic, and HR 7329, a β Pic moving group member with a wide brown dwarf companion (Lowrance et al. 2000). Including the detections of planets around HR 8799 and β Pic, Vigan et al. (2012) measure the occurrence rate of 3–14 $M_{\rm Jup}$ planets between 5–320 AU to be $8.7^{+10.1}_{-2.8}$% at 68% confidence.

The complete statistical analysis for the entire sample is presented in Galicher et al. (2016, submitted). They merge their own results for 292 stars with the GDPS and NaCo-LP surveys, totaling a combined sample of 356 targets. From this they infer an occurrence rate of $1.05^{+2.80}_{-0.70}$% (95% confidence interval) for 0.5–14 $M_{\rm Jup}$ planets between 20–300 AU. They do not find evidence that this frequency depends on stellar host mass. In addition, 16 of the 59 binaries resolved in IDPS are new.

4.2.9. *PALMS: Planets Around Low-Mass Stars*

The PALMS survey (PI: B. Bowler) is a deep imaging search for planets and brown dwarfs orbiting low-mass stars (0.1–0.6 $M_{\odot}$) carried out at Keck Observatory with NIRC2 and Subaru Telescope with HiCIAO. Deep coronagraphic observations were acquired for 78 single young M dwarfs in H- and Ks-bands between 2010–2013 using angular differential imaging. An additional 27 stars were found to be close binaries. Targets largely originate from Shkolnik et al. (2009), Shkolnik et al. (2012), and an additional *GALEX*-selected sample (E. Shkolnik et al., in preparation). Most of these lie within 40 pc and have ages between 20–620 Myr; about one third of the sample are members of young moving groups. The observations and PSF subtraction pipeline are described in Bowler et al. (2015b).

Four substellar companions were found in this program: 1RXS J235133.3+312720 B (Bowler et al. 2012a), GJ 3629 B (Bowler et al. 2012b), 1RXS J034231.8+121622 B (Bowler et al. 2015b), and 2MASS J15594729+4403595 B (Bowler et al. 2015b). 1RXS J235133.3+312720 B is a particularly useful benchmark brown dwarf because it orbits a member of a young moving group (AB Dor) and therefore has a well-constrained age (≈120 Myr).

The statistical results from the survey are presented in Bowler et al. (2015b). No planets were found, implying an occurrence rate of <10.3% for 1–13 $M_{\rm Jup}$ planets between 10–100 AU at the 95% confidence level assuming hot-start models and <16.0% assuming cold-start models. For the most massive planets between 5–13 $M_{\rm Jup}$, the upper limits are <6.0% and <9.9% for hot- and cold-start cooling models.

The second, parallel phase of the PALMS survey is an ongoing program targeting a larger sample of ∼400 young M dwarfs primarily at Keck with shallower contrasts (Bowler et al., in prep.). Initial discoveries include two substellar companions: 2MASS J01225093–2439505 B, an L-type member of AB Dor at the planet/brown dwarf boundary with an unusually red spectrum (Bowler et al. 2013; Hinkley et al. 2015a), and 2MASS J02155892–0929121 C (Bowler et al. 2015c), a brown dwarf in a close quadruple system which probably belongs to the Tuc-Hor moving group.

4.2.10. *NaCo-LP: VLT Large Program to Probe the Occurrence of Exoplanets and Brown Dwarfs at Wide Orbits*

The NaCo-LP survey was a Large Program at the VLT focused on 86 young, bright, primarily FGK stars (PI: J.-L. Beuzit). H-band observations were carried out with NaCo in ADI mode between 2009–2013 (Chauvin et al. 2015). The target sample is described in detail in Desidera et al. (2015); stars were chosen to be single, have ages $\lesssim$200 Myr, and lie within 100 pc. Many of these stars were identified as new members of young moving groups.

Although no new substellar companions were discovered, an intriguing white dwarf was found orbiting HD 8049, an ostensibly young K2 star that may instead be much older due to mass exchange with its now evolved companion (Zurlo et al. 2013). New observations of the spatially resolved debris disk around HD 61005 ("the Moth") were presented by Buenzli et al. (2010), and 11 new close binaries were resolved during this program (Chauvin et al. 2015).

The statistical analysis of the sample of single stars was performed in Chauvin et al. (2015). Based on a subsample of 51 young FGK stars, they found that <15% of Sun-like stars host planets with masses >5 $M_{\rm Jup}$ between 100–500 AU and <10% host >10 $M_{\rm Jup}$ planets between 50–500 AU at the 95% confidence level. Reggiani et al. (2016) use these NaCo-LP null results together with additional deep archival observations to study the companion mass function as it relates to binary star formation and planet formation. From their full sample of 199 Sun-like stars, they find that the results from direct imaging are consistent with the superposition of the planet mass function determined from radial velocity surveys and the stellar companion mass ratio distribution down to 5 $M_{\rm Jup}$, suggesting that many planetary-mass companions uncovered with direct imaging may originate from the tail of the brown dwarf mass distribution instead of being the most massive representatives of the giant planet population.

4.3. *Other First Generation Surveys*

Several smaller, more focused surveys have also been carried out with angular differential imaging: Apai et al.

2008 targeted 8 debris disk hosts with NaCo using simultaneous differential imaging; Ehrenreich et al. (2010) imaged 38 high-mass stars primarily with NaCo; Janson et al. (2011a) observed 15 B and A stars with NIRI; Delorme et al. (2012) presented observations of 16 young M dwarfs in L'-band with NaCo; Maire et al. (2014) targeted 16 young AFGK stars with NaCo's four-quadrant phase mask, simultaneous differential imaging, and angular differential imaging; Meshkat et al. (2015a) used NaCo's Apodizing Phase Plate coronagraph in L' band to image six young debris disk hosts with gaps as part of the Holey Debris Disk survey; and Meshkat et al. (2015b) also used the APP at NaCo to image a sample of 13 A- and F-type main sequence stars in search of planets, uncovering a probable brown dwarf around HD 984 (Meshkat et al. 2015c). The Lyot Project is another survey with important contributions for its early use of coronagraphy behind an extreme adaptive optics system (Oppenheimer et al. 2004). This survey was carried out at the 3.6-m AEOS telescope equipped with a 941-actuator deformable mirror and targeted 86 nearby bright stars using angular differential imaging (Leconte et al. 2010).

4.4. *The Second Generation: Extreme Adaptive Optics, Exceptional Strehl Ratios, and Optimized Integral Field Units*

The transition to second-generation planet-finding instruments began over the past few years. This new era is characterized by regular implementation of high-order ("extreme") adaptive optics systems with thousands of actuators and exceptionally low residual wavefront errors; pyramid wavefront sensors providing better sensitivity and higher precision wavefront correction; Strehl ratios approaching (and often exceeding) 90% at near-infrared wavelengths; high-contrast integral field units designed for on-axis observations enabling speckle subtraction and low-resolution spectroscopy; sensitivity to smaller inner working angles than first-generation instruments; and advanced coronagraphy.

4.4.1. *Project 1640*

Project 1640 is a large ongoing survey (PI: R. Oppenheimer) and high-contrast imaging instrument with the same name located behind the PALM-3000 second-generation adaptive optics system at the Palomar Observatory 200-inch (5.1-meter) Hale Telescope. The instrument itself contains an apodized-pupil Lyot coronagraph and integral field unit that samples 32 spectral channels across Y, J, and H bands (Hinkley et al. 2011), producing a low-resolution spectrum to broadly characterize the physical properties of faint companions (Roberts et al. 2012; Rice et al. 2015). The survey consists of two phases, the first (now concluded) with the original Palomar Adaptive Optics System (PALM-241; Troy et al. 2000) and a second ongoing three-year program focusing on nearby massive stars with the upgraded PALM-3000 adaptive optics system (Dekany et al. 2013). The data reduction pipeline is described in Zimmerman et al. (2011) and a detailed treatment of speckle subtraction, precision astrometry, and robust spectrophotometry can be found in Crepp et al. (2011), Pueyo et al. (2012), Oppenheimer et al. (2013), Fergus et al. (2014), and Pueyo et al. (2015).

Results from the Project 1640 survey include several discoveries of faint stellar companions to massive A stars (Zimmerman et al. 2010; Hinkley et al. 2010) and follow-up astrometric and spectral characterization of known substellar companions (Crepp et al. 2015; Hinkley et al. 2013). In addition, Oppenheimer et al. (2013) and Pueyo et al. (2015) presented detailed spectroscopic and astrometric analysis of the HR 8799 planets and found intriguing evidence for mutually dissimilar spectral properties and signs of non-coplanar orbits.

4.4.2. *LEECH: LBTI Exozodi Exoplanet Common Hunt*

LEECH is an ongoing ∼70-night high-contrast imaging program (PI: A. Skemer) at the twin 8.4-m Large Binocular Telescope. Survey observations began in 2013 and are carried out in angular differential imaging mode in L'-band with LMIRcam utilizing deformable secondary mirrors to maximize sensitivity at mid-IR wavelengths by limiting thermal emissivity from warm optics (Skemer et al. 2014b). The target sample focuses on intermediate-age stars <1 Gyr including members of the ∼500 Myr Ursa Majoris moving group, massive BA stars, and nearby young FGK stars.

In addition to searching for new companions, this survey is also characterizing known planets using the unique mid-IR instrumentation, sensitivity, and filter suite at the LBT. Maire et al. (2015b) refined the orbits of the HR 8799 planets and found them to be consistent with 8:4:2:1 mean motion resonances. Skemer et al. (2016) observed GJ 504 b in three narrow-band filters spanning 3.7–4.0 μm. Model fits indicate an exceptionally low effective temperature of ≈540 K and enhanced metallicity, possibly pointing to an origin through core accretion. Additionally, Schlieder et al. (2016) presented LEECH observations and dynamical mass measurements the Ursa Majoris binary NO UMa. Recently the integral field unit Arizona Lenslets for Exoplanet Spectroscopy (ALES; Skemer et al. 2015) was installed inside LMIRcam and will enable integral-field spectroscopy of planets between 3–5 μm for the first time.

4.4.3. *GPIES: Gemini Planet Imager Exoplanet Survey*

GPIES is an ongoing 890-hour, 600-star survey to image extrasolar giant planets and debris disks with the Gemini Planet Imager at Gemini-South (PI: B. Macintosh). GPI is expressly built to image planets at small inner working angles; its high-order adaptive optics system incorporates an apodized pupil Lyot coronagraph, integral field spectrograph, imaging polarimeter, and (imminent) non-redundant masking capabilities (Macintosh et al. 2014). Survey observations targeting young nearby stars began in 2014 and will span three years.

Macintosh et al. (2015) presented the discovery of 51 Eri b, the first exoplanet found in GPIES and the lowest-mass planet imaged in thermal emission to date. This remarkable young, methanated T dwarf has a contrast of 14.5 mag in H-band at a separation of $0\farcs45$, which translates into a mass of only 2 $M_{\rm Jup}$ at 13 AU assuming hot-start cooling models. It is also the only imaged planet consistent with the most pessimistic cold-start evolutionary models, in which case its mass may be as high as 12 $M_{\rm Jup}$. De Rosa et al. (2015) obtained follow-up observations with GPI and showed that 51 Eri b shares a com-

mon proper motion with its host and exhibits slight (but significant) orbital motion. Other initial results from this survey include astrometry and a refined orbit for β Pic b (Macintosh et al. 2014), as well as resolved imaging of the debris disks around HD 106906 (Kalas et al. 2015) and HD 131835 (Hung et al. 2015).

4.4.4. *SPHERE GTO Survey*

SPHERE (Spectro-Polarimetric High-contrast Exoplanet Research) is an extreme adaptive optics system (SAXO) and versatile instrument for high-contrast imaging and spectroscopy at the VLT with a broad range of capabilities (Beuzit et al. 2008). IRDIS (Dohlen et al. 2008) offers classical and dual-band imaging (Vigan et al. 2010), dual-polarization imaging (Langlois et al. 2014), and long-slit spectroscopy (Vigan et al. 2008); IFS provides low-resolution (R∼30–50) integral field spectroscopy spanning 0.95–1.65 μm (Claudi et al. 2008); and ZIMPOL enables diffraction-limited imaging and polarimetry in the optical (Thalmann et al. 2008). As part of a guaranteed time observing program, the SPHERE GTO team is carrying out a large ongoing survey (PI: J.-L. Beuzit) with a range of science goals. About 200 nights of this time are devoted to a deep near-infrared imaging survey (SHINE: SpHere Infrared survEy) to search for and characterize exoplanets around 400–600 stars, while the remaining ∼60 nights will be used for a broad range of science including spatially-resolved observations of circumstellar disks and optical imaging of planets.

Initial results from the SHINE survey include observations of the brown dwarf GJ 758 B (Vigan et al. 2016), PZ Tel B and HD 1160 B (Maire et al. 2016), HD 106906 (Lagrange et al. 2016), and the HR 8799 planets (Zurlo et al. 2016; Bonnefoy et al. 2016). Other results have focused on resolved imaging of the debris disk surrounding HD 61005, which may be a product of a recent planetesimal collision (Olofsson et al. 2016), and HD 135344 B, host of a transition disk with striking spiral arm structure (Stolker et al. 2016). Boccaletti et al. (2015) uncovered intriguing and temporally evolving features in AU Mic's debris disk. In addition, Garufi et al. (2016) presented deep IRDIS near-infrared images and visible ZIMPOL polarimetric observations of HD 100546 revealing a complex disk environment with considerable structure and resolved K-band emission at the location of the candidate protoplanet HD 100546 b.

4.4.5. *Other Second Generation Instruments and Surveys*

A number of other novel instruments and forthcoming surveys bear highlighting. MagAO (PI: L. Close) at the Magellan 6.5-m Clay telescope is a versatile adaptive optics system consisting of a 585-actuator adaptive secondary mirror, pyramid wavefront sensor, and two science cameras offering simultaneous diffraction-limited imaging spanning the visible (0.6–1.05 μm) with VisAO and near-infrared (1–5.3 μm) with Clio2 (Close et al. 2012; Morzinski et al. 2014; Morzinski et al. 2015). Strehl ratios of ∼20–30% in the optical are opening up new science fronts including deep red-optical observations of exoplanets (Males et al. 2014; Wu et al. 2015), characterization of accreting protoplanets in Hα (Sallum et al. 2015a), and high spatial resolution imaging down to ∼20 mas (Close et al. 2013). Vector apodizing phase plate coronagraphs were recently installed in MagAO and other upgrades such as an optical integral field unit are possible in the future.

Subaru Coronagraphic Extreme Adaptive Optics (SCExAO; PI: O. Guyon) is being built for the Subaru telescope and is the newest extreme adaptive optics system on a large telescope. A detailed description of all facets of this instrument is described in Jovanovic et al. (2015). In short, a pyramid wavefront sensor is coupled with a 2000-element deformable mirror to produce Strehl ratios in excess of 90%. The instrument is particularly flexible, allowing for a variety of setups and instrument subcomponents including speckle nulling to suppress static and slowly changing speckles (Martinache et al. 2014), a near-infrared science camera (currently HiCIAO), sub-diffraction-limited interferometric science in the visible with VAMPIRES (Norris et al. 2015) and FIRST (Huby et al. 2012), high-contrast integral field spectroscopy (Brandt et al. 2014b), and coronagraphy with phase-induced amplitude apodization (Guyon 2003) and vector vortex coronagraphs (Mawet et al. 2010).

4.5. *The Occurrence Rate of Giant Planets on Wide Orbits: Meta-Analysis of Imaging Surveys*

The frequency and mass-period distribution of planets spanning various orbital distances, stellar host masses, and system ages provides valuable clues about the dominant processes shaping the formation and evolution of planetary systems. These measurements are best addressed with large samples and uniform statistical analyses. Nielsen et al. (2008) carried out the first such large-scale study based on adaptive optics imaging surveys from Biller et al. (2007) and Masciadri et al. (2005). From their sample of 60 unique stars they found an upper limit of 20% for >4 $M_{\rm Jup}$ planets between 20–100 AU at the 95% confidence level. This was expanded to 118 targets in Nielsen & Close (2010) by including the GDPS survey of Lafrenière et al. (2007b), resulting in the same upper limit and planet mass regime but for a broader range of separations of 8–911 AU at 68% confidence. Vigan et al. (2012) and Rameau et al. (2013a) combined their own observations of high-mass stars with previous surveys and measured occurrence rates of $8.7^{+10.1}_{-2.8}$% (for 3–14 $M_{\rm Jup}$ planets between 5–320 AU) and $16.1^{+8.7}_{-5.3}$% (for 1–13 $M_{\rm Jup}$ planets between 1–1000 AU), respectively. Brandt et al. (2014a) incorporated the SEEDS, GDPS, and the NICI moving group surveys and found a frequency of 1.0–3.1% for 5–70 $M_{\rm Jup}$ companions between 10–100 AU. Recently, Galicher et al. (2016, submitted) combined results from IDPS, GDPS, and the NaCo Survey of Young Nearby Austral Stars and found an occurrence rate of $1.05^{+2.80}_{-0.70}$% for 0.5–14 $M_{\rm Jup}$ companions between 20–300 AU based on a sample of 356 unique stars. Breaking this into stellar mass bins did not reveal any signs of a trend with stellar host mass.

Here I reexamine the occurrence rate of giant planets with a meta-analysis of the largest and deepest high-contrast imaging surveys. 696 contrast curves are assembled from the literature from the programs outlined in Section 4.2. For stars with more than one observation, the deeper contrast curve at 1″ is chosen. Targets with stellar companions within 100 AU are removed from the sample because binaries can both inhibit planet for-

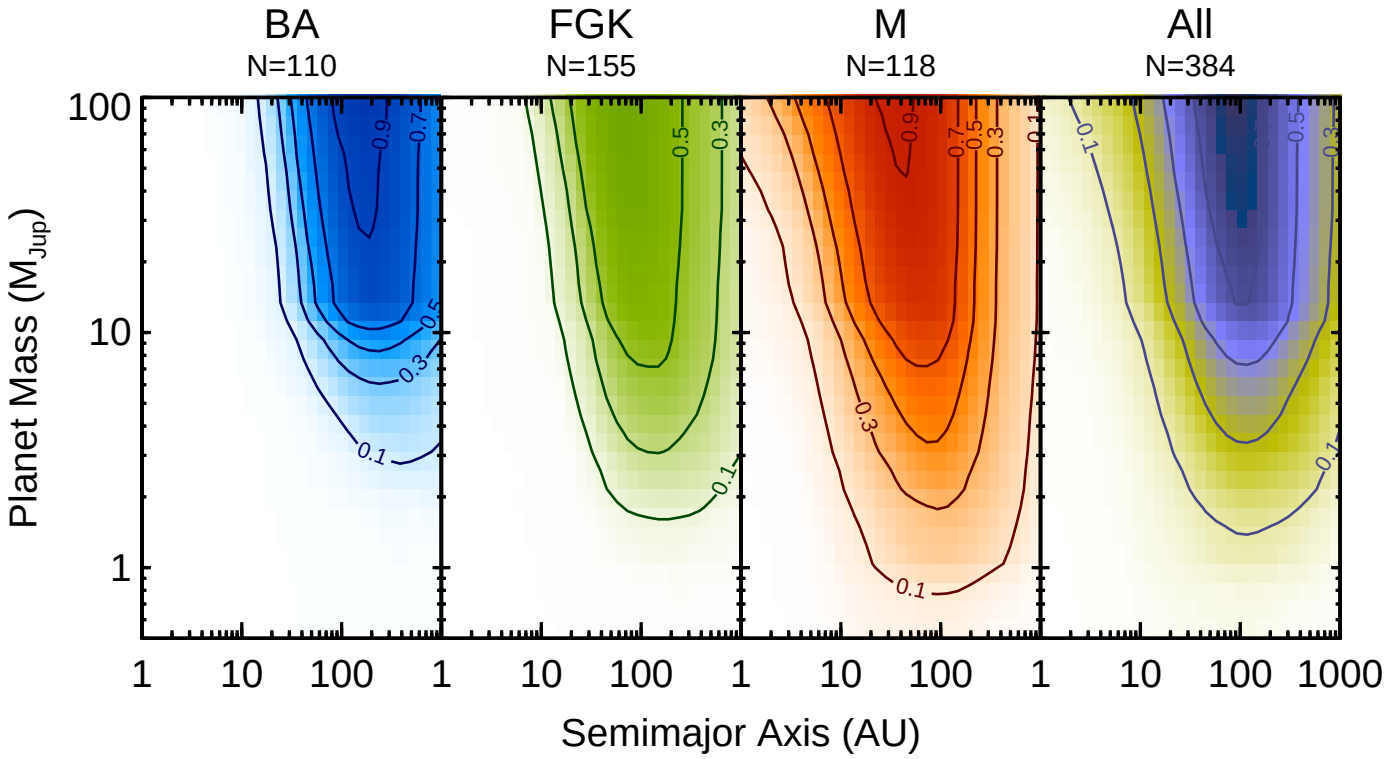

FIG. 11.— Mean sensitivity maps from a meta-analysis of 384 unique stars with published high-contrast imaging observations. M dwarfs provide the highest sensitivities to lower planet masses in the contrast-limited regime. Altogether, current surveys probe the lowest masses at separations of ∼30–300 AU. Contours denote 10%, 30%, 50%, 70%, and 90% sensitivity limits.

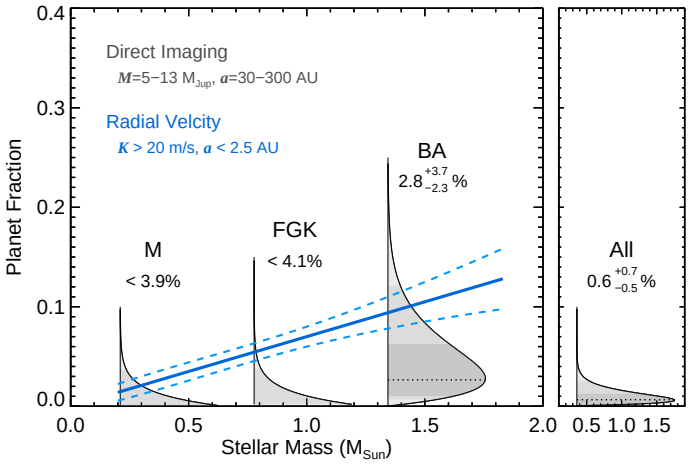

FIG. 12.— Probability distributions for the occurrence rate giant planets from a meta-analysis of direct imaging surveys in the literature. $2.8^{+3.7}_{-2.3}$% of BA stars, <4.1% of FGK stars, and <3.9% of M dwarfs harbor giant planets between 5–13 $M_{\rm Jup}$ and 30–300 AU. The correlation between stellar host mass and giant planet frequency at small separations (<2.5 AU) from Johnson et al. (2010) is shown in blue. Larger sample sizes are needed to discern any such correlation on wide orbits. $0.6^{+0.7}_{-0.5}$% of stars of any mass host giant planets over the same mass and separation range.

mation and dynamically disturb planetary orbits. Most candidate planets uncovered during these surveys are rejected as background stars from second epoch observations, but some candidates are either not recovered or are newly revealed in follow-up data. Because of finite telescope allocation, some of these candidates remain untested for common proper motion. These ambiguous candidates cannot be ignored in a statistical analysis because one (or more) could be indeed be bound. In these cases, contrast curves are individually truncated one standard deviation above the brightest candidate. Ages are taken from the literature except for members of young moving groups, for which the most recent (and systematically older) ages of young moving groups from Bell et al. (2015) are adopted. Most ages in the sample are less than 300 Myr and within 100 pc. Altogether this leaves 384 unique stars spanning B2–M6 spectral types: 76 from Bowler et al. (2015b), 72 from Biller et al. (2013), 61 from Nielsen et al. (2013), 54 from Lafrenière et al. (2007b), 45 from Brandt et al. (2014c), 30 from Janson et al. (2013c), 25 from Vigan et al. (2012), 14 from Wahhaj et al. (2013b), and 7 from Janson et al. (2011a).

Sensitivity maps and planet occurrence rates are derived following Bowler et al. (2015b). For a given planet mass and semimajor axis, a population of artificial planets on random circular orbits are generated in a Monte Carlo fashion and converted into apparent magnitudes and separations using Cond hot-start evolutionary models from Baraffe et al. (2003), the age of the host star, and the distance to the system, including uncertainties in age and distance. These are compared with the measured contrast curve to infer the fractional sensitivity at each grid point spanning 30 logarithmically-uniform bins in mass and separation between 1–1000 AU and 0.5–100 $M_{\rm Jup}$. When available, fractional field of view coverage is taken into account. Contrasts measured in CH_4S filters are converted to H-band using an empir-

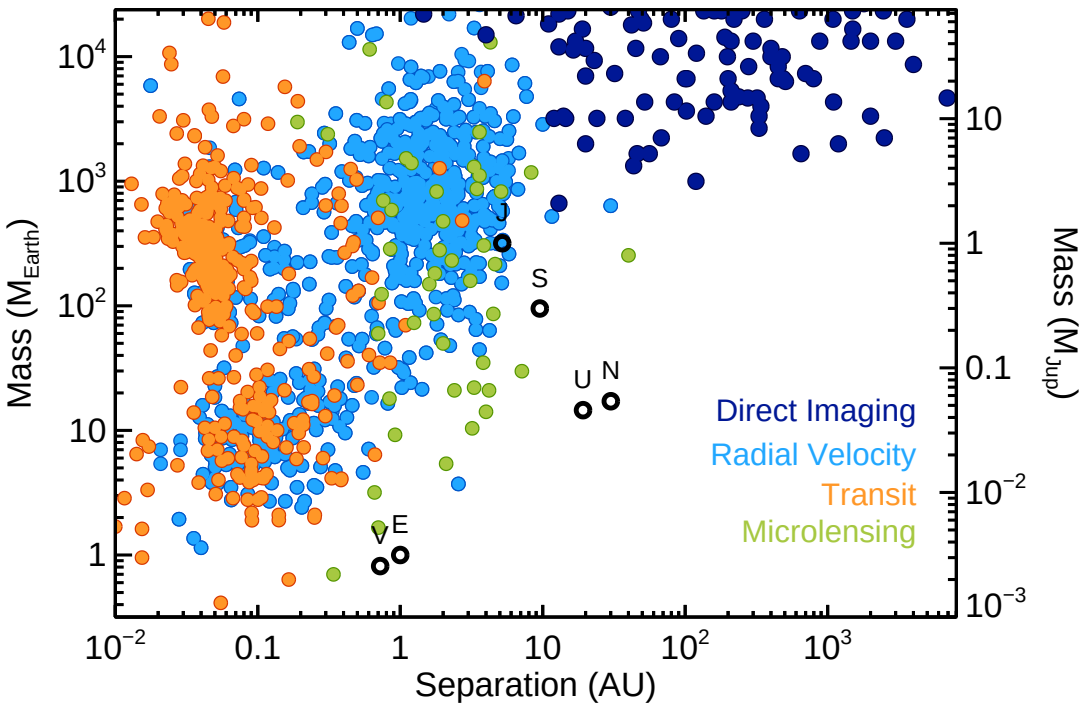

FIG. 13.— The demographics of exoplanets from direct imaging (dark blue), radial velocity (light blue), transit (orange), and microlensing (green) surveys. Planets detected with radial velocities are minimum masses. It remains unclear whether imaged planets and brown dwarfs represent distinct populations or whether they form a continuous distribution down to the fragmentation limit. Directly imaged substellar companions are compiled from the literature, while planets found with other methods are from exoplanets.eu as of April 2016.

ical color-spectral type relationship based on synthetic colors of ultracool dwarfs from the SpeX Prism Library (Burgasser 2014) as well as the spectral type-effective temperature sequence from Golimowski et al. (2004a)[5].

The mean sensitivity maps for all 384 targets and separate bins containing BA stars (110 targets), FGK stars (155 targets), and M dwarfs (118 targets) are shown in Figure 11. In general, surveys of high-mass stars probe higher planet masses than deep imaging around M dwarfs owing to differences in the host stars' intrinsic luminosities. The most sensitive region for all stars is between ∼30–300 AU, with less coverage at extremely wide separations because of limited fields of view and at small separations in contrast-limited regimes.

The occurrence rate of giant planets for all targets and for each stellar mass bin are listed in Table 3, which assumes logarithmically-uniform distributions in mass and separation (see Section 6.5 of Bowler et al. 2015b for details). The mode and 68.3% minimum credible interval (also known as the highest posterior density interval) of the planet frequency probability distribution are reported. Two massive stars in the sample host planets that were either discovered or successfully recovered in these surveys: β Pic, with a planet at 9 AU, and HR 8799, with planets spanning 15–70 AU. HR 8799 is treated as a single detection. The most precise occurrence rate measurement is between 5–13 $M_{\rm Jup}$ and 30–300 AU. Over these ranges, the frequency of planets orbiting BA, FGK, and M stars is $2.8^{+3.7}_{-2.3}$%, <4.1%, and <3.9%, respectively (Figure 12). Here upper limits are 95% confidence intervals. Although there are hints of a higher giant planet occurrence rate around massive stars analogous to the well-established correlation at small separations (Johnson et al. 2007; Lovis & Mayor 2007; Johnson et al. 2010; Bowler et al. 2010b), this trend is not yet statistically significant at wide orbital distances and requires larger sample sizes in each stellar mass bin to unambiguously test this correlation. Marginalizing over stellar host mass, the overall giant planet occurrence rate for the full sample of 384 stars is $0.6^{+0.7}_{-0.5}$%, which happens to be comparable to the frequency of hot Jupiters around FGK stars in the field (1.2 ± 0.4%; Wright et al. 2012) and in the *Kepler* sample (0.5 ± 0.1%; Howard et al. 2012). However, compared to the high occurrence rate of giant planets (0.3–10 $M_{\rm Jup}$) with orbital periods out to 2000 days (∼10%; Cumming et al. 2008), massive gas giants are clearly quite rare at wide orbital distances.

5. BROWN DWARFS, GIANT PLANETS, AND THE COMPANION MASS FUNCTION

Direct imaging has shown that planetary-mass companions exist at unexpectedly wide separations but the provenance of these objects remains elusive. There is substantial evidence that the tail-end of the star formation process can produce objects extending from low-mass stars at the hydrogen burning limit (≈75 $M_{\rm Jup}$) to brown dwarfs at the opacity limit for fragmenta-

[5] Synthesized colors of ultracool dwarfs using the Keck/NIRC2 CH_4S and $H_{\rm MKO}$ filter profiles yields the following relation: CH_4S–$H_{\rm MKO}$ = $\sum_{i=0}^{4} c_i {\rm SpT}^i$, where c_0=0.03913178, c_1=0.008678245, c_2=–0.001542768, c_3=0.0001033761, c_4=–2.902588×10^{-6}, and SpT is the numerical near-infrared spectral type (M0=1.0, L0=10.0, T0=20.0). This relation is valid from M3–T8 and the rms of the fit is 0.025 mag. Golimowski et al. (2004a) provide an empirical $T_{\rm eff}$(SpT) relationship, but the inverse SpT($T_{\rm eff}$) is necessary for this filter conversion at a given mass and age. Refitting the same data from Golimowski et al. yields the following: SpT = $\sum_{i=0}^{4} c_i {T_{\rm eff}}^i$, where c_0=36.56779, c_1=–0.004666549, c_2=–9.872890×10^{-6}, c_3=4.108142×10^{-09}, c_4=– 4.854263×10^{-13}. This is valid for 700 K < $T_{\rm eff}$ < 3900 K, the rms is 1.89 mag, and SpT is the same numerical near-infrared spectral type as above.

tion (≈5–10 $M_{\rm Jup}$), which corresponds to the minimum mass of a pressure-supported fragment during the collapse of a molecular cloud core (Low & Lynden-Bell 1976; Silk 1977; Boss 2001; Bate et al. 2002; Bate 2009). Indeed, isolated objects with inferred masses below 10 $M_{\rm Jup}$ have been found in a range of contexts over the past decade: in star-forming regions (Lucas et al. 2001; Luhman et al. 2009a; Scholz et al. 2012; Muzic et al. 2015), among closer young stellar associations (Liu et al. 2013; Gagné et al. 2015a; Kellogg et al. 2016; Schneider et al. 2016), and at much older ages as Y dwarfs in the field (Cushing et al. 2011; Kirkpatrick et al. 2012; Beichman et al. 2013). Similarly, several systems with *companions* below ≈10 $M_{\rm Jup}$ are difficult to explain with any formation scenario other than cloud fragmentation: 2M1207–3932 Ab is a ∼25 $M_{\rm Jup}$ brown dwarf with a ∼5 $M_{\rm Jup}$ companion at an orbital distance of 40 AU (Chauvin et al. 2004) and 2M0441+2301 AabBab is a quadruple system comprising a low-mass star, two brown dwarfs, and a 10 $M_{\rm Jup}$ object in a hierarchical and distinctly non-planetary configuration (Todorov et al. 2010).

From the radial velocity perspective, the distribution of gas giant minimum masses is generally well-fit with a decaying power law (Butler et al. 2006; Johnson 2009; Lopez & Jenkins 2012) or exponential function (Jenkins et al. 2016) that tapers off beyond ∼10 $M_{\rm Jup}$. This is evident in Figure 13, although inhomogeneous radial velocity detection biases which exclude lower-mass planets at wide separations are not taken into account. The dominant formation channel for this population of close-in giant planets is thought to be core accretion plus gas capture, in which growing cores reach a critical mass and undergo runaway gas accretion (e.g., Helled et al. 2013).

The totality of evidence indicates that the decreasing brown dwarf companion mass function almost certainly overlaps with the the rising giant planet mass function in the 5–20 $M_{\rm Jup}$ mass range. No strict mass cutoff can therefore unambiguously divide giant planets from brown dwarfs, and many of the imaged companions below 13 $M_{\rm Jup}$ listed in Table 1 probably originate from the dwindling brown dwarf companion mass function.

Another approach to separate these populations is to consider formation channel: planets originate in disks while brown dwarfs form like stars from the gravitational collapse of molecular cloud cores. However, not only are the relic signatures of formation difficult to discern for individual discoveries, but objects spanning the planetary up to the stellar mass regimes may also form in large Toomre-unstable circumstellar disks at separations of tens to hundreds of AU (e.g., Durisen et al. 2007; Kratter & Lodato 2016). Any binary narrative based on origin in a disk versus a cloud core is therefore also problematic. Furthermore, both giant planets and brown dwarf companions may migrate, dynamically scatter, or undergo periodic Kozai-Lidov orbital oscillations if a third body is present, further mixing these populations and complicating the interpretation of very low-mass companions uncovered with direct imaging.

The deuterium-burning limit at ≈13 $M_{\rm Jup}$ is generally acknowledged as a nebulous, imperfect, and ultimately artificial division between brown dwarfs and giant planets. Moreover, this boundary is not fixed and may depend on planet composition, core mass, and accretion history (Spiegel et al. 2011; Bodenheimer et al. 2013; Mordasini 2013). Uncertainties in planet luminosities, evolutionary histories, metallicities, and ages can also produce large systematic errors in inferred planet masses (see Section 3), rendering inconsequential any sharp boundary set by mass. However, despite these shortcomings, this border lies in the planet/brown dwarf "mass valley" and may still serve as a pragmatic (if flawed) qualitative division between two populations formed *predominantly* with their host stars and *predominantly* in protoplanetary disks.

Observational tests of formation routes will eventually provide the necessary tools to understand the relationship between these populations. This can be carried out at an individual level with environmental clues such as coplanarity of multi-planet systems or orbital alignment within a debris disk; enhanced metallicities or abundance ratios relative to host stars (Oberg et al. 2011); or overall system orbital architecture. Similarly, the statistical properties of brown dwarfs and giant planets can be used to identify dominant formation channels: the separation distribution of objects formed through cloud fragmentation should resemble that of binary stars; disk instability and core accretion may result in a bimodal period distribution for giant planets (Boley 2009); planet scattering to wide orbits should produce a rising mass function at low planet masses as opposed to a truncated mass distribution at the fragmentation limit for cloud fragmentation and disk instability; and the companion mass function and mass ratio distribution are expected to smoothly extend from low-mass stars down to the fragmentation limit if a common formation channel in at play (Brandt et al. 2014a; Reggiani et al. 2016). Testing these scenarios will require much larger sample sizes given the low occurrence rates uncovered in direct imaging surveys.

6. CONCLUSIONS AND FUTURE OUTLOOK

High-contrast imaging is still in its nascence. Radial velocity, transit, and microlensing surveys have unambiguously demonstrated that giant planets are much rarer than super-Earths and rocky planets at separations $\lesssim$10 AU. In that light, the discovery of truly massive planets at tens, hundreds, and even thousands of AU with direct imaging is fortuitous, even if the overall occurrence rate of this population is quite low. Each detection technique has produced many micro paradigm shifts over the past twenty years that disrupt and rearrange perceptions about the demographics and architectures of planetary systems. Hot Jupiters, correlations with stellar mass and metallicity, the ubiquity of super-Earths, compact systems of small planets, resonant configurations, orbital misalignments, the prevalence of habitable-zone Earth-sized planets, circumbinary planets, and featureless clouds and hazes are an incomplete inventory within just a few AU (e.g., Winn & Fabrycky 2015). The most important themes to emerge from direct imaging are that massive planets exist but are uncommon at wide separations (>10 AU), and at young ages the low-gravity atmospheres of giant planets do not resemble those of older, similar-temperature brown dwarfs.

There are many clear directions forward in this field. Deeper contrasts and smaller inner working angles will probe richer portions of planetary mass-

and separation distributions. Thirty meter-class telescopes with extreme adaptive optics systems will regularly probe sub-Jovian masses at separations down to 5 AU. This next generation will uncover more planets and enable a complete mapping of the evolution of giant planet atmospheres over time. Other fertile avenues for high-contrast imaging include precise measurements of atmospheric composition (Konopacky et al. 2013; Barman et al. 2015), doppler imaging (Crossfield 2014; Crossfield et al. 2014), photometric monitoring to map variability of rotationally-modulated features (e.g., Apai et al. 2016), synergy with other detection methods (e.g., Lagrange et al. 2013; Sozzetti et al. 2013; Montet et al. 2014; Clanton & Gaudi 2016), advances in stellar age-dating at the individual and population levels, merging high-contrast imaging with high-resolution spectroscopy (Snellen et al. 2014; Snellen et al. 2015), surveying the companion mass function to sub-Jovian masses, polarimetric observations of photospheric clouds (e.g., Marley et al. 2013; Jensen-Clem et al. 2016), statistical correlations with stellar host properties, probing the earliest stages of protoplanet assembly (Kraus & Ireland 2012; Sallum et al. 2015a), astrometric orbit monitoring and constraints on dynamical histories, and robust dynamical mass measurements to test evolutionary models and probe initial conditions (e.g., Dupuy et al. 2009; Crepp et al. 2012a). High-contrast imaging has a promising future and will play an ever-growing role in investigating the architecture, atmospheres, and origin of exoplanets.

It is a pleasure to thank the referee, Rebecca Oppenheimer, as well as Lynne Hillenbrand, Dimitri Mawet, Sasha Hinkley, and Trent Dupuy for their thoughtful comments and constructive feedback on this review. Michael Liu, Arthur Vigan, Christian Marois, Motohide Tamura, Gaël Chauvin, Andy Skemer, Adam Kraus, and Bruce Macintosh contributed helpful suggestions on past and ongoing imaging surveys. Bruce Macintosh, Eric Nielsen, Andy Skemer, and Raphaël Galicher kindly provided images for Figure 9. Trent Dupuy generously shared his compilation of late-T and Y dwarfs used in Figure 7. This research has made use of the Exoplanet Orbit Database, the Exoplanet Data Explorer at exoplanets.org, and the SpeX Prism Spectral Libraries maintained by Adam Burgasser. NASA's Astrophysics Data System Bibliographic Services together with the VizieR catalogue access tool and SIMBAD database operated at CDS, Strasbourg, France, were invaluable resources for this work.

REFERENCES

Absil, O., & Mawet, D. 2009, Astron Astrophys Rev, 18, 317
Absil, O., Le Bouquin, J.-B., Berger, J.-P., et al. 2011, A&A, 535, A68
Absil, O., Milli, J., Mawet, D., et al. 2013, A&A, 559, L12
Ahmic, M., Jayawardhana, R., Brandeker, A., et al. 2007, The Astrophysical Journal, 671, 2074
Allard, F., Homeier, D., & Freytag, B. 2012, Philosophical Transactions of the Royal Society A: Mathematical, Physical and Engineering Sciences, 370, 2765
Allers, K. N., & Liu, M. C. 2013, The Astrophysical Journal, 772, 79
Allers, K. N., Liu, M. C., Dupuy, T. J., & Cushing, M. C. 2010, The Astrophysical Journal, 715, 561
Amara, A., & Quanz, S. P. 2012, Monthly Notices RAS, 427, 948
Anderson, E., & Francis, C. 2012, Astronomy Letters, 38, 331
Andrews, S. M. 2015, Publications of the Astronomical Society of the ...
Andrews, S. M., Rosenfeld, K. A., Kraus, A. L., & Wilner, D. J. 2013, ApJ, 771, 129
Apai, D., Janson, M., Moro-Martín, A., et al. 2008, The Astrophysical Journal, 672, 1196
Apai, D., Kasper, M., Skemer, A., et al. 2016, ApJ, 820, 1
Artigau, E., Gagné, J., Faherty, J., et al. 2015, ApJ, 806, 1
Aumann, H. H. 1985, Publ. Astron. Soc. Pac., 97, 885
Aumann, H. H., Beichman, C. A., Gillet, F. C., et al. 1984, Astrophys. J., 278, L23
Backman, D., Marengo, M., & Stapelfeldt, K. 2009, The Astrophysical ...
Bailey, J. 2014, Publications of the Astronomical Society of Australia, 31, e043
Bailey, V., Meshkat, T., Reiter, M., et al. 2014, The Astrophysical Journal, 780, L4
Baraffe, I., Chabrier, G., Allard, F., & Hauschildt, P. H. 2002, A&A, 382, 563
Baraffe, I., Chabrier, G., Barman, T. S., Allard, F., & Hauschildt, P. H. 2003, A&A, 402, 701
Baraffe, I., Homeier, D., Allard, F., & Chabrier, G. 2015, arXiv, 1503.04107v1
Barenfeld, S. A., Bubar, E. J., Mamajek, E. E., & Young, P. A. 2013, The Astrophysical Journal, 766, 6
Barman, T. S., Konopacky, Q. M., Macintosh, B., & Marois, C. 2015, ApJ, 804, 1
Barman, T. S., Macintosh, B., Konopacky, Q. M., & Marois, C. 2011a, The Astrophysical Journal, 733, 65
—. 2011b, The Astrophysical Journal, 735, L39
Basri, G., & Brown, M. E. 2006, Annual Review of Earth and Planetary Sciences, 34, 193
Bate, M. R. 2009, Monthly Notices RAS, 392, 590
Bate, M. R., Bonnell, I. A., & Bromm, V. 2002, Monthly Notices RAS, 332, L65
Beichman, C., Gelino, C. R., Kirkpatrick, J. D., et al. 2013, ApJ, 764, 101
—. 2014, ApJ, 783, 68
Bell, C. P. M., Mamajek, E. E., & Naylor, T. 2015, Monthly Notices RAS, 454, 593
Benedict, G. F., McArthur, B. E., Gatewood, G., et al. 2006, The Astronomical Journal, 132, 2206
Benest, D., & Duvent, J. L. 1995, A&A, 299, 621
Bergfors, C., Brandner, W., Janson, M., Köhler, R., & Henning, T. 2011, A&A, 528, A134
Beust, H., Augereau, J.-C., Bonsor, A., et al. 2014, A&A, 561, A43
Beuzit, J.-L., Mouillet, D., Oppenheimer, B. R., & Monnier, J. D. 2007, Protostars and Planets V, 717
Beuzit, J.-L., Ségransan, D., Forveille, T., et al. 2004, A&A, 425, 997
Beuzit, J.-L., Feldt, M., Dohlen, K., et al. 2008, 7014, 701418
Biller, B., Allers, K., Liu, M., Close, L. M., & Dupuy, T. 2011, The Astrophysical Journal, 730, 39
Biller, B., Artigau, É., Wahhaj, Z., et al. 2008, Proc. SPIE, 7015, 70156Q
Biller, B., Lacour, S., Juhász, A., et al. 2012, The Astrophysical Journal Letters, 753, L38
Biller, B. A., Close, L. M., Masciadri, E., et al. 2007, The Astrophysical Journal Supplement Series, 173, 143
Biller, B. A., Liu, M. C., Wahhaj, Z., et al. 2010, The Astrophysical Journal, 720, L82
—. 2013, ApJ, 777, 160
Biller, B. A., Males, J., Rodigas, T., et al. 2014, The Astrophysical Journal Letters, 792, L22
Biller, B. A., Vos, J., Bonavita, M., et al. 2015a, The Astrophysical Journal Letters, 813, 1
Biller, B. A., Liu, M. C., Rice, K., et al. 2015b, Monthly Notices RAS, 450, 4446

Binks, A. S., & Jeffries, R. D. 2014, MNRAS Letters, 438, L11
Binks, A. S., Jeffries, R. D., & Maxted, P. F. L. 2015, Monthly Notices RAS, 452, 173
Boccaletti, A., Lagrange, A.-M., Bonnefoy, M., Galicher, R., & Chauvin, G. 2013, A&A, 551, L14
Boccaletti, A., Thalmann, C., Lagrange, A.-M., et al. 2015, Nature, 526, 230
Bodenheimer, P., D'angelo, G., Lissauer, J. J., Fortney, J. J., & Saumon, D. 2013, The Astrophysical Journal, 770, 120
Boley, A. C. 2009, ApJL, 695, L53
Boley, A. C., Payne, M. J., Corder, S., et al. 2012, The Astrophysical Journal, 750, L21
Bond, H. E., Gilliland, R. L., Schaefer, G. H., et al. 2015, ApJ, 813, 1
Bonnefoy, M., Chauvin, G., Rojo, P., et al. 2010, A&A, 512, A52
Bonnefoy, M., Lagrange, A.-M., Boccaletti, A., et al. 2011, A&A, 1
Bonnefoy, M., Boccaletti, A., Lagrange, A.-M., et al. 2013, A&A, 555, A107
Bonnefoy, M., Currie, T., Marleau, G. D., et al. 2014a, A&A, 562, A111
Bonnefoy, M., Marleau, G. D., Galicher, R., et al. 2014b, A&A, 567, L9
Bonnefoy, M., Zurlo, A., Baudino, J. L., et al. 2016, A&A, 587, A58
Bonnet-Bidaud, J. M., & Pantin, E. 2008, A&A, 489, 651
Boss, A. P. 2001, The Astrophysical Journal Letters, 551, L167
Bowler, B. P., Andrews, S. M., Kraus, A. L., et al. 2015a, The Astrophysical Journal Letters, 805, 1
Bowler, B. P., & Hillenbrand, L. A. 2015, The Astrophysical Journal Letters, 811, L30
Bowler, B. P., Liu, M. C., Dupuy, T. J., & Cushing, M. C. 2010a, The Astrophysical Journal, 723, 850
Bowler, B. P., Liu, M. C., Kraus, A. L., & Mann, A. W. 2014, ApJ, 784, 65
Bowler, B. P., Liu, M. C., Kraus, A. L., Mann, A. W., & Ireland, M. J. 2011, The Astrophysical Journal, 743, 148
Bowler, B. P., Liu, M. C., Shkolnik, E. L., & Dupuy, T. J. 2013, The Astrophysical Journal, 774, 55
Bowler, B. P., Liu, M. C., Shkolnik, E. L., et al. 2012a, The Astrophysical Journal, 753, 142
Bowler, B. P., Liu, M. C., Shkolnik, E. L., & Tamura, M. 2012b, The Astrophysical Journal, 756, 69
—. 2015b, The Astrophysical Journal Supplement Series, 216, 7
Bowler, B. P., Johnson, J. A., Marcy, G. W., et al. 2010b, The Astrophysical Journal, 709, 396
Bowler, B. P., Shkolnik, E. L., Liu, M. C., et al. 2015c, The Astrophysical Journal, 806, 62
Brandner, W., Zinnecker, H., Alcalá, J. M., et al. 2000, AJ, 120, 950
Brandt, T. D., McElwain, M. W., Turner, E. L., et al. 2013, The Astrophysical Journal, 764, 183
—. 2014a, ApJ, 794, 159
Brandt, T. D., McElwain, M. W., Janson, M., et al. 2014b, In Proc. SPIE, 9148, 1, 91849
Brandt, T. D., Kuzuhara, M., McElwain, M. W., et al. 2014c, ApJ, 786, 1
Brown, R. A. 2015, ApJ, 805, 1
Bryan, M. L., Knutson, H. A., Howard, A. W., et al. 2016, ApJ, 821, 1
Buenzli, E., Thalmann, C., Vigan, A., et al. 2010, A&A, 524, L1
Burgasser, A. J. 2014, arXiv, 1406.4887v1
Burgasser, A. J., Reid, I. N., Siegler, N., et al. 2007, Protostars and Planets V, 427
Burgasser, A. J., Simcoe, R. A., Bochanski, J. J., et al. 2010, The Astrophysical Journal, 725, 1405
Burningham, B., Leggett, S. K., Homeier, D., et al. 2011, Monthly Notices RAS, 414, 3590
Burrows, A., Hubbard, W. B., Lunine, J. I., & Liebert, J. 2001, Reviews of Modern Physics, 73, 719
Burrows, A., & Liebert, J. 1993, Reviews of Modern Physics, 65, 301
Burrows, A., Marley, M., Hubbard, W. B., et al. 1997, Astrophysical Journal, 491, 856
Butler, R. P., Wright, J. T., Marcy, G. W., et al. 2006, The Astrophysical Journal, 646, 505
Caceres, C., Hardy, A., Schreiber, M. R., et al. 2015, The Astrophysical Journal Letters, 806, 1
Cantalloube, F., Mouillet, D., Mugnier, L. M., et al. 2015, A&A, 582, A89
Cardoso, C. V., Mccaughrean, M. J., King, R. R., et al. 2009, in AIP Conf. Proc 1094, 15th Cambridge Workshop on CoolStars, Stellar Systems and the Sun, ed. E. Stempels (Melville, NY: AIP),, 509
Carson, J., Thalmann, C., Janson, M., et al. 2013, The Astrophysical Journal, 763, L32
Carson, J. C., Eikenberry, S. S., Brandl, B. R., Wilson, J. C., & Hayward, T. L. 2005, The Astronomical Journal, 130, 1212
Carson, J. C., Eikenberry, S. S., Smith, J. J., & Cordes, J. M. 2006, The Astronomical Journal, 132, 1146
Chabrier, G. 2001, The Astrophysical Journal, 554, 1274
Chabrier, G., Baraffe, I., Selsis, F., et al. 2007, Protostars and Planets V, 623
Chabrier, G., Johansen, A., Janson, M., & Rafikov, R. 2014, in Protostars and Planets VI, Henrik Beuther, Ralf S. Klessen, Cornelis P. Dullemond, and Thomas Henning (eds.), University of Arizona Press, Tucson, 914 pp., p.619-642
Chauvin, G., Beust, H., Lagrange, A.-M., & Eggenberger, A. 2011, A&A, 528, A8
Chauvin, G., Lagrange, A.-M., Dumas, C., et al. 2004, A&A, 425, L29
—. 2005a, A&A, 438, L25
Chauvin, G., Lagrange, A.-M., Udry, S., et al. 2006, A&A, 456, 1165
Chauvin, G., Lagrange, A.-M., Udry, S., & Mayor, M. 2007, A&A, 475, 723
Chauvin, G., Thomson, M., Dumas, C., et al. 2003, A&A, 404, 157
Chauvin, G., Lagrange, A.-M., Zuckerman, B., et al. 2005b, A&A, 438, L29
Chauvin, G., Lagrange, A.-M., Lacombe, F., et al. 2005c, A&A, 430, 1027
Chauvin, G., Lagrange, A.-M., Bonavita, M., et al. 2010, A&A, 509, A52
Chauvin, G., Lagrange, A.-M., Beust, H., et al. 2012, A&A, 542, A41
Chauvin, G., Vigan, A., Bonnefoy, M., et al. 2015, A&A, 573, A127
Cheetham, A., Huélamo, N., Lacour, S., de Gregorio-Monsalvo, I., & Tuthill, P. 2015, Monthly Notices RAS Letters, 450, L1
Chiang, E., Kite, E., Kalas, P., Graham, J. R., & Clampin, M. 2009, The Astrophysical Journal, 693, 734
Chun, M., Toomey, D., Wahhaj, Z., et al. 2008, SPIE, 7015, 1
Cieza, L. A., Padgett, D. L., Allen, L. E., et al. 2009, ApJL, 696, L84
Clanton, C., & Gaudi, B. S. 2016, ApJ, 819, 1
Claudi, R. U., Turatto, M., Gratton, R. G., et al. 2008, in SPIE Astronomical Telescopes + Instrumentation, ed. I. S. McLean & M. M. Casali (SPIE), 70143E
Close, L. M., Males, J. R., Kopon, D. A., et al. 2012, Adaptive Optics Systems III. Proceedings of the SPIE, 8447
Close, L. M., Males, J. R., Morzinski, K., et al. 2013, ApJ, 774, 94
Close, L. M., Follette, K. B., Males, J. R., et al. 2014, The Astrophysical Journal, 781, L30
Crepp, J. R., Gonzales, E. J., Bechter, E. B., et al. 2016, arXiv, arXiv:1604.00398
Crepp, J. R., Johnson, J. A., Howard, A. W., et al. 2014, ApJ, 781, 29
—. 2013a, The Astrophysical Journal, 774, 1
Crepp, J. R., Pueyo, L., Brenner, D., et al. 2011, The Astrophysical Journal, 729, 132
Crepp, J. R., Johnson, J. A., Fischer, D. A., et al. 2012a, The Astrophysical Journal, 751, 97
Crepp, J. R., Johnson, J. A., Howard, A. W., et al. 2012b, The Astrophysical Journal, 761, 39
—. 2013b, ApJ, 771, 46
Crepp, J. R., Rice, E. L., Veicht, A., et al. 2015, The Astrophysical Journal Letters, 798, L43
Crossfield, I. J. M. 2014, A&A, 566, A130
—. 2015, Publications of the Astronomical Society of the Pacific, 127, 941
Crossfield, I. J. M., Biller, B., Schlieder, J. E., et al. 2014, Nature, 505, 654

Cumming, A., Butler, R. P., Marcy, G. W., et al. 2008, PASP, 120, 531
Currie, T., Bailey, V., Fabrycky, D., et al. 2010, The Astrophysical Journal, 721, L177
Currie, T., Burrows, A., & Daemgen, S. 2014a, ApJ, 787, 104
Currie, T., Cloutier, R., Brittain, S., et al. 2015, The Astrophysical Journal Letters, 814, 1
Currie, T., Cloutier, R., Debes, J. H., Kenyon, S. J., & Kaisler, D. 2013, The Astrophysical Journal Letters, 777, L6
Currie, T., Daemgen, S., Debes, J., et al. 2014b, The Astrophysical Journal, 780, L30
Currie, T., Fukagawa, M., Thalmann, C., Matsumura, S., & Plavchan, P. 2012a, The Astrophysical Journal, 755, L34
Currie, T., Thalmann, C., Matsumura, S., et al. 2011a, The Astrophysical Journal, 736, L33
Currie, T., Burrows, A., Itoh, Y., et al. 2011b, The Astrophysical Journal, 729, 128
Currie, T., Debes, J., Rodigas, T. J., et al. 2012b, The Astrophysical Journal Letters, 760, L32
Currie, T., Burrows, A., Girard, J. H., et al. 2014c, ApJ, 795, 133
Currie, T., Muto, T., Kudo, T., et al. 2014d, The Astrophysical Journal Letters, 796, L30
Cushing, M. C., Marley, M. S., Saumon, D., et al. 2008, The Astrophysical Journal, 678, 1372
Cushing, M. C., Kirkpatrick, J. D., Gelino, C. R., et al. 2011, The Astrophysical Journal, 743, 50
Daemgen, S., Bonavita, M., Jayawardhana, R., LaFreniere, D., & Janson, M. 2015, ApJ, 799, 155
Davies, R., & Kasper, M. 2012, Annu. Rev. Astro. Astrophys., 50, 305
Dawson, R. I., Murray-Clay, R. A., & Fabrycky, D. C. 2011, The Astrophysical Journal, 743, L17
De Rosa, R. J., Nielsen, E. L., Blunt, S. C., et al. 2015, The Astrophysical Journal Letters, 814, 1
De Rosa, R. J., Rameau, J., Patience, J., et al. 2016, arXiv, 1604.01411v1
Deacon, N. R., Schlieder, J. E., & Murphy, S. J. 2016, Monthly Notices RAS, 457, 3191
Deacon, N. R., Liu, M. C., Magnier, E. A., et al. 2014, ApJ, 792, 119
Dekany, R., Roberts, J., Burruss, R., et al. 2013, ApJ, 776, 130
Delorme, P., Lagrange, A. M., Chauvin, G., et al. 2012, A&A, 539, A72
Delorme, P., Gagné, J., Girard, J. H., et al. 2013, A&A, 553, L5
Dent, W. R. F., Walker, H. J., Holland, W. S., & Greaves, J. S. 2000, Monthly Notices RAS, 314, 702
Dent, W. R. F., Wyatt, M. C., Roberge, A., et al. 2014, Science, 1490
Desidera, S., Covino, E., Messina, S., et al. 2015, A&A, 573, A126
Dohlen, K., Langlois, M., Saisse, M., et al. 2008, in SPIE Astronomical Telescopes + Instrumentation, ed. I. S. McLean & M. M. Casali, Lab. d'Astrophysique de Marseille, CNRS, Univ. de Provence (France) (SPIE), 70143L
Dong, R., Fung, J., & Chiang, E. 2016a, arXiv, 1602.04814v1
Dong, R., Hall, C., Rice, K., & Chiang, E. 2015, The Astrophysical Journal Letters, 812, L32
Dong, R., Zhu, Z., Fung, J., et al. 2016b, The Astrophysical Journal Letters, 816, L12
Dou, J., Ren, D., Zhao, G., et al. 2015, ApJ, 802, 1
Duchêne, G. 2010, The Astrophysical Journal, 709, L114
Duchêne, G., & Kraus, A. 2013, Annu. Rev. Astro. Astrophys., 51, 269
Dupuy, T. J., Kratter, K. M., Kraus, A. L., et al. 2016, ApJ, 817, 1
Dupuy, T. J., & Kraus, A. L. 2013, Science, 341, 1492
Dupuy, T. J., & Liu, M. C. 2011, The Astrophysical Journal, 733, 122
—. 2012, The Astrophysical Journal Supplement, 201, 19
Dupuy, T. J., Liu, M. C., & Ireland, M. J. 2009, The Astrophysical Journal, 692, 729
—. 2014, ApJ, 790, 133
Dupuy, T. J., Liu, M. C., & Leggett, S. K. 2015a, ApJ, 803, 1
Dupuy, T. J., Liu, M. C., Leggett, S. K., et al. 2015b, ApJ, 805, 1
Durisen, R. H., Boss, A. P., Mayer, L., et al. 2007, in Protostars and Planets V, e. B. Reipurth, D. Jewitt, & K. Keil (Tucson, AZ: Univ. Arizona Press), 607
Ehrenreich, D., Lagrange, A.-M., Montagnier, G., et al. 2010, A&A, 523, A73
Eiroa, C., Marshall, J. P., Mora, A., et al. 2013, A&A, 555, A11
Els, S. G., Sterzik, M. F., Marchis, F., et al. 2001, A&A, 370, L1
Espaillat, C., Muzerolle, J., Najita, J., et al. 2014, Protostars and Planets VI, 497
Esposito, S., Mesa, D., Skemer, A., et al. 2012, A&A, 549, A52
Fabrycky, D. C., & Murray-Clay, R. A. 2010, The Astrophysical Journal, 710, 1408
Faherty, J. K., Rice, E. L., Cruz, K. L., Mamajek, E. E., & Núñez, A. 2012, The Astronomical Journal, 145, 2
Farihi, J., Bond, H. E., Dufour, P., et al. 2013, Monthly Notices RAS, 430, 652
Feigelson, E. D., Lawson, W. A., & Stark, M. 2006, The Astronomical ...
Fergus, R., Hogg, D. W., Oppenheimer, R., Brenner, D., & Pueyo, L. 2014, ApJ, 794, 161
Filippazzo, J. C., Rice, E. L., Faherty, J., et al. 2015, ApJ, 810, 1
Fitzgerald, M. P., Kalas, P. G., & Graham, J. R. 2009, The Astrophysical Journal, 706, L41
Fortney, J. J., Marley, M. S., Saumon, D., & Lodders, K. 2008, The Astrophysical Journal, 683, 1104
Fortney, J. J., & Nettelmann, N. 2009, Space Sci Rev, 1
Forveille, T., S gransan, D., Delorme, P., et al. 2004, A&A, 427, L1
Fuhrmann, K., & Chini, R. 2015, ApJ, 806, 1
Fukagawa, M., Itoh, Y., Tamura, M., et al. 2009, The Astrophysical Journal, 696, L1
Gagné, J., Burgasser, A. J., Faherty, J. K., et al. 2015a, The Astrophysical Journal Letters, 808, 1
Gagné, J., LaFreniere, D., Doyon, R., Malo, L., & Artigau, E. 2014, ApJ, 783, 121
—. 2015b, ApJ, 798, 73
Gagné, J., Faherty, J. K., Cruz, K. L., et al. 2015c, The Astrophysical Journal Supplement Series, 219, 1
Gaidos, E., Mann, A. W., Lépine, S., et al. 2014, Monthly Notices RAS, 443, 2561
Galicher, R., Marois, C., Macintosh, B., Barman, T., & Konopacky, Q. 2011, The Astrophysical Journal, 739, L41
Galicher, R., Rameau, J., Bonnefoy, M., et al. 2014, A&A, 565, L4
Garcia, E. V., Dupuy, T. J., Allers, K. N., Liu, M. C., & Deacon, N. R. 2015, ApJ, 804, 1
Garufi, A., Quanz, S. P., Schmid, H. M., et al. 2016, arXiv, 1601.04983v1
Gauza, B., Bejar, V. J. S., Pérez-Garrido, A., et al. 2015, The Astrophysical Journal, 804, 96
Geißler, K., Kellner, S., Brandner, W., et al. 2007, A&A, 461, 665
Ginski, C., Mugrauer, M., Seeliger, M., et al. 2016, Monthly Notices RAS, 457, 2173
Gizis, J. E. 2002, The Astrophysical Journal, 575, 484
Goldman, B., Marsat, S., Henning, T., Clemens, C., & Greiner, J. 2010, Monthly Notices RAS, 405, 1140
Golimowski, D. A., Leggett, S. K., Marley, M. S., et al. 2004a, The Astronomical Journal, 127, 3516
Golimowski, D. A., Henry, T. J., Krist, J. E., et al. 2004b, The Astronomical Journal, 128, 1733
Gonzalez, C. A. G., Absil, O., Absil, P. A., et al. 2016, arXiv, 1602.08381v1
Goździewski, K., & Migaszewski, C. 2009, Monthly Notices RAS Letters, 397, L16
—. 2014, Monthly Notices RAS, 440, 3140
Greaves, J. S., Holland, W. S., Moriarty-Schieven, G., et al. 1998, The Astrophysical Journal, 506, L133
Greaves, J. S., Holland, W. S., Wyatt, M. C., et al. 2005, ApJL, 619, L187
Greco, J. P., & Brandt, T. D. 2016, arXiv, 1602.00691v1
Greco, J. P., & Burrows, A. 2015, ApJ, 808, 1
Guyon, O. 2003, A&A, 404, 379
Guyon, O., Pluzhnik, E. A., Galicher, R., et al. 2005, The Astrophysical Journal, 622, 744
Guyon, O., Pluzhnik, E. A., Kuchner, M. J., Collins, B., & Ridgway, S. T. 2006, The Astrophysical Journal Supplement Series, 167, 81
Hagelberg, J., Ségransan, D., Udry, S., & Wildi, F. 2016, Monthly Notices RAS, 455, 2178
Han, E., Wang, S. X., Wright, J. T., et al. 2014, Publications of the Astronomical Society of the Pacific, 126, 827

Hashimoto, J., Tamura, M., Muto, T., et al. 2011, The Astrophysical Journal, 729, L17
Hatzes, A. P., Cochran, W. D., McArthur, B., et al. 2000, The Astrophysical Journal, 544, L145
Hayward, T. L., Biller, B. A., Liu, M. C., et al. 2014, Publications of the Astronomical Society of the Pacific, 126, 1112
Heap, S. R., Lindler, D. J., Lanz, T. M., et al. 2000, The Astrophysical Journal, 539, 435
Heinze, A. N., Hinz, P. M., Kenworthy, M., et al. 2010a, The Astrophysical Journal, 714, 1570
Heinze, A. N., Hinz, P. M., Kenworthy, M., Miller, D., & Sivanandam, S. 2008, The Astrophysical Journal, 688, 583
Heinze, A. N., Hinz, P. M., Sivanandam, S., et al. 2010b, The Astrophysical Journal, 714, 1551
Helled, R., Bodenheimer, P., Podolak, M., et al. 2013, in Protostars and Planets VI, ed. H. Beuther et al. (Tucson, AZ: Univ. Arizona Press), 643
Helling, C., & Casewell, S. 2014, Astron Astrophys Rev, 22, 80
Helling, C., Woitke, P., Rimmer, P., et al. 2014, Life, 4, 142
Helling, C., Ackerman, A., Allard, F., et al. 2008, Monthly Notices RAS, 391, 1854
Henry, T. J., & McCarthy, D. W. J. 1990, Astrophysical Journal, 350, 334
Herczeg, G. J., & Hillenbrand, L. A. 2015, The Astrophysical Journal, 808, 23
Hinkley, S., Oppenheimer, B. R., Soummer, R., et al. 2007, The Astrophysical Journal, 654, 633
Hinkley, S., Oppenheimer, B. R., Brenner, D., et al. 2010, The Astrophysical Journal, 712, 421
Hinkley, S., Oppenheimer, B. R., Zimmerman, N., et al. 2011, Publications of the Astronomical Society of the Pacific, 123, 74
Hinkley, S., Pueyo, L., Faherty, J. K., et al. 2013, ApJ, 779, 153
Hinkley, S., Bowler, B. P., Vigan, A., et al. 2015a, The Astrophysical Journal Letters, 805, 1
Hinkley, S., Kraus, A. L., Ireland, M. J., et al. 2015b, The Astrophysical Journal Letters, 806, 1
Hinz, P. M., Heinze, A. N., Sivanandam, S., et al. 2006, ApJ, 653, 1486
Hinz, P. M., Rodigas, T. J., Kenworthy, M. A., et al. 2010, The Astrophysical Journal, 716, 417
Howard, A. W., Johnson, J. A., Marcy, G. W., et al. 2010, The Astrophysical Journal, 721, 1467
Howard, A. W., Marcy, G. W., Bryson, S. T., et al. 2012, The Astrophysical Journal Supplement Series, 201, 15
Howard, A. W., Marcy, G. W., Fischer, D. A., et al. 2014, ApJ, 794, 51
Huby, E., Perrin, G., Marchis, F., et al. 2012, A&A, 541, A55
Huélamo, N., Lacour, S., Tuthill, P., et al. 2011, A&A, 528, L7
Hung, L.-W., Duchene, G., Arriaga, P., et al. 2015, The Astrophysical Journal Letters, 815, 1
Ingraham, P., Marley, M. S., Saumon, D., et al. 2014, The Astrophysical Journal Letters, 794, L15
Ireland, M. J., Kraus, A., Martinache, F., Law, N., & Hillenbrand, L. A. 2011, The Astrophysical Journal, 726, 113
Ireland, M. J., & Kraus, A. L. 2008, The Astrophysical Journal, 678, L59
—. 2014, IAU, 8, 199
Irwin, A. W., Fletcher, J. M., Yang, S. L. S., Walker, G. A. H., & Goodenough, C. 1992, Astronomical Society of the Pacific, 104, 489
Isella, A., Chandler, C. J., Carpenter, J. M., Pérez, L. M., & Ricci, L. 2014, ApJ, 788, 129
Itoh, Y., Oasa, Y., & Fukagawa, M. 2006, The Astrophysical Journal
Itoh, Y., Hayashi, M., Tamura, M., et al. 2005, The Astrophysical Journal, 620, 984
Itoh, Y., Tamura, M., Hayashi, M., et al. 2008, Publications of the Astronomical Society of Japan, 60, 209
Janson, M., Bonavita, M., Klahr, H., et al. 2011a, The Astrophysical Journal, 736, 89
Janson, M., Carson, J. C., Lafrenière, D., et al. 2012, The Astrophysical Journal, 747, 116
Janson, M., LaFreniere, D., Jayawardhana, R., et al. 2013a, ApJ, 773, 170
Janson, M., Quanz, S. P., Carson, J. C., et al. 2015, A&A, 574, A120
Janson, M., Reffert, S., Brandner, W., et al. 2008, A&A, 488, 771
Janson, M., Brandner, W., Henning, T., et al. 2007, The Astronomical Journal, 133, 2442
Janson, M., Apai, D., Zechmeister, M., et al. 2009, Monthly Notices RAS, 399, 377
Janson, M., Carson, J., Thalmann, C., et al. 2011b, ApJ, 728, 85
Janson, M., Brandt, T. D., Kuzuhara, M., et al. 2013b, The Astrophysical Journal, 778, L4
Janson, M., Brandt, T. D., Moro-Martín, A., et al. 2013c, ApJ, 773, 73
Janson, M., Bergfors, C., Brandner, W., et al. 2014, The Astrophysical Journal Supplement Series, 214, 17
Jeffries, R. D. 2014, EAS Publications Series, 65, 289
Jenkins, J. S., Jones, H. R. A., Biller, B., et al. 2010, A&A, 515, A17
Jenkins, J. S., Jones, H. R. A., Tuomi, M., et al. 2016, arXiv, 1603.09391v1
Jensen-Clem, R., Millar-Blanchaer, M., Mawet, D., et al. 2016, ApJ, 820, 1
Jilkova, L., & Zwart, S. P. 2015, Monthly Notices RAS, 451, 804
Johnson, J. A. 2009, Publications of the Astronomical Society of the Pacific, 121, 309
Johnson, J. A., Aller, K. M., Howard, A. W., & Crepp, J. R. 2010, Publications of the Astronomical Society of the Pacific, 122, 905
Johnson, J. A., Butler, R. P., Marcy, G. W., et al. 2007, The Astrophysical Journal, 670, 833
Jones, J., White, R. J., Quinn, S., et al. 2016, The Astrophysical Journal Letters, 822, 1
Jovanovic, N., Martinache, F., Guyon, O., et al. 2015, Publications of the Astronomical Society of Pacific, 127, 890
Kalas, P., Graham, J., Chiang, E., & Fitzgerald, M. 2008a, Science Express
Kalas, P., Graham, J. R., & Clampin, M. 2005, Nature, 435, 1067
Kalas, P., Graham, J. R., Fitzgerald, M. P., & Clampin, M. 2013, ApJ, 775, 56
Kalas, P., & Jewitt, D. 1995, Astronomical Journal v.110, 110, 794
Kalas, P., Graham, J. R., Chiang, E., et al. 2008b, Science, 322, 1345
Kalas, P. G., Rajan, A., Wang, J. J., et al. 2015, ApJ, 814, 1
Kasper, M., Apai, D., Janson, M., & Brandner, W. 2007, A&A, 472, 321
Kellogg, K., Metchev, S., Gagné, J., & Faherty, J. 2016, The Astrophysical Journal Letters, 821, 1
Kennedy, G. M., & Wyatt, M. C. 2011, Monthly Notices RAS, 412, 2137
Kenworthy, M. A., Codona, J. L., Hinz, P. M., et al. 2007, ApJ, 660, 762
Kenworthy, M. A., Mamajek, E. E., Hinz, P. M., et al. 2009, The Astrophysical Journal, 697, 1928
Kenworthy, M. A., Meshkat, T., Quanz, S. P., et al. 2013, ApJ, 764, 7
Kenyon, S. J., & Bromley, B. C. 2004, The Astronomical Journal
Kenyon, S. J., Currie, T., & Bromley, B. C. 2014, ApJ, 786, 70
Kirkpatrick, J. D., Gelino, C. R., Cushing, M. C., et al. 2012, The Astrophysical Journal, 753, 156
Kiss, L. L., Moór, A., Szalai, T., et al. 2010, Monthly Notices RAS, 411, 117
Knutson, H. A., Fulton, B. J., Montet, B. T., et al. 2014, ApJ, 785, 126
Konopacky, Q. M., Barman, T. S., Macintosh, B. A., & Marois, C. 2013, Science, 339, 1398
Konopacky, Q. M., Marois, C., Macintosh, B. A., et al. 2016, arXiv, 1604.08157v1
Kratter, K. M., & Lodato, G. 2016, arXiv, 1603.01280v1
Kraus, A. L., Andrews, S. M., Bowler, B. P., et al. 2015, The Astrophysical Journal, 798, L23
Kraus, A. L., & Hillenbrand, L. A. 2012, The Astrophysical Journal, 757, 141
Kraus, A. L., & Ireland, M. J. 2012, The Astrophysical Journal, 745, 5
Kraus, A. L., Ireland, M. J., Cieza, L. A., et al. 2014a, ApJ, 781, 20
Kraus, A. L., Ireland, M. J., Hillenbrand, L. A., & Martinache, F. 2012, The Astrophysical Journal, 745, 19
Kraus, A. L., Ireland, M. J., Huber, D., Mann, A. W., & Dupuy, T. J. 2016, arXiv, 1604.05744v1

Kraus, A. L., Ireland, M. J., Martinache, F., & Lloyd, J. P. 2008, The Astrophysical Journal, 679, 762
Kraus, A. L., Shkolnik, E. L., Allers, K. N., & Liu, M. C. 2014b, AJ, 147, 146
Kraus, A. L., White, R. J., & Hillenbrand, L. A. 2005, ApJ, 633, 452
Krivov, A. V. 2010, Research in Astron. Astrophys., 383
Kuchner, M. J., & Brown, M. E. 2000, Publications of the Astronomical Society of the Pacific, 112, 827
Kumar, S. S. 1963, Astrophysical Journal, 137, 1121
Kuzuhara, M., Tamura, M., Ishii, M., et al. 2011, The Astronomical Journal, 141, 119
Kuzuhara, M., Tamura, M., Kudo, T., et al. 2013, The Astrophysical Journal, 774, 11
Lachapelle, F.-R., LaFreniere, D., Gagné, J., et al. 2015, ApJ, 802, 1
Lacour, S., Biller, B., Cheetham, A., et al. 2015, arXiv, 1511.09390v1
Lafrenière, D., Jayawardhana, R., & van Kerkwijk, M. H. 2008, The Astrophysical Journal, 689, L153
—. 2010, The Astrophysical Journal, 719, 497
Lafrenière, D., Jayawardhana, R., van Kerkwijk, M. H., Brandeker, A., & Janson, M. 2014, ApJ, 785, 47
Lafrenière, D., Marois, C., Doyon, R., & Barman, T. 2009, The Astrophysical Journal, 694, L148
Lafrenière, D., Marois, C., Doyon, R., Nadeau, D., & Artigau, É. 2007a, The Astrophysical Journal, 660, 770
Lafrenière, D., Doyon, R., Marois, C., et al. 2007b, The Astrophysical Journal, 670, 1367
Lagrange, A.-M. 2014, Philosophical Transactions of the Royal Society A: Mathematical, Physical and Engineering Sciences, 372, 20130090
Lagrange, A.-M., Beust, H., Udry, S., Chauvin, G., & Mayor, M. 2006, A&A, 459, 955
Lagrange, A.-M., Meunier, N., Chauvin, G., et al. 2013, A&A, 559, A83
Lagrange, A.-M., Gratadour, D., Chauvin, G., et al. 2009a, A&A, 493, L21
Lagrange, A.-M., Kasper, M., Boccaletti, A., et al. 2009b, A&A, 506, 927
Lagrange, A.-M., Bonnefoy, M., Chauvin, G., et al. 2010, Science, 329, 57
Lagrange, A.-M., Langlois, M., Gratton, R., et al. 2016, A&A, 586, L8
Langlois, M., Dohlen, K., Vigan, A., et al. 2014, in SPIE Astronomical Telescopes + Instrumentation, ed. S. K. Ramsay, I. S. McLean, & H. Takami (SPIE), 91471R
Larwood, J. D., & Kalas, P. G. 2001, MNRAS, 323, 402
Leconte, J., Soummer, R., Hinkley, S., et al. 2010, The Astrophysical Journal, 716, 1551
Lee, J.-M., Heng, K., & Irwin, P. G. J. 2013, ApJ, 778, 97
Lépine, S., & Simon, M. 2009, The Astronomical Journal, 137, 3632
Line, M. R., Fortney, J. J., Marley, M. S., & Sorahana, S. 2014, ApJ, 793, 33
Liu, M. C. 2004, Science, 305, 1442
Liu, M. C., Dupuy, T. J., Bowler, B. P., Leggett, S. K., & Best, W. M. J. 2012, The Astrophysical Journal, 758, 57
Liu, M. C., Fischer, D. A., Graham, J. R., et al. 2002, The Astrophysical Journal, 571, 519
Liu, M. C., Wahhaj, Z., Biller, B. A., et al. 2010, SPIE, 7736, 77361K
Liu, M. C., Delorme, P., Dupuy, T. J., et al. 2011, The Astrophysical Journal, 740, 108
Liu, M. C., Magnier, E. A., Deacon, N. R., et al. 2013, The Astrophysical Journal, 777, L20
Lodato, G., Delgado-Donate, E., & Clarke, C. J. 2005, Monthly Notices RAS Letters, 364, L91
Looper, D. L., Mohanty, S., Bochanski, J. J., et al. 2010, The Astrophysical Journal, 714, 45
Lopez, S., & Jenkins, J. S. 2012, ApJ, 756, 177
Lovis, C., & Mayor, M. 2007, A&A, 472, 657
Low, C., & Lynden-Bell, D. 1976, Royal Astronomical Society, 176, 367
Lowrance, P. J., McCarthy, C., Becklin, E. E., et al. 1999, The Astrophysical Journal, 512, L69
Lowrance, P. J., Schneider, G., Kirkpatrick, J. D., et al. 2000, The Astrophysical Journal, 541, 390
Lowrance, P. J., Becklin, E. E., Schneider, G., et al. 2005, The Astronomical Journal, 130, 1845
Lucas, P. W., Roche, P. F., Allard, F., & Hauschildt, P. H. 2001, Monthly Notices RAS, 326, 695
Luhman, K. L., Burgasser, A. J., & Bochanski, J. J. 2011, The Astrophysical Journal, 730, L9
Luhman, K. L., Burgasser, A. J., Labbé, I., et al. 2012, The Astrophysical Journal, 744, 135
Luhman, K. L., & Jayawardhana, R. 2002, The Astrophysical Journal, 566, 1132
Luhman, K. L., Mamajek, E. E., Allen, P. R., & Cruz, K. L. 2009a, The Astrophysical Journal, 703, 399
Luhman, K. L., Mamajek, E. E., Allen, P. R., Muench, A. A., & Finkbeiner, D. P. 2009b, The Astrophysical Journal, 691, 1265
Luhman, K. L., Mcleod, K. K., & Goldenson, N. 2005, The Astrophysical Journal, 623, 1141
Luhman, K. L., Wilson, J. C., Brandner, W., et al. 2006, The Astrophysical Journal, 649, 894
Luhman, K. L., Patten, B. M., Marengo, M., et al. 2007, The Astrophysical Journal, 654, 570
Macintosh, B., Graham, J. R., Ingraham, P., et al. 2014, Proceedings of the National Academy of Sciences, 111, 12661
Macintosh, B., Graham, J. R., Barman, T., et al. 2015, Science
Macintosh, B. A., Becklin, E. E., Kaisler, D., Konopacky, Q., & Zuckerman, B. 2003, The Astrophysical Journal, 594, 538
Macintosh, B. A., Max, C., Zuckerman, B., et al. 2001, Young Stars Near Earth: Progress and Prospects, 244, 309
Madhusudhan, N., Knutson, H., Fortney, J., & Barman, T. 2014, arXiv, 1402.1169v1
Maire, A. L., Boccaletti, A., Rameau, J., et al. 2014, A&A, 566, A126
Maire, A. L., Skemer, A. J., Hinz, P. M., et al. 2015a, A&A, 576, A133
—. 2015b, A&A, 579, C2
Maire, A. L., Bonnefoy, M., Ginski, C., et al. 2016, A&A, 587, A56
Males, J. R., Close, L. M., Morzinski, K. M., et al. 2014, ApJ, 786, 32
Malo, L., Artigau, E., Doyon, R., et al. 2014, ApJ, 788, 81
Malo, L., Doyon, R., Lafrenière, D., et al. 2013, ApJ, 762, 88
Mamajek, E. E. 2012, The Astrophysical Journal, 754, L20
—. 2016, In Young Stars & Planets Near the Sun, Proceedings of the International Astronomical Union, IAU Symposium, 314, 21
Mamajek, E. E., & Bell, C. P. M. 2014, Monthly Notices RAS, 445, 2169
Mamajek, E. E., Bartlett, J. L., Seifahrt, A., et al. 2013, The Astronomical Journal, 146, 154
Marengo, M., Megeath, S. T., Fazio, G. G., et al. 2006, The Astrophysical Journal, 647, 1437
Marengo, M., Stapelfeldt, K., Werner, M. W., et al. 2009, The Astrophysical Journal, 700, 1647
Marleau, G. D., & Cumming, A. 2013, Monthly Notices RAS, 437, 1378
Marley, M. S., Ackerman, A. S., Cuzzi, J. N., & Kitzmann, D. 2013, arXiv, astro-ph.EP
Marley, M. S., Fortney, J., Seager, S., & Barman, T. 2007a, Protostars and Planets V, 733
Marley, M. S., Fortney, J. J., Hubickyj, O., Bodenheimer, P., & Lissauer, J. J. 2007b, The Astrophysical Journal, 655, 541
Marley, M. S., & Robinson, T. D. 2015, Annu. Rev. Astro. Astrophys., 53, 279
Marley, M. S., Saumon, D., Cushing, M., et al. 2012, The Astrophysical Journal, 754, 135
Marois, C., Correia, C., Galicher, R., et al. 2014, in SPIE Astronomical Telescopes + Instrumentation, ed. E. Marchetti, L. M. Close, & J.-P. Veran (SPIE), 91480U
Marois, C., Lafrenière, D., Doyon, R., Macintosh, B., & Nadeau, D. 2006, The Astrophysical Journal, 641, 556
Marois, C., Macintosh, B., Barman, T., et al. 2008, Science, 322, 1348
Marois, C., Macintosh, B., & Véran, J.-P. 2010a, Proc. SPIE, 7736, 77361J
Marois, C., Zuckerman, B., Konopacky, Q. M., Macintosh, B., & Barman, T. 2010b, Nature, 468, 1080

Marshall, J. P., Moro-Martin, A., Eiroa, C., et al. 2014, A&A, 565, A15
Martinache, F., Guyon, O., Jovanovic, N., et al. 2014, Publications of the Astronomical Society of Pacific, 126, 565
Masciadri, E., Mundt, R., Henning, T., Alvarez, C., & barrado y Navascués, D. 2005, The Astrophysical Journal, 625, 1004
Matthews, B. C., Krivov, A. V., Wyatt, M. C., Bryden, G., & Eiroa, C. 2014a, in Protostars and Planets VI, Henrik Beuther, Ralf S. Klessen, Cornelis P. Dullemond, and Thomas Henning (eds.), University of Arizona Press, Tucson, 521
Matthews, C. T., Crepp, J. R., Skemer, A., et al. 2014b, The Astrophysical Journal Letters, 783, L25
Mawet, D., Riaud, P., Absil, O., & Surdej, J. 2005, The Astrophysical Journal
Mawet, D., Serabyn, E., Liewer, K., et al. 2010, The Astrophysical Journal, 709, 53
Mawet, D., Absil, O., Montagnier, G., et al. 2012a, A&A, 544, A131
Mawet, D., Pueyo, L., Lawson, P., et al. 2012b, in SPIE Astronomical Telescopes + Instrumentation, ed. M. C. Clampin, G. G. Fazio, H. A. MacEwen, & J. M. Oschmann (SPIE), 844204
Mawet, D., Milli, J., Wahhaj, Z., et al. 2014, ApJ, 792, 97
Mawet, D., David, T., Bottom, M., et al. 2015, ApJ, 811, 1
Mayama, S., Hashimoto, J., Muto, T., et al. 2012, The Astrophysical Journal Letters, 760, L26
McCarthy, C., & Zuckerman, B. 2004, The Astronomical Journal, 127, 2871
Mccarthy, K., & Wilhelm, R. J. 2014, The Astronomical Journal, 148, 70
Mennesson, B., Serabyn, E., Hanot, C., et al. 2011, ApJ, 736, 14
Meshkat, T., Bailey, V. P., Su, K. Y. L., et al. 2015a, ApJ, 800, 5
Meshkat, T., Kenworthy, M. A., Quanz, S. P., & Amara, A. 2013a, ApJ, 780, 17
Meshkat, T., Kenworthy, M. A., Reggiani, M., et al. 2015b, Monthly Notices RAS, 453, 2534
Meshkat, T., Bailey, V., Rameau, J., et al. 2013b, The Astrophysical Journal, 775, L40
Meshkat, T., Bonnefoy, M., Mamajek, E. E., et al. 2015c, Monthly Notices RAS, 453, 2379
Metchev, S., Marois, C., & Zuckerman, B. 2009, The Astrophysical Journal, 705, L204
Metchev, S. A., & Hillenbrand, L. A. 2004, The Astrophysical Journal, 617, 1330
—. 2006, The Astrophysical Journal, 651, 1166
—. 2009, The Astrophysical Journal Supplement Series, 181, 62
Metchev, S. A., Hillenbrand, L. A., & White, R. J. 2003, The Astrophysical Journal, 582, 1102
Metchev, S. A., Heinze, A., Apai, D., et al. 2015, ApJ, 799, 154
Meyer, M. R., Carpenter, J. M., Mamajek, E. E., et al. 2008, ApJL, 673, L181
Millar-Blanchaer, M. A., Graham, J. R., Pueyo, L., et al. 2015, ApJ, 811, 1
Milli, J., Lagrange, A.-M., Mawet, D., et al. 2014, A&A, 566, A91
Mohanty, S., Greaves, J., Mortlock, D., et al. 2013, ApJ, 773, 168
Mollière, P., & Mordasini, C. 2012, A&A, 547, A105
Montet, B. T., Crepp, J. R., Johnson, J. A., Howard, A. W., & Marcy, G. W. 2014, ApJ, 781, 28
Montet, B. T., Bowler, B. P., Shkolnik, E. L., et al. 2015, The Astrophysical Journal Letters, 813, 1
Moor, A., Szabo, G. M., Kiss, L. L., et al. 2013, Monthly Notices RAS, 1
Mordasini, C. 2013, A&A, 558, A113
Mordasini, C., Alibert, Y., Klahr, H., & Henning, T. 2012, A&A, 547, A111
Moro-Martin, A., Wyatt, M. C., Malhotra, R., & Trilling, D. E. 2008, The Solar System Beyond Neptune, 465
Moro-Martin, A., Marshall, J. P., Kennedy, G., et al. 2015, ApJ, 801, 1
Morzinski, K. M., Close, L. M., Males, J. R., et al. 2014, in SPIE Astronomical Telescopes + Instrumentation, ed. E. Marchetti, L. M. Close, & J.-P. Veran (SPIE), 914804
Morzinski, K. M., Males, J. R., Skemer, A. J., et al. 2015, ApJ, 815, 1
Mouillet, D., Larwood, J. D., Papaloizou, J. C. B., & Lagrange, A.-M. 1997, Monthly Notices RAS, 292, 896
Mugrauer, M., & Neuhäuser, R. 2005, Monthly Notices RAS Letters, 361, L15
Mugrauer, M., Neuh User, R., Guenther, E. W., et al. 2004, A&A, 417, 1031
Muto, T., Grady, C. A., Hashimoto, J., et al. 2012, The Astrophysical Journal, 748, L22
Muzic, K., Scholz, A., Geers, V. C., & Jayawardhana, R. 2015, ApJ, 810, 1
Nakajima, T., Durrance, S. T., Golimowski, D. A., & Kulkarni, S. R. 1994, The Astrophysical Journal, 428, 797
Nakajima, T., Morino, J.-I., Tsuji, T., et al. 2005, Astronomische Nachrichten, 326, 952
Naud, M.-E., Artigau, E., Malo, L., et al. 2014, ApJ, 787, 5
Neuhäuser, R., Guenther, E. W., Alves, J., et al. 2003, Astronomische Nachrichten, 324, 535
Neuhäuser, R., Mugrauer, M., Fukagawa, M., Torres, G., & Schmidt, T. 2007, A&A, 462, 777
Ngo, H., Knutson, H. A., Hinkley, S., et al. 2015, ApJ, 800, 138
Nielsen, E. L., & Close, L. M. 2010, The Astrophysical Journal, 717, 878
Nielsen, E. L., Close, L. M., Biller, B. A., Masciadri, E., & Lenzen, R. 2008, The Astrophysical Journal, 674, 466
Nielsen, E. L., Liu, M. C., Wahhaj, Z., et al. 2012, The Astrophysical Journal, 750, 53
—. 2013, ApJ, 776, 4
—. 2014, ApJ, 794, 158
Norris, B., Schworer, G., Tuthill, P., et al. 2015, Monthly Notices RAS, 447, 2894
Oberg, K. I., Murray-Clay, R., & Bergin, E. A. 2011, The Astrophysical Journal, 743, L16
Olofsson, J., Benisty, M., Le Bouquin, J.-B., et al. 2013, A&A, 552, A4
Olofsson, J., Samland, M., Avenhaus, H., et al. 2016, arXiv, 1601.07861v1
Oppenheimer, B. R., Golimowski, D. A., Kulkarni, S. R., et al. 2001, The Astronomical Journal, 121, 2189
Oppenheimer, B. R., & Hinkley, S. 2009, Annu. Rev. Astro. Astrophys., 47, 253
Oppenheimer, B. R., Kulkarni, S. R., & Stauffer, J. R. 2000, Protostars and Planets IV (Book - Tucson: University of Arizona Press; eds Mannings, 1313
Oppenheimer, B. R., Digby, A. P., Newburgh, L., et al. 2004, in Astronomical Telescopes and Instrumentation, ed. D. Bonaccini Calia, B. L. Ellerbroek, & R. Ragazzoni (SPIE), 433–442
Oppenheimer, B. R., Baranec, C., Beichman, C., et al. 2013, The Astrophysical Journal, 768, 24
Owen, J. E. 2016, Publications of the Astronomical Society of Australia, 33, e005
Owen, J. E., & Menou, K. 2016, The Astrophysical Journal Letters, 819, 1
Ozernoy, L. M., Gorkavyi, N. N., Mather, J. C., & Taidakova, T. A. 2000, The Astrophysical Journal, 537, L147
Patience, J., King, R. R., De Rosa, R. J., & Marois, C. 2010, A&A, 517, A76
Pecaut, M. J., Mamajek, E. E., & Bubar, E. J. 2012, The Astrophysical Journal, 746, 154
Perez, S., Dunhill, A., Casassus, S., et al. 2015, The Astrophysical Journal Letters, 811, 1
Perryman, M. 2011, The Exoplanet Handbook (Cambridge University Press)
Perryman, M., Hartman, J., Bakos, G. Á., & Lindegren, L. 2014, ApJ, 797, 14
Petr-Gotzens, M. G., Cuby, J. G., Smith, M. D., & Sterzik, M. F. 2010, A&A, 522, A78
Pueyo, L., Crepp, J. R., Vasisht, G., et al. 2012, The Astrophysical Journal Supplement Series, 199, 6
Pueyo, L., Soummer, R., Hoffmann, J., et al. 2015, ApJ, 803, 31
Quanz, S. P. 2015, Astrophys. Space Sci., 1
Quanz, S. P., Amara, A., Meyer, M. R., et al. 2015, ApJ, 807, 1
—. 2013, The Astrophysical Journal, 766, L1
Quanz, S. P., Meyer, M. R., Kenworthy, M. A., et al. 2010, The Astrophysical Journal Letters, 722, L49
Queloz, D., Mayor, M., Weber, L., et al. 2000, A&A, 354, 99
Radigan, J., LaFreniere, D., Jayawardhana, R., & Artigau, E. 2014, ApJ, 793, 75

Rajan, A., Barman, T., Soummer, R., et al. 2015, The Astrophysical Journal Letters, 809, 1
Rameau, J., Chauvin, G., Lagrange, A.-M., et al. 2015, A&A
—. 2013a, A&A, 553, A60
—. 2013b, The Astrophysical Journal, 779, L26
—. 2013c, The Astrophysical . . . , 772, L15
Rameau, J., Nielsen, E. L., De Rosa, R. J., et al. 2016, arXiv, 1604.05139v1
Rebolo, R., Zapatero Osorio, M. R., Madruga, S., et al. 1998, Science, 282, 1309
Reggiani, M., Quanz, S. P., Meyer, M. R., et al. 2014, The Astrophysical Journal Letters, 792, L23
Reggiani, M., Meyer, M. R., Chauvin, G., et al. 2016, A&A, 586, A147
Reid, I. N., Cruz, K. L., Kirkpatrick, J. D., et al. 2008, The Astronomical Journal, 136, 1290
Reid, I. N., & Walkowicz, L. M. 2006, The Publications of the Astronomical Society of the Pacific, 118, 671
Riaz, B., & Martín, E. L. 2011, A&A, 525, A10
Riaz, B., Martín, E. L., Petr-Gotzens, M. G., & Monin, J.-L. 2013, A&A, 559, A109
Rice, E. L., Oppenheimer, R., Zimmerman, N., Roberts, Jr, L. C., & Hinkley, S. 2015, Publications of the Astronomical Society of the Pacific, 127, 479
Riedel, A. R., Finch, C. T., Henry, T. J., et al. 2014, The Astronomical Journal, 147, 85
Rieke, G. H., Su, K. Y. L., Stansberry, J. A., et al. 2005, The Astrophysical Journal, 620, 1010
Roberts, L. C., Rice, E. L., Beichman, C. A., et al. 2012, The Astronomical Journal, 144, 14
Robinson, T. D., Stapelfeldt, K. R., & Marley, M. S. 2016, Publications of the Astronomical Society of the Pacific, 128, 1
Rodigas, T. J., Follette, K. B., Weinberger, A., Close, L., & Hines, D. C. 2014, The Astrophysical Journal Letters, 791, L37
Rodigas, T. J., Males, J. R., Hinz, P. M., Mamajek, E. E., & Knox, R. P. 2011, The Astrophysical Journal, 732, 10
Rodigas, T. J., Weinberger, A., Mamajek, E. E., et al. 2015, ApJ, 811, 1
Rodigas, T. J., Arriagada, P., Faherty, J., et al. 2016, ApJ, 818, 1
Rodriguez, D. R., Bessell, M. S., Zuckerman, B., & Kastner, J. H. 2011a, The Astrophysical Journal, 727, 62
Rodriguez, D. R., Zuckerman, B., Kastner, J. H., et al. 2013, ApJ, 774, 101
Rodriguez, D. R., Zuckerman, B., Melis, C., & Song, I. 2011b, The Astrophysical Journal, 732, L29
Rosotti, G. P., Juhasz, A., Booth, R. A., & Clarke, C. J. 2016, MNRAS, 1
Rouan, D., Riaud, P., Boccaletti, A., Clénet, Y., & Labeyrie, A. 2000, The Publications of the Astronomical Society of the Pacific, 112, 1479
Ryu, T., Sato, B., Kuzuhara, M., et al. 2016, arXiv, 1603.02017v1
Sallum, S., Follette, K. B., Eisner, J. A., et al. 2015a, Nature, 527, 342
Sallum, S., Eisner, J. A., Close, L. M., et al. 2015b, ApJ, 801, 85
Santos, N. C., Mayor, M., Naef, D., et al. 2002, A&A, 392, 215
Sartoretti, P., Brown, R. A., & Latham, D. W. 1998, Astronomy and . . .
Saumon, D., & Marley, M. S. 2008, The Astrophysical Journal, 689, 1327
Savransky, D. 2015, ApJ, 800, 100
Schlieder, J. E., Lépine, S., & Simon, M. 2010, The Astronomical Journal, 140, 119
—. 2012a, The Astronomical Journal, 143, 80
—. 2012b, The Astronomical Journal, 144, 109
Schlieder, J. E., Skemer, A. J., Maire, A.-L., et al. 2016, ApJ, 818, 1
Schneider, A. C., Windsor, J., Cushing, M. C., Kirkpatrick, J. D., & Wright, E. L. 2016, The Astrophysical Journal Letters, 822, 1
Schnupp, C., Bergfors, C., Brandner, W., et al. 2010, arXiv, astro-ph.SR
Scholz, A., Jayawardhana, R., Muzic, K., et al. 2012, ApJ, 756, 24
Scholz, R.-D. 2010, A&A, 515, A92
Schroeder, D. J., Golimowski, D. A., Brukardt, R. A., et al. 2000, The Astronomical . . .
Serabyn, E., Mawet, D., & Burruss, R. 2010, Nature, 464, 1018
Shkolnik, E., Liu, M. C., & Reid, I. N. 2009, The Astrophysical Journal, 699, 649
Shkolnik, E. L., Anglada-Escudé, G., Liu, M. C., et al. 2012, The Astrophysical Journal, 758, 56
Silk, J. 1977, Astrophysical Journal, 214, 152
Skemer, A. J., & Close, L. M. 2011, ApJ, 730, 53
Skemer, A. J., Marley, M. S., Hinz, P. M., et al. 2014a, ApJ, 792, 17
Skemer, A. J., Hinz, P., Esposito, S., et al. 2014b, in SPIE Astronomical Telescopes + Instrumentation, ed. E. Marchetti, L. M. Close, & J.-P. Veran (SPIE), 91480L
Skemer, A. J., Hinz, P., Montoya, M., et al. 2015, in SPIE Optical Engineering + Applications, ed. S. Shaklan (SPIE), 96051D
Skemer, A. J., Morley, C. V., Zimmerman, N. T., et al. 2016, ApJ, 817, 1
Smith, B. A., & Terrile, R. J. 1984, Science
Snellen, I., de Kok, R., Birkby, J. L., et al. 2015, A&A, 576, A59
Snellen, I. A. G., Brandl, B. R., de Kok, R. J., et al. 2014, Nature, 508, 63
Soderblom, D. R. 2010, Annu. Rev. Astro. Astrophys., 48, 581
Soderblom, D. R., Hillenbrand, L. A., Jeffries, R. D., Mamajek, E. E., & Naylor, T. 2014, . . . and Planets VI
Song, I., Zuckerman, B., & Bessell, M. S. 2003, The Astrophysical Journal, 599, 342
Soummer, R. 2005, The Astrophysical Journal, 618, L161
Soummer, R., Hagan, J. B., Pueyo, L., et al. 2011, The Astrophysical Journal, 741, 55
Soummer, R., Pueyo, L., & Larkin, J. 2012, The Astrophysical Journal, 755, L28
Sozzetti, A., Giacobbe, P., Lattanzi, M. G., et al. 2013, Monthly Notices RAS, 437, 497
Spergel, D., Gehrels, N., Baltay, C., et al. 2015, arXiv, 1
Spiegel, D. S., & Burrows, A. 2012, The Astrophysical Journal, 745, 174
Spiegel, D. S., Burrows, A., & Milsom, J. A. 2011, The Astrophysical Journal, 727, 57
Stevenson, D. J. 1991, IN: Annual review of astronomy and astrophysics. Vol. 29 (A92-18081 05-90). Palo Alto, 29, 163
Stolker, T., Dominik, C., Avenhaus, H., et al. 2016, arXiv, 1603.00481v1
Stone, J. M., Skemer, A. J., Kratter, K. M., et al. 2016, The Astrophysical Journal Letters, 818, 1
Stumpf, M. B., Brandner, W., Joergens, V., et al. 2010, The Astrophysical Journal, 724, 1
Su, K., Rieke, G. H., & Misselt, K. A. 2005, The Astrophysical . . .
Su, K. Y. L., Rieke, G. H., Malhotra, R., et al. 2013, ApJ, 763, 118
Sudol, J. J., & Haghighipour, N. 2012, ApJ, 755, 38
Tamura, M. 2016, Proceedings of the Japan Academy. Ser. B: Physical and Biological Sciences, 92, 45
Tamura, M., SEEDS team, Usuda, T., Tamura, M., & Ishii, M. 2009, in EXOPLANETS AND DISKS: THEIR FORMATION AND DIVERSITY: Proceedings of the International Conference, AA(National Astronomical Observatory of Japan, Mitaka, Tokyo 181-8588 motohide.tamuraatnao.ac.jp) (AIP), 11–16
Tanner, A., Beichman, C., Akeson, R., et al. 2007, The Publications of the Astronomical Society of the Pacific, 119, 747
Tanner, A. M., Gelino, C. R., & Law, N. M. 2010, Publications of the Astronomical Society of the Pacific, 122, 1195
Terebey, S., van Buren, D., Matthews, K., & Padgett, D. L. 2000, The Astronomical Journal, 119, 2341
Terebey, S., van Buren, D., Padgett, D. L., Hancock, T., & Brundage, M. 1998, The Astrophysical Journal, 507, L71
Thalmann, C., Schmid, H. M., Boccaletti, A., et al. 2008, in SPIE Astronomical Telescopes + Instrumentation, ed. I. S. McLean & M. M. Casali (SPIE), 70143F
Thalmann, C., Carson, J., Janson, M., et al. 2009, The Astrophysical Journal, 707, L123
Thalmann, C., Grady, C. A., Goto, M., et al. 2010, The Astrophysical Journal Letters, 718, L87
Thalmann, C., Usuda, T., Kenworthy, M., et al. 2011, The Astrophysical Journal, 732, L34
Thalmann, C., Desidera, S., Bonavita, M., et al. 2014, A&A, 572, A91
Thomas, S., Belikov, R., & Bendek, E. 2015, ApJ, 810, 1
Tinney, C. G., Faherty, J. K., Kirkpatrick, J. D., et al. 2014, ApJ, 796, 39

Todorov, K., Luhman, K. L., & Mcleod, K. K. 2010, The Astrophysical Journal, 714, L84
Todorov, K. O., Line, M. R., Pineda, J. E., et al. 2015, arXiv, 1504.00217v3
Todorov, K. O., Luhman, K. L., Konopacky, Q. M., et al. 2014, ApJ, 788, 40
Tokovinin, A. 2014, The Astronomical Journal, 147, 87
Torres, C. A. O., Quast, G. R., Melo, C. H. F., & Sterzik, M. F. 2008, in Young Nearby Loose Associations, ed. B. Reipurth (San Francisco, CA: ASP), 757
Torres, G. 1999, The Publications of the Astronomical Society of the Pacific, 111, 169
Traub, W. A., & Oppenheimer, B. R. 2010, Exoplanets, 111
Traub, W. A., Belikov, R., Guyon, O., et al. 2014, in SPIE Astronomical Telescopes + Instrumentation, ed. J. M. Oschmann, M. Clampin, G. G. Fazio, & H. A. MacEwen (SPIE), 91430N
Trilling, D. E., Bryden, G., Beichman, C. A., et al. 2008, The Astrophysical Journal, 674, 1086
Troy, M., Dekany, R. G., Brack, G., et al. 2000, Proc. SPIE Vol. 4007, 4007, 31
Vigan, A., Gry, C., Salter, G., et al. 2015, Monthly Notices RAS, 454, 129
Vigan, A., Langlois, M., Moutou, C., & Dohlen, K. 2008, A&A, 489, 1345
Vigan, A., Moutou, C., Langlois, M., et al. 2010, Monthly Notices RAS, 407, 71
Vigan, A., Patience, J., Marois, C., et al. 2012, A&A, 544, 9
Vigan, A., Bonnefoy, M., Ginski, C., et al. 2016, A&A, 587, A55
Wahhaj, Z., Koerner, D. W., Ressler, M. E., et al. 2003, The Astrophysical Journal, 584, L27
Wahhaj, Z., Liu, M. C., Biller, B. A., et al. 2011, The Astrophysical Journal, 729, 139
—. 2013a, ApJ, 779, 80
Wahhaj, Z., Liu, M. C., Nielsen, E. L., et al. 2013b, The Astrophysical Journal, 773, 179
Wahhaj, Z., Liu, M. C., Biller, B. A., et al. 2014, arXiv, 1404.6525v1
Wahhaj, Z., Cieza, L. A., Mawet, D., et al. 2015, A&A, 581, A24
Wang, J., Xie, J.-W., Barclay, T., & Fischer, D. A. 2014, ApJ, 783, 4
White, R. J., & Ghez, A. M. 2001, The Astrophysical Journal, 556, 265
Williams, J. P., & Cieza, L. A. 2011, Annu. Rev. Astro. Astrophys., 49, 67
Wilner, D. J., Holman, M. J., & Kuchner, M. J. 2002, The Astrophysical . . .
Winn, J. N., & Fabrycky, D. C. 2015, Annu. Rev. Astro. Astrophys., 53, 409
Winters, J. G., Henry, T. J., Lurie, J. C., et al. 2015, The Astronomical Journal, 149, 1
Wöllert, M., Brandner, W., Reffert, S., et al. 2014, A&A, 564, A10
Wright, J. T., Marcy, G. W., Howard, A. W., et al. 2012, ApJ, 753, 160
Wright, J. T., Fakhouri, O., Marcy, G. W., et al. 2011, Publications of the Astronomical Society of the Pacific, 123, 412
Wu, Y.-L., Close, L. M., Males, J. R., et al. 2015, The Astrophysical Journal Letters, 807, 1
Wyatt, M. C. 2008, Annu. Rev. Astro. Astrophys., 46, 339
Wyatt, M. C., Holmes, E. K., Piña, R. K., et al. 1999, ApJ, 527, 918
Wyatt, M. C., Kennedy, G., Sibthorpe, B., et al. 2012, Monthly Notices RAS, 424, 1206
Yamamoto, K., Matsuo, T., Shibai, H., et al. 2013, PASJ, 1306.3100
Zahnle, K. J., & Marley, M. S. 2014, ApJ, 797, 41
Zapatero Osorio, M. R., Rebolo, R., Bihain, G., et al. 2010, The Astrophysical Journal, 715, 1408
Zhou, Y., Apai, D., Schneider, G. H., Marley, M. S., & Showman, A. P. 2016, ApJ, 818, 1
Zhou, Y., Herczeg, G. J., Kraus, A. L., Metchev, S., & Cruz, K. L. 2014, The Astrophysical Journal, 783, L17
Zhu, Z., Dong, R., Stone, J. M., & Rafikov, R. R. 2015, ApJ, 813, 1
Zimmerman, N., Brenner, D., Oppenheimer, B. R., et al. 2011, Publications of the Astronomical Society of the Pacific, 123, 746
Zimmerman, N., Oppenheimer, B. R., Hinkley, S., et al. 2010, The Astrophysical Journal, 709, 733
Zucker, S., Mazeh, T., Santos, N. C., Udry, S., & Mayor, M. 2003, A&A, 404, 775
—. 2004, A&A, 426, 695
Zuckerman, B. 2001, Annu. Rev. Astro. Astrophys., 39, 549
Zuckerman, B., Rhee, J. H., Song, I., & Bessell, M. S. 2011, The Astrophysical Journal, 732, 61
Zuckerman, B., & Song, I. 2004, Annu. Rev. Astro. Astrophys., 42, 685
Zuckerman, B., Song, I., Bessell, M. S., & Webb, R. A. 2001, The Astrophysical Journal, 562, L87
Zurlo, A., Vigan, A., Hagelberg, J., et al. 2013, A&A, 554, A21
Zurlo, A., Vigan, A., Galicher, R., et al. 2016, A&A, 587, A57

TABLE 1
Directly Imaged Planets and Planet Candidates with Inferred Masses $\lesssim$13 $M_{\rm Jup}$

Name	Mass[a] ($M_{\rm Jup}$)	Luminosity (log ($L_{\rm Bol}/L_\odot$))	Age (Myr)	Sep. ($''$)	Sep. (AU)	NIR SpT	Orbital Motion?	Pri. Mult.[b]	Pri. Mass ($M_\odot$)	Referenc
Close-in Planets (<100 AU)										
51 Eri b	2 ± 1	–5.6 ± 0.2	23 ± 3	0.45	13	T4.5–T6	Yes	S	1.75	1, 2, 3
HD 95086 b	5 ± 2	–4.96 ± 0.10	17 ± 4	0.6	56	L/T:	Yes	S	1.6	4–7
HR 8799 b	5 ± 1	–5.1 ± 0.1	40 ± 5	1.7	68	∼L/Tpec	Yes	S	1.5	8–11
LkCa 15 b[c]	6 ± 4	···	2 ± 1	0.08	20	···	Yes	S	1.0	12–15
HR 8799 c	7 ± 2	–4.7 ± 0.1	40 ± 5	0.95	38	∼L/Tpec	Yes	S	1.5	8–11
HR 8799 d	7 ± 2	–4.7 ± 0.2	40 ± 5	0.62	24	∼L7pec	Yes	S	1.5	8, 10, 1
HR 8799 e	7 ± 2	–4.7 ± 0.2	40 ± 5	0.38	14	∼L7pec	Yes	S	1.5	10, 11, 1
β Pic b	12.7 ± 0.3	–3.78 ± 0.03	23 ± 3	0.4	9	L1	Yes	S	1.6	17–20
Planetary-Mass Companions on Wide Orbits (>100 AU)										
WD 0806-661 b	7.5 ± 1.5	···	2000 ± 500	130	2500	Y?	No	S	2.0[d]	21–23
Ross 458 c	9 ± 3	–5.62 ± 0.03	150–800	102	1190	T8.5pec	No	B	0.6, 0.09	24–28
ROXs 42B b	10 ± 4	–3.07 ± 0.07	3 ± 2	1.2	140	L1	Yes	B	0.89, 0.36	29–33
HD 106906 b	11 ± 2	–3.64 ± 0.08	13 ± 2	7.1	650	L2.5	No	B	1.5	34, 35
GU Psc b	11 ± 2	–4.75 ± 0.15	120 ± 10	42	2000	T3.5	No	S	0.30	36
CHXR 73 b	13 ± 6	–2.85 ± 0.14	2 ± 1	1.3	210	≥M9.5	No	S	0.30	37
SR12 C	13 ± 2	–2.87 ± 0.20	3 ± 2	8.7	1100	M9.0	No	B	1.0, 0.5	31, 38
TYC 9486-927-1 b	12–15	···	10–45	217	6900	L3	No	S	0.4	39, 40
Planetary-Mass Companions Orbiting Brown Dwarfs										
2M1207–3932 b	5 ± 2	–4.68 ± 0.05	10 ± 3	0.8	41	L3	No	S	0.024	41–44, 1
2M0441+2301 Bb	10 ± 2	–3.03 ± 0.09	2 ± 1	12/0.1	1800/15	L1	Yes	B/S	0.2, 0.018	45–47
Candidate Planets and Companions Near the Deuterium-Burning Limit										
1RXS J1609–2105 B	14 ± 2	–3.36 ± 0.09	11 ± 2	2.2	330	L2	No	S	0.85	48–51
2M0103–5515 b	13–35	–3.49 ± 0.11	45 ± 4	1.7	84	···	Yes	B	0.19, 0.17	52, 53, 1
2M0122–2439 B	12–27	–4.19 ± 0.10	120 ± 10	1.4	52	L4	No	S	0.4	53, 54
2M0219–3925 B	14 ± 1	–3.84 ± 0.05	45 ± 4	4.0	156	L4	No	S	0.11	55
AB Pic B	13–30	–3.7 ± 0.2	45 ± 4	5.5	250	L0	No	S	0.95	56, 57
CFBDSIR J1458+1013 B	5–20	–6.74 ± 0.19	1000–5000	0.1	2.6	Y0:	Yes	S	0.01–0.04	58, 59
DH Tau B	8–22	–2.71 ± 0.12	2 ± 1	2.3	340	M9.25	No	S	0.5	60, 37, 1
Fomalhaut b	$\lesssim$2	···	440 ± 40	13	119	···	Yes	S	1.92	61–64
FU Tau B	∼16	–2.60	2 ± 1	5.7	800	M9.25	No	S	0.05	65
FW Tau b	∼10–100	···	2 ± 1	2.3	330	pec	No	B	0.3, 0.3	29, 31, 6
G196-3 B	12–25	–3.8 ± 0.2	20–85	16	400	L3	No	S	0.43	67–69, 53
GJ 504 b	3–30	–6.13 ± 0.03	100–6500	2.5	44	T:	Yes	S	1.16	70–73
GJ 758 B	10–40	–6.1 ± 0.2	1000–6000	1.9	29	T8:	Yes	S	1.0	74–77
GSC 6214-210 B	15 ± 2	–3.1 ± 0.1	11 ± 2	2.2	320	M9.5	No	S	0.9	50, 31, 78
HD 100546 b	∼10 ± 5	···	5–10	0.48	53	···	No	S	2.4	80–82
HD 100546 c	<20	···	5–10	0.13	13	···	No	S	2.4	83
HD 203030 B	12–30	–4.64 ± 0.07	130–400	12	490	L7.5	Yes	S	0.95	84, 85
HN Peg B	12–31	–4.77 ± 0.03	300 ± 200	43	800	T2.5	No	S	1.07	85, 86
κ And b	12–66	–3.76 ± 0.06	40–300	1.1	55	L1	No	S	2.8	87–90
LkCa 15 c[c]	<10	···	2 ± 1	0.08	15	···	Yes	S	1.0	14, 15
LkCa 15 d	<10	···	2 ± 1	0.09	18	···	Yes	S	1.0	14, 15
LP 261-75 B	12–26	–4.43 ± 0.09	100–200	14	450	L4.5	No	S	0.22	91, 53
ROXs12 B	16 ± 4	···	8 ± 3	1.8	210	···	Yes	S	0.9	29, 33
SDSS2249+0044 A	12–60	–3.9 ± 0.3	20–300	0.3/49	17/2600	L3	No	S/S	···	92
SDSS2249+0044 B	8–52	–4.2 ± 0.3	20–300	0.3	17	L5	No	S	0.03	92
VHS1256–1257 b	10–21	–5.05 ± 0.22	150–300	8.1	102	L7	No	B	0.07, 0.07	93, 94
WISE J0146+4234 B	4–16	–7.01 ± 0.22	1000-10000	0.09	1	Y0	Yes	S	0.005–0.016	95
WISE J1217+1626 B	5–20	–6.79 ± 0.18	1000–5000	0.08	8	Y0	No	S	0.01–0.04	96

References. — (1) Macintosh et al. (2015); (2) De Rosa et al. (2015); (3) Mamajek & Bell (2014); (4) Rameau et al. (2013c); (5) Meshkat et al. (201 (6) De Rosa et al. (2016); (7) Rameau et al. (2016); (8) Marois et al. (2008); (9) Rajan et al. (2015); (10) Bonnefoy et al. (2016); (11) Bell et al. (2015); (Kraus & Ireland (2012); (13) Ireland & Kraus (2014); (14) Sallum et al. (2015a); (15) Andrews et al. (2013); (16) Marois et al. (2010b); (17) Lagrange et (2009a); (18) Lagrange et al. (2010); (19) Morzinski et al. (2015); (20) Bonnefoy et al. (2013); (21) Luhman et al. (2011); (22) Luhman et al. (2012); (Rodriguez et al. 2011b; (24) Goldman et al. (2010); (25) Scholz (2010); (26) Burgasser et al. (2010); (27) Burningham et al. (2011); (28) Beuzit et (2004); (29) Kraus et al. (2014a); (30) Currie et al. (2014b); (31) Bowler et al. (2014); (32) Currie et al. (2014a); (33) Bryan et al., submitted; (Bailey et al. (2014); (35) Lagrange et al. (2016); (36) Naud et al. (2014); (37) Luhman et al. (2006); (38) Kuzuhara et al. (2011); (39) Deacon et al. (20 (40) Reid et al. (2008); (41) Chauvin et al. (2004); (42) Chauvin et al. (2005a); (43) Barman et al. (2011b); (44) Allers & Liu (2013); (45) Todorov et (2010); (46) Todorov et al. (2014); (47) Bowler & Hillenbrand (2015); (48) Lafrenière et al. (2008); (49) Lafrenière et al. (2010); (50) Ireland et al. (20 (51) Wu et al. (2015); (52) Delorme et al. (2013); (53) Bowler et al. (2013); (54) Hinkley et al. (2015a); (55) Artigau et al. (2015); (56) Chauvin et al. (200 (57) Bonnefoy et al. (2010); (58) Liu et al. (2011); (59) Liu et al. (2012); (60) Itoh et al. (2005); (61) Kalas et al. (2008b); (62) Kalas et al. (2013); (Mamajek (2012); (64) Janson et al. (2012); (65) Luhman et al. (2009b); (66) White & Ghez (2001); (67) Rebolo et al. (1998); (68) Zapatero Osorio et (2010); (69) Gaidos et al. (2014); (70) Kuzuhara et al. (2013); (71) Janson et al. (2013b); (72) Fuhrmann & Chini (2015); (73) Skemer et al. (2016); (Thalmann et al. (2009); (75) Currie et al. (2010); (76) Janson et al. (2011b); (77) Vigan et al. (2016); (78) Bowler et al. (2011); (79) Lachapelle et (2015); (80) Quanz et al. (2013); (81) Currie et al. (2014d); (82) Quanz et al. (2015); (83) Currie et al. (2015); (84) Metchev & Hillenbrand (2006); (Tokovinin (2014); (86) Luhman et al. (2007); (87) Carson et al. (2013); (88) Hinkley et al. (2013); (89) Bonnefoy et al. (2014a); (90) Jones et al. 2016; (Reid & Walkowicz (2006); (92) Allers et al. (2010); (93) Gauza et al. (2015); (94) Stone et al. (2016); (95) Dupuy et al. (2015a); (96) Liu et al. (2012)

[a] Inferred masses assume hot-start evolutionary models.

[b] Multiplicity of the host star interior to the companion's orbit.

[c] LkCa 15 "b" from Kraus & Ireland (2012) is planet "c" in Sallum et al. (2015a). Here I use the original nomenclature from Kraus et al; LkCa15 c in table is the candidate planet "b" from Sallum et al.

TABLE 2
Directly Imaged Stellar and Substellar Companions Inducing Shallow Radial Velocity Trends

Name	Separation ($''$)	Separation (AU)	Nature of Companion	Comp. Mass ($M_\odot$)	Companion SpT	Planet Host?	dv/dt (m s^{-1} yr^{-1})	References
HD 19467 B	1.65	51	BD	0.050	T5.5	No	–1.37 ± 0.09	1, 2
HD 4747 B	0.60	11.3	BD	0.057	···	No	–30.7 ± 0.6[a]	3
HR 7672 B	0.5	18	BD	0.066	L4.5	No	–24 ± 0.6[a]	4, 5
HIP 71898 B	3.0	30	LMS	0.074	L0	No	8.6 ± 0.4	6, 7, 8
HD 5608 B	0.6	34	LMS	0.10	···	Yes	–5.51 ± 0.45	9
HD 68017 B	0.59	13	LMS	0.15	[M5]	No	16.3 ± 0.9[a]	10
HD 7449 B	0.54	18	LMS	0.2	[M4.5]	Yes	···[a]	11
Gl 15 B	41	146	LMS	0.2	M3.5	Yes	–0.27 ± 0.09	12
HD 104304 B	1.0	13	LMS	0.21	[M4]	No	···[a]	13
HD 109272 B	1.2	59	LMS	0.28	···	No	2.4 ± 0.2	9
HD 71881 B	0.85	35	LMS	0.29	[M3]	No	–10.3 ± 0.2	10
Kepler-444 BC	1.8	66	LMS	0.29+0.25	[M]	Yes	–7.8 ± 0.5	14
HD 164509 B	0.75	39	LMS	0.33	[M]	Yes	–3.3 ± 0.5	15
HD 126614 B	0.49	33	LMS	0.33	[M]	Yes	16.2 ± 0.2	16
HD 197037	3.7	24	LMS	0.34	[M]	Yes	–1.9 ± 0.3	17
HAT-P-10 B	0.34	42	LMS	0.36	[M]	Yes	–5.1 ± 1.4	18, 19
HD 41004 A	0.5	22	LMS	0.4	K1	Yes	105 ± 10[a]	20, 21, 22
HD 77407 B	1.7	50	LMS	0.4	[M2]	No	···	23
γ Cep B	0.88	20	LMS	0.41	[M4]	Yes	···[a]	24
HD 8375 C	0.3	17	LMS	0.5	[M1]	No	52.9 ± 1.9	25
HD 196885 B	0.7	23	LMS	0.5	M1	Yes	···[a]	26, 27
HD 114174 B	0.69	18	WD	0.54	···	No	61.1 ± 0.1[a]	28, 29
HD 8049 B	1.5	50	WD	0.56	···	No	···	30
HD 195109 B	2.4	92	LMS	0.58	···	Yes	1.9	15
Gl 86 B	2.3	28	WD	0.59	DQ6	Yes	131	31–36
Procyon B	4.3	15	WD	0.59	DQZ	No	···[a]	37, 38, 39
γ Hya B	1.6	66	LMS	0.61	···	No	4.1 ± 0.2	9
HD 53665 B	0.14	103	LMS	0.7	[K7]	No	5.3 ± 0.3	40

References. — (1) Crepp et al. (2014); (2) Crepp et al. (2015); (3) Crepp et al. (2016); (4) Liu et al. (2002); (5) Crepp et al. (2012a); (6) Montet et al. (2014); (7) Golimowski et al. (2004b) (8) Forveille et al. (2004); (9) Ryu et al. (2016); (10) Crepp et al. (2012b); (11) Rodigas et al. (2016); (12) Howard et al. (2014); (13) Schnupp et al. (2010); (14) Dupuy et al. (2016); (15) Bryan et al. (2016); (16) Howard et al. (2010); (17) Ginski et al. (2016); (18) Knutson et al. (2014); (19) Ngo et al. (2015); (20) Santos et al. (2002); (21) Zucker et al. (2003); (22) Zucker et al. (2004); (23) Mugrauer et al. (2004); (24) Neuhäuser et al. (2007); (25) Crepp et al. (2013b); (26) Chauvin et al. (2007); (27) Chauvin et al. (2011); (28) Crepp et al. (2013a); (29) Matthews et al. (2014b); (30) Zurlo et al. (2013); (31) Queloz et al. (2000); (32) Els et al. (2001); (33) Mugrauer & Neuhäuser (2005); (34) Chauvin et al. (2006); (35) Lagrange et al. (2006); (36) Farihi et al. (2013); (37) Irwin et al. (1992); (38) Torres (1999); (39) Bond et al. (2015); (40) Crepp et al. (2012b).

[a] Radial velocities show both acceleration and curvature.

TABLE 3
THE FREQUENCY OF 5–13 $M_{\rm Jup}$ PLANETS ON WIDE ORBITS

Sample	Number of Stars	Occurrence Rate (10–100 AU)	Occurrence Rate (30–300 AU)	Occurrence Rate (10–1000 AU)	Occurrence Rate (100–1000 AU)
BA	110	$7.7^{+9.0}_{-6.0}$%	$2.8^{+3.7}_{-2.3}$%	$3.5^{+4.7}_{-2.5}$%	<6.4%
FGK	155	<6.8%	<4.1%	<5.8%	<5.1%
M	118	<4.2%	<3.9%	<5.4%	<7.3%
All Stars	384	$0.8^{+1.2}_{-0.5}$%	$0.6^{+0.7}_{-0.5}$%	$0.8^{+1.0}_{-0.6}$%	<2.1%

NOTE. — Assumes circular orbits, logarithmically-flat planet mass-period distributions, and hot-start evolutionary models from Baraffe et al. (2003). All binaries within 100 AU of the host stars have been removed. Occurrence rates are 68% credible intervals and upper limits are 95% confidence values.

APPENDIX

ASTROMETRY OF HR 8799 BCDE AND β PIC B

TABLE 4
ASTROMETRY OF HR 8799 BCDE AND β PIC B UNTIL 2016

UT Date	Epoch	Telescope/ Instrument	ρ ($''$)	θ ($^\circ$)	$\Delta_{\rm R.A.}$ ($''$)	$\Delta_{\rm Dec}$ ($''$)	Reference
			HR 8799 b				
1998 Oct 30	1998.828	*HST*/NICMOS	1.721 ± 0.012	55.1 ± 0.4	1.411 ± 0.009	0.986 ± 0.009	Lafrenière et al. (200
1998 Oct 30[a]	1998.828	*HST*/NICMOS	1.738 ± 0.018	54.7 ± 0.4	[1.418 ± 0.016]	[1.00 ± 0.014]	Soummer et al. (201
2002 Jul 19	2002.545	Subaru/CIAO	[1.74 ± 0.03]	[58.2 ± 0.6]	1.481 ± 0.023	0.919 ± 0.017	Fukagawa et al. (200
2004 Jul 14	2004.534	Keck/NIRC2	[1.716 ± 0.007]	[59.0 ± 0.17]	1.471 ± 0.005	0.884 ± 0.005	Marois et al. (2008
2005 Jul 15	2005.534	Keck/NIRC2	[1.724 ± 0.007]	[60.2 ± 0.17]	1.496 ± 0.005	0.856 ± 0.005	Currie et al. (2012a
2007 Aug 02	2007.583	Keck/NIRC2	[1.726 ± 0.004]	[61.8 ± 0.1]	1.522 ± 0.003	0.815 ± 0.003	Metchev et al. (200
2007 Aug 02[a]	2007.583	Keck/NIRC2	[1.721 ± 0.004]	[60.90 ± 0.10]	1.504 ± 0.003	0.837 ± 0.003	Konopacky et al. (20
2007 Oct 25	2007.813	Gemini-N/NIRI	[1.713 ± 0.007]	[62.0 ± 0.17]	1.512 ± 0.005	0.805 ± 0.005	Marois et al. (2008
2007 Oct 25[a]	2007.813	Keck/NIRC2	[1.717 ± 0.010]	[60.9 ± 0.2]	1.500 ± 0.007	0.836 ± 0.007	Konopacky et al. (20
2008 Jul 11	2008.523	Keck/NIRC2	[1.723 ± 0.006]	[62.4 ± 0.13]	1.527 ± 0.004	0.799 ± 0.004	Marois et al. (2008
2008 Aug 12	2008.613	Keck/NIRC2	[1.724 ± 0.003]	[62.3 ± 0.07]	1.527 ± 0.002	0.801 ± 0.002	Marois et al. (2008
2008 Sep 18	2008.715	Keck/NIRC2	[1.724 ± 0.004]	[62.4 ± 0.10]	1.528 ± 0.003	0.798 ± 0.003	Marois et al. (2008
2008 Sep 18[a]	2008.715	Keck/NIRC2	[1.723 ± 0.006]	[61.65 ± 0.13]	1.516 ± 0.004	0.818 ± 0.004	Konopacky et al. (20
2008 Nov 21	2008.890	MMT/Clio	[1.728 ± 0.017]	[63.2 ± 0.4]	1.54 ± 0.01	0.780 ± 0.014	Hinz et al. (2010)
2008 Nov 21[a]	2008.890	MMT/Clio	[1.73 ± 0.03]	[62.5 ± 0.7]	1.532 ± 0.02	0.796 ± 0.02	Currie et al. (2011b
2009 Aug 15	2009.619	Subaru/IRCS	[1.725 ± 0.014]	[62.9 ± 0.3]	1.536 ± 0.01	0.785 ± 0.01	Currie et al. (2011b
2009 Sep 12	2009.695	MMT/Clio	[1.72 ± 0.04]	[63.2 ± 1.0]	1.538 ± 0.03	0.777 ± 0.03	Currie et al. (2011b
2009 Oct 06	2009.761	VLT/NaCo	[1.74 ± 0.03]	[62.0 ± 0.7]	1.535 ± 0.02	0.816 ± 0.02	Bergfors et al. (201
2009 Oct 08	2009.767	VLT/NaCo	[1.720 ± 0.010]	[62.9 ± 0.2]	1.532 ± 0.007	0.783 ± 0.007	Currie et al. (2011b
2009 Jul 11	2009.523	Palomar/WCS	1.73 ± 0.10	62.9 ± 1.5	1.54 ± 0.04	0.79 ± 0.06	Serabyn et al. (201
2009 Jul 30	2009.575	Keck/NIRC2	[1.721 ± 0.006]	[62.42 ± 0.13]	1.526 ± 0.004	0.797 ± 0.004	Konopacky et al. (20
2009 Aug 01	2009.580	Keck/NIRC2	[1.725 ± 0.010]	[62.6 ± 0.2]	1.531 ± 0.007	0.794 ± 0.007	Konopacky et al. (20
2009 Nov 01	2009.832	Keck/NIRC2	[1.74 ± 0.03]	[62.5 ± 0.6]	1.54 ± 0.019	0.80 ± 0.019	Galicher et al. (201
2009 Nov 01	2009.832	Keck/NIRC2	[1.719 ± 0.014]	[62.5 ± 0.3]	1.524 ± 0.010	0.795 ± 0.010	Konopacky et al. (20
2010 Jul 13	2010.528	Keck/NIRC2	[1.720 ± 0.007]	[62.93 ± 0.17]	1.532 ± 0.005	0.783 ± 0.005	Konopacky et al. (20
2010 Oct 30	2010.827	Keck/NIRC2	[1.716 ± 0.021]	[63.5 ± 0.5]	1.535 ± 0.015	0.766 ± 0.015	Konopacky et al. (20
2010 Oct 30[a]	2010.827	Keck/NIRC2	[1.717 ± 0.007]	[64.2 ± 0.17]	1.546 ± 0.005	0.748 ± 0.005	Currie et al. (2012a
2011 Jul 21	2011.550	Keck/NIRC2	[1.719 ± 0.007]	[63.69 ± 0.17]	1.541 ± 0.005	0.762 ± 0.005	Konopacky et al. (20
2011 Oct 16	2011.789	LBT/PISCES	[1.741 ± 0.016]	[65.1 ± 0.4]	1.579 ± 0.011	0.734 ± 0.011	Esposito et al. (201
2011 Nov 09	2011.854	LBT/PISCES	[1.708 ± 0.016]	[64.9 ± 0.4]	1.546 ± 0.011	0.725 ± 0.011	Esposito et al. (201
2012 Jun 14	2012.452	Palomar/P1640	[1.715 ± 0.007]	[65.7 ± 0.17]	1.563 ± 0.005	0.706 ± 0.005	Pueyo et al. (2015
2012 Jul 22	2012.556	Keck/NIRC2	[1.716 ± 0.007]	[64.20 ± 0.17]	1.545 ± 0.005	0.747 ± 0.005	Konopacky et al. (20
2012 Oct 26	2012.819	Keck/NIRC2	[1.718 ± 0.006]	[64.37 ± 0.13]	1.549 ± 0.004	0.743 ± 0.004	Konopacky et al. (20
2013 Oct 16	2013.789	Keck/NIRC2	[1.706 ± 0.031]	[64.9 ± 0.7]	1.545 ± 0.022	0.724 ± 0.022	Konopacky et al. (20
2013 Oct 21	2013.802	LBT/LMIRCam	1.717 ± 0.013	65.46 ± 0.44	1.562 ± 0.008	0.713 ± 0.013	Maire et al. (2015a
2014 Jul 13	2014.528	VLT/SPHERE	[1.722 ± 0.008]	[65.8 ± 1.7]	1.570 ± 0.006	0.707 ± 0.006	Zurlo et al. (2016)
2014 Jul 17	2014.539	Keck/NIRC2	[1.720 ± 0.018]	[65.1 ± 0.4]	1.560 ± 0.013	0.725 ± 0.013	Konopacky et al. (20
2014 Dec 04–08	2014.93	VLT/SPHERE	[1.724 ± 0.007]	[65.9 ± 0.17]	1.574 ± 0.005	0.703 ± 0.005	Zurlo et al. (2016)
2014 Dec 05–09	2014.93	VLT/SPHERE	1.729 ± 0.007	65.93 ± 0.15	[1.579 ± 0.007]	[0.705 ± 0.007]	Apai et al. (2016)
			HR 8799 c				
1998 Oct 30	1998.828	*HST*/NICMOS	0.966 ± 0.022	300 ± 0.8	[–0.84 ± 0.02]	[0.483 ± 0.016]	Soummer et al. (201
2004 Jul 14	2004.534	Keck/NIRC2	[0.960 ± 0.007]	[309.6 ± 0.3]	–0.739 ± 0.005	0.612 ± 0.005	Marois et al. (2008
2005 Jul 15	2005.534	Keck/NIRC2	[0.951 ± 0.007]	[311.5 ± 0.3]	–0.713 ± 0.005	0.630 ± 0.005	Currie et al. (2012a
2007 Aug 02	2007.583	Keck/NIRC2	[0.952 ± 0.007]	[315.1 ± 0.3]	–0.672 ± 0.005	0.674 ± 0.005	Metchev et al. (200
2007 Aug 02[a]	2007.583	Keck/NIRC2	[0.957 ± 0.006]	[314.5 ± 0.2]	–0.683 ± 0.004	0.671 ± 0.004	Konopacky et al. (20
2007 Oct 25	2007.813	Gemini-N/NIRI	[0.958 ± 0.007]	[315.3 ± 0.3]	–0.674 ± 0.005	0.681 ± 0.005	Marois et al. (2008
2007 Oct 25[a]	2007.813	Keck/NIRC2	[0.957 ± 0.010]	[314.9 ± 0.4]	–0.678 ± 0.007	0.676 ± 0.007	Konopacky et al. (20
2008 Jul 11	2008.523	Keck/NIRC2	[0.961 ± 0.006]	[316.8 ± 0.2]	–0.658 ± 0.004	0.701 ± 0.004	Marois et al. (2008
2008 Aug 12	2008.613	Keck/NIRC2	[0.964 ± 0.003]	[317.06 ± 0.12]	–0.657 ± 0.002	0.706 ± 0.002	Marois et al. (2008
2008 Sep 18	2008.715	Keck/NIRC2	[0.964 ± 0.004]	[317.06 ± 0.18]	–0.657 ± 0.003	0.706 ± 0.003	Marois et al. (2008
2008 Sep 18[a]	2008.715	Keck/NIRC2	[0.959 ± 0.004]	[316.27 ± 0.18]	–0.663 ± 0.003	0.693 ± 0.003	Konopacky et al. (20
2008 Nov 21	2008.890	MMT/Clio	[0.921 ± 0.03]	[316.8 ± 1.1]	–0.631 ± 0.015	0.671 ± 0.02	Hinz et al. (2010)
2008 Nov 21[a]	2008.890	MMT/Clio	[0.958 ± 0.03]	[316.9 ± 1.2]	–0.654 ± 0.02	0.700 ± 0.02	Currie et al. (2011b
2009 Jan 09	2009.022	MMT/Clio	[0.90 ± 0.04]	[317.4 ± 1.9]	–0.612 ± 0.03	0.665 ± 0.03	Hinz et al. (2010)
2009 Jul 11	2009.523	Palomar/WCS	1.00 ± 0.06	315.9 ± 1.5	–0.70 ± 0.05	0.72 ± 0.05	Serabyn et al. (201
2009 Jul 30	2009.575	Keck/NIRC2	[0.957 ± 0.006]	[318.1 ± 0.2]	–0.639 ± 0.004	0.712 ± 0.004	Konopacky et al. (20
2009 Aug 01	2009.580	Keck/NIRC2	[0.962 ± 0.013]	[318.7 ± 0.5]	–0.635 ± 0.009	0.722 ± 0.009	Konopacky et al. (20
2009 Sep 12	2009.695	MMT/Clio	[0.96 ± 0.03]	[319.2 ± 1.2]	–0.625 ± 0.02	0.725 ± 0.02	Hinz et al. (2010)
2009 Sep 12[a]	2009.695	MMT/Clio	[0.942 ± 0.04]	[317.7 ± 1.8]	–0.634 ± 0.03	0.697 ± 0.03	Currie et al. (2011b
2009 Oct 06	2009.761	VLT/NaCo	[0.940 ± 0.06]	[317 ± 2]	–0.636 ± 0.04	0.692 ± 0.04	Bergfors et al. (201
2009 Oct 08	2009.767	VLT/NaCo	[0.952 ± 0.010]	[318.8 ± 0.4]	–0.627 ± 0.007	0.716 ± 0.007	Currie et al. (2011b
2009 Nov 01	2009.832	Keck/NIRC2	[0.957 ± 0.018]	[318.8 ± 0.8]	–0.63 ± 0.013	0.72 ± 0.013	Galicher et al. (201

TABLE 4 — *Continued*

UT Date	Epoch	Telescope/ Instrument	ρ ($''$)	θ ($^\circ$)	$\Delta_{\rm R.A.}$ ($''$)	$\Delta_{\rm Dec}$ ($''$)	Reference
2009 Nov 01	2009.832	Keck/NIRC2	[0.961 ± 0.013]	[318.5 ± 0.5]	–0.636 ± 0.009	0.720 ± 0.009	Konopacky et al. (20
2010 Jul 13	2010.528	Keck/NIRC2	[0.956 ± 0.006]	[319.6 ± 0.2]	–0.619 ± 0.004	0.728 ± 0.004	Konopacky et al. (20
2010 Oct 30	2010.827	Keck/NIRC2	[0.960 ± 0.017]	[320.8 ± 0.7]	–0.607 ± 0.012	0.744 ± 0.012	Konopacky et al. (20
2010 Oct 30	2010.827[a]	Keck/NIRC2	[0.949 ± 0.007]	[320.9 ± 0.3]	–0.598 ± 0.005	0.737 ± 0.005	Currie et al. (2012a
2011 Jul 21	2011.550	Keck/NIRC2	[0.955 ± 0.006]	[321.5 ± 0.2]	–0.595 ± 0.004	0.747 ± 0.004	Konopacky et al. (20
2011 Oct 16	2011.789	LBT/PISCES	[0.938 ± 0.014]	[323.3 ± 0.6]	–0.561 ± 0.010	0.752 ± 0.010	Esposito et al. (201
2011 Nov 09	2011.854	LBT/PISCES	[0.960 ± 0.014]	[323.0 ± 0.6]	–0.578 ± 0.010	0.767 ± 0.010	Esposito et al. (201
2012 Jun 14	2012.452	Palomar/P1640	[0.947 ± 0.006]	[323.9 ± 0.2]	–0.558 ± 0.004	0.765 ± 0.004	Pueyo et al. (2015
2012 Jul 22	2012.556	Keck/NIRC2	[0.956 ± 0.007]	[322.8 ± 0.3]	–0.578 ± 0.005	0.761 ± 0.005	Konopacky et al. (20
2012 Oct 26	2012.819	Keck/NIRC2	[0.958 ± 0.004]	[323.32 ± 0.18]	–0.572 ± 0.003	0.768 ± 0.003	Konopacky et al. (20
2013 Oct 16	2013.789	Keck/NIRC2	[0.953 ± 0.031]	[325.3 ± 1.3]	–0.542 ± 0.022	0.784 ± 0.022	Konopacky et al. (20
2013 Oct 21	2013.802	LBT/LMIRCam	0.951 ± 0.014	325.5 ± 0.9	–0.538 ± 0.006	0.784 ± 0.013	Maire et al. (2015a
2014 Jul 13	2014.528	VLT/SPHERE	[0.948 ± 0.006]	[326.6 ± 0.2]	–0.522 ± 0.004	0.791 ± 0.004	Zurlo et al. (2016)
2014 Jul 17	2014.539	Keck/NIRC2	[0.964 ± 0.018]	[325.9 ± 0.8]	–0.540 ± 0.013	0.799 ± 0.013	Konopacky et al. (20
2014 Dec 04–08	2014.93	VLT/SPHERE	[0.951 ± 0.006]	[327.0 ± 0.2]	–0.518 ± 0.004	0.797 ± 0.004	Zurlo et al. (2016)
2014 Dec 05–09	2014.93	VLT/SPHERE	0.947 ± 0.007	327.8 ± 0.4	[–0.504 ± 0.007]	[0.802 ± 0.007]	Apai et al. (2016)
			HR 8799 d				
1998 Oct 30	1998.828	*HST*/NICMOS	0.549 ± 0.028	166 ± 3	[0.13 ± 0.03]	[–0.53 ± 0.03]	Soummer et al. (201
2005 Jul 15	2005.534	Keck/NIRC2	[0.585 ± 0.014]	[188.6 ± 1.0]	–0.087 ± 0.010	–0.578 ± 0.010	Currie et al. (2012a
2007 Aug 02	2007.583	Keck/NIRC2	[0.613 ± 0.011]	[196.1 ± 0.7]	–0.170 ± 0.008	–0.589 ± 0.008	Metchev et al. (200
2007 Aug 02[a,b]	2007.583	Keck/NIRC2	[0.615 ± 0.007]	[196.9 ± 0.5]	–0.179 ± 0.005	–0.588 ± 0.005	Konopacky et al. (20
2007 Oct 25[a]	2007.813	Keck/NIRC2	[0.614 ± 0.014]	[196.5 ± 0.9]	–0.175 ± 0.010	–0.589 ± 0.010	Konopacky et al. (20
2008 Jul 11	2008.523	Keck/NIRC2	[0.618 ± 0.006]	[199.7 ± 0.4]	–0.208 ± 0.004	–0.582 ± 0.004	Marois et al. (2008
2008 Aug 12	2008.613	Keck/NIRC2	[0.621 ± 0.003]	[200.36 ± 0.18]	–0.216 ± 0.002	–0.582 ± 0.002	Marois et al. (2008
2008 Sep 18	2008.715	Keck/NIRC2	[0.621 ± 0.004]	[200.4 ± 0.3]	–0.216 ± 0.003	–0.582 ± 0.003	Marois et al. (2008
2008 Sep 18[a]	2008.715	Keck/NIRC2	[0.622 ± 0.006]	[199.0 ± 0.4]	–0.202 ± 0.004	–0.588 ± 0.004	Konopacky et al. (20
2008 Nov 21	2008.890	MMT/Clio	[0.68 ± 0.02]	[198.9 ± 1.7]	–0.22 ± 0.021	–0.644 ± 0.013	Hinz et al. (2010)
2008 Nov 21[a]	2008.890	MMT/Clio	[0.646 ± 0.03]	[199.6 ± 1.8]	–0.217 ± 0.02	–0.608 ± 0.02	Currie et al. (2011b
2009 Jul 11	2009.523	Palomar/WCS	0.64 ± 0.04	197.5 ± 1.5	–0.19 ± 0.07	–0.61 ± 0.03	Serabyn et al. (201
2009 Jul 30	2009.575	Keck/NIRC2	[0.624 ± 0.004]	[202.3 ± 0.3]	–0.237 ± 0.003	–0.577 ± 0.003	Konopacky et al. (20
2009 Aug 01	2009.580	Keck/NIRC2	[0.622 ± 0.010]	[203.7 ± 0.6]	–0.250 ± 0.007	–0.570 ± 0.007	Konopacky et al. (20
2009 Sep 12	2009.695	MMT/Clio	[0.65 ± 0.04]	[205 ± 3]	–0.28 ± 0.03	–0.59 ± 0.03	Hinz et al. (2010)
2009 Oct 06	2009.761	VLT/NaCo	[0.66 ± 0.10]	[204 ± 6]	–0.270 ± 0.07	–0.600 ± 0.07	Bergfors et al. (201
2009 Oct 08	2009.767	VLT/NaCo	[0.634 ± 0.010]	[202.4 ± 0.6]	–0.241 ± 0.007	–0.586 ± 0.007	Currie et al. (2011b
2009 Nov 01	2009.832	Keck/NIRC2	[0.63 ± 0.02]	[202.5 ± 1.3]	–0.24 ± 0.014	–0.58 ± 0.014	Galicher et al. (201
2009 Nov 01	2009.832	Keck/NIRC2	[0.626 ± 0.010]	[203.7 ± 0.6]	–0.251 ± 0.007	–0.573 ± 0.007	Konopacky et al. (20
2010 Jul 13	2010.528	Keck/NIRC2	[0.634 ± 0.006]	[204.7 ± 0.4]	–0.265 ± 0.004	–0.576 ± 0.004	Konopacky et al. (20
2010 Oct 30	2010.827	Keck/NIRC2	[0.634 ± 0.018]	[207.8 ± 1.2]	–0.296 ± 0.013	–0.561 ± 0.013	Konopacky et al. (20
2010 Oct 30[a]	2010.827	Keck/NIRC2	[0.634 ± 0.007]	[206.5 ± 0.6]	–0.283 ± 0.005	–0.567 ± 0.005	Currie et al. (2012a
2011 Jul 21	2011.550	Keck/NIRC2	[0.638 ± 0.007]	[208.3 ± 0.4]	–0.303 ± 0.005	–0.562 ± 0.005	Konopacky et al. (20
2011 Oct 16	2011.789	LBT/PISCES	[0.637 ± 0.014]	[208.0 ± 0.9]	–0.299 ± 0.010	–0.563 ± 0.010	Esposito et al. (201
2011 Nov 09	2011.854	LBT/PISCES	[0.635 ± 0.014]	[210.2 ± 0.9]	–0.320 ± 0.010	–0.549 ± 0.010	Esposito et al. (201
2012 Jun 14	2012.452	Palomar/P1640	[0.620 ± 0.008]	[211.4 ± 0.6]	–0.323 ± 0.006	–0.529 ± 0.006	Pueyo et al. (2015
2012 Jul 22	2012.556	Keck/NIRC2	[0.650 ± 0.007]	[211.4 ± 0.4]	–0.339 ± 0.005	–0.555 ± 0.005	Konopacky et al. (20
2013 Oct 16	2013.789	Keck/NIRC2	[0.647 ± 0.023]	[216.2 ± 1.4]	–0.382 ± 0.016	–0.522 ± 0.016	Konopacky et al. (20
2013 Oct 21	2013.802	LBT/LMIRCam	0.657 ± 0.013	215.0 ± 1.2	–0.377 ± 0.007	–0.538 ± 0.011	Maire et al. (2015a
2012 Oct 26	2012.819	Keck/NIRC2	[0.648 ± 0.006]	[212.3 ± 0.4]	–0.346 ± 0.004	–0.548 ± 0.004	Konopacky et al. (20
2014 Jul 13	2014.528	VLT/SPHERE	[0.658 ± 0.008]	[216.3 ± 0.5]	–0.390 ± 0.005	–0.530 ± 0.006	Zurlo et al. (2016)
2014 Jul 17	2014.539	Keck/NIRC2	[0.667 ± 0.016]	[216.8 ± 0.9]	–0.400 ± 0.011	–0.534 ± 0.011	Konopacky et al. (20
2014 Aug 12	2014.611	VLT/SPHERE	[0.658 ± 0.006]	[216.5 ± 0.3]	–0.391 ± 0.004	–0.529 ± 0.004	Zurlo et al. (2016)
2014 Dec 04–08	2014.93	VLT/SPHERE	[0.660 ± 0.006]	[217.5 ± 0.3]	–0.402 ± 0.004	–0.523 ± 0.004	Zurlo et al. (2016)
2014 Dec 05–09	2014.93	VLT/SPHERE	0.654 ± 0.007	217.6 ± 0.8	[–0.400 ± 0.009]	[–0.518 ± 0.008]	Apai et al. (2016)
			HR 8799 e				
2009 Jul 30	2009.575	Keck/NIRC2	[0.372 ± 0.010]	[235.4 ± 1.1]	–0.306 ± 0.007	–0.211 ± 0.007	Konopacky et al. (20
2009 Jul 31	2009.578	Keck/NIRC2	[0.369 ± 0.03]	[234 ± 3]	–0.299 ± 0.019	–0.217 ± 0.019	Marois et al. (2010b
2009 Aug 01	2009.580	Keck/NIRC2	[0.368 ± 0.018]	[235 ± 2]	–0.303 ± 0.013	–0.209 ± 0.013	Marois et al. (2010b
2009 Aug 01[a]	2009.580	Keck/NIRC2	[0.373 ± 0.014]	[238.5 ± 1.5]	–0.318 ± 0.010	–0.195 ± 0.010	Konopacky et al. (20
2009 Oct 08	2009.767	VLT/NaCo	[0.375 ± 0.010]	[234.7 ± 1.1]	–0.306 ± 0.007	–0.217 ± 0.007	Currie et al. (2011b
2009 Nov 01	2009.832	Keck/NIRC2	[0.362 ± 0.014]	[237.2 ± 1.6]	–0.304 ± 0.010	–0.196 ± 0.010	Marois et al. (2010b
2009 Nov 01[a]	2009.832	Keck/NIRC2	[0.362 ± 0.013]	[238.9 ± 1.4]	–0.310 ± 0.009	–0.187 ± 0.009	Konopacky et al. (20
2010 Jul 13	2010.528	Keck/NIRC2	[0.368 ± 0.011]	[242.0 ± 1.3]	–0.325 ± 0.008	–0.173 ± 0.008	Marois et al. (2010b
2010 Jul 13[a]	2010.528	Keck/NIRC2	[0.363 ± 0.008]	[242.8 ± 1.0]	–0.323 ± 0.006	–0.166 ± 0.006	Konopacky et al. (20
2010 Jul 21	2010.550	Keck/NIRC2	[0.368 ± 0.016]	[241.6 ± 1.7]	–0.324 ± 0.011	–0.175 ± 0.011	Marois et al. (2010b
2010 Oct 30	2010.827	Keck/NIRC2	[0.371 ± 0.014]	[244.1 ± 1.5]	–0.334 ± 0.010	–0.162 ± 0.010	Marois et al. (2010b
2010 Oct 30[a]	2010.827	Keck/NIRC2	[0.370 ± 0.027]	[247.2 ± 2.5]	–0.341 ± 0.016	–0.143 ± 0.016	Konopacky et al. (20
2011 Jul 21	2011.550	Keck/NIRC2	[0.375 ± 0.011]	[249.7 ± 1.2]	–0.352 ± 0.008	–0.130 ± 0.008	Konopacky et al. (20
2011 Oct 16	2011.789	LBT/PISCES	[0.347 ± 0.016]	[249.9 ± 1.8]	–0.326 ± 0.011	–0.119 ± 0.011	Esposito et al. (201
2011 Nov 09	2011.854	LBT/PISCES	[0.403 ± 0.016]	[251.6 ± 1.6]	–0.382 ± 0.011	–0.127 ± 0.011	Esposito et al. (201
2012 Jun 14	2012.452	Palomar/P1640	[0.377 ± 0.008]	[256.2 ± 0.9]	–0.366 ± 0.006	–0.090 ± 0.006	Pueyo et al. (2015
2012 Jul 22	2012.556	Keck/NIRC2	[0.382 ± 0.011]	[257.3 ± 1.2]	–0.373 ± 0.008	–0.084 ± 0.008	Konopacky et al. (20
2012 Oct 26	2012.819	Keck/NIRC2	[0.378 ± 0.013]	[258.4 ± 1.4]	–0.370 ± 0.009	–0.076 ± 0.009	Konopacky et al. (20

TABLE 4 — *Continued*

UT Date	Epoch	Telescope/ Instrument	ρ ($''$)	θ ($^\circ$)	$\Delta_{\mathrm{R.A.}}$ ($''$)	Δ_{Dec} ($''$)	Reference
2013 Oct 16	2013.789	Keck/NIRC2	[0.373 ± 0.018]	[267.4 ± 2.0]	–0.373 ± 0.013	–0.017 ± 0.013	Konopacky et al. (20
2013 Oct 21	2013.802	LBT/LMIRCam	0.395 ± 0.012	264.8 ± 1.7	–0.394 ± 0.011	–0.036 ± 0.017	Maire et al. (2015a
2014 Jul 13	2014.528	VLT/SPHERE	[0.386 ± 0.012]	[268.8 ± 1.3]	–0.386 ± 0.009	–0.008 ± 0.009	Zurlo et al. (2016)
2014 Jul 17	2014.539	Keck/NIRC2	[0.387 ± 0.016]	[270.4 ± 1.7]	–0.387 ± 0.011	0.003 ± 0.011	Konopacky et al. (20
2014 Aug 12	2014.611	VLT/SPHERE	[0.384 ± 0.003]	[269.3 ± 0.3]	–0.384 ± 0.002	–0.005 ± 0.002	Zurlo et al. (2016)
2014 Dec 04–08	2014.93	VLT/SPHERE	[0.384 ± 0.014]	[272.1 ± 1.5]	–0.384 ± 0.010	0.014 ± 0.010	Zurlo et al. (2016)
2014 Dec 05–09	2014.93	VLT/SPHERE	0.381 ± 0.007	272.5 ± 0.7	[–0.381 ± 0.007]	[0.016 ± 0.005]	Apai et al. (2016)
				β Pic b			
2003 Nov 10	2003.857	VLT/NaCo	0.411 ± 0.008	31.8 ± 1.3	[0.217 ± 0.009]	[0.349 ± 0.008]	Lagrange et al. (200
2003 Nov 10	2003.857	VLT/NaCo	0.411 ± 0.008	31.5 ± 1.3	[0.215 ± 0.009]	[0.350 ± 0.008]	Lagrange et al. (200
2003 Nov 10[a]	2003.857	VLT/NaCo	0.413 ± 0.022	34.4 ± 3.5	[0.233 ± 0.022]	0.341 ± 0.022	Chauvin et al. (201
2003 Nov 13	2003.865	VLT/NaCo	0.401 ± 0.008	32.1 ± 1.4	[0.213 ± 0.009]	[0.340 ± 0.009]	Lagrange et al. (200
2008 Nov 11	2008.862	VLT/NaCo	0.210 ± 0.027	211.5 ± 1.9	[–0.110 ± 0.015]	[–0.179 ± 0.023]	Currie et al. (2011a
2009 Oct 25	2009.813	VLT/NaCo	0.298 ± 0.016	210.6 ± 3.6	[–0.152 ± 0.018]	[–0.257 ± 0.017]	Lagrange et al. (201
2009 Oct 25[a]	2009.813	VLT/NaCo	0.299 ± 0.014	210.7 ± 2.9	–0.153 ± 0.014	–0.257 ± 0.014	Chauvin et al. (201
2009 Nov–Dec[c]	2009.9	VLT/NaCo	0.299 ± 0.016	209.4 ± 3.5	[–0.147 ± 0.018]	[–0.260 ± 0.017]	Lagrange et al. (201
2009 Dec 03	2009.920	Gemini-S/NICI	0.323 ± 0.010	209.3 ± 1.8	[–0.158 ± 0.010]	[–0.282 ± 0.010]	Nielsen et al. (2014
2009 Dec 03	2009.920	Gemini-S/NICI	0.339 ± 0.010	209.2 ± 1.7	[–0.165 ± 0.010]	[–0.296 ± 0.010]	Nielsen et al. (2014
2009 Dec 26	2009.983	VLT/NaCo	0.302 ± 0.016	212.8 ± 3.7	[–0.164 ± 0.019]	[–0.254 ± 0.017]	Lagrange et al. (201
2009 Dec 26[a]	2009.983	VLT/NaCo	0.299 ± 0.013	211.1 ± 1.7	[–0.154 ± 0.010]	[–0.256 ± 0.012]	Milli et al. (2014)
2009 Dec 29	2009.991	VLT/NaCo	0.314 ± 0.016	211.5 ± 3.5	[–0.164 ± 0.018]	[–0.268 ± 0.017]	Lagrange et al. (201
2009 Dec 29[a]	2009.991	VLT/NaCo	0.326 ± 0.013	210.6 ± 1.2	[–0.166 ± 0.009]	[–0.280 ± 0.012]	Currie et al. (2011a
2009 Dec 29[a]	2009.991	VLT/NaCo	0.306 ± 0.009	212.1 ± 1.7	–0.163 ± 0.009]	[–0.260 ± 0.008	Chauvin et al. (201
2010 Mar 20[d]	2010.214	VLT/NaCo	0.345 ± 0.007	209.4 ± 0.3	[–0.169 ± 0.004]	[–0.301 ± 0.006]	Bonnefoy et al. (201
2010 Apr 03	2010.252	VLT/NaCo+APP	0.354 ± 0.012	209.1 ± 2.1	[–0.172 ± 0.013]	[–0.309 ± 0.012]	Quanz et al. (2010
2010 Apr 10[d]	2010.271	VLT/NaCo	0.355 ± 0.002	208.4 ± 1.1	[–0.169 ± 0.006]	[–0.312 ± 0.004]	Bonnefoy et al. (201
2010 Apr 10[a]	2010.271	VLT/NaCo	0.346 ± 0.007	209.9 ± 1.2	–0.173 ± 0.007	–0.300 ± 0.007	Chauvin et al. (201
2010 Sep 28	2010.739	VLT/NaCo	0.383 ± 0.011	210.3 ± 1.7	–0.193 ± 0.011	–0.331 ± 0.011	Chauvin et al. (201
2010 Sep 28[a]	2010.739	VLT/NaCo	0.385 ± 0.011	210.1 ± 1.5	[–0.193 ± 0.010]	[–0.333 ± 0.011]	Milli et al. (2014)
2010 Nov 16	2010.873	VLT/NaCo	0.387 ± 0.008	212.4 ± 1.4	–0.207 ± 0.008	–0.326 ± 0.010	Chauvin et al. (201
2010 Nov 17	2010.876	VLT/NaCo	0.390 ± 0.013	212.3 ± 2.1	–0.209 ± 0.013	–0.330 ± 0.014	Chauvin et al. (201
2010 Dec 25	2010.980	Gemini-S/NICI	0.404 ± 0.010	212.1 ± 0.7	[–0.215 ± 0.007]	[–0.342 ± 0.009]	Boccaletti et al. (20
2010 Dec 25[a]	2010.980	Gemini-S/NICI	0.407 ± 0.005	212.9 ± 1.4	[–0.221 ± 0.009]	[–0.342 ± 0.007]	Nielsen et al. (2014
2011 Jan 02	2011.003	VLT/NaCo	0.408 ± 0.009	211.1 ± 1.5	–0.211 ± 0.009	–0.350 ± 0.010	Chauvin et al. (201
2011 Mar 26	2011.230	VLT/NaCo	0.426 ± 0.013	210.1 ± 1.8	–0.214 ± 0.012	–0.367 ± 0.014	Chauvin et al. (201
2011 Oct 12	2011.778	VLT/NaCo	0.439 ± 0.005	212.9 ± 0.5	[–0.238 ± 0.003]	[–0.369 ± 0.003]	Milli et al. (2014)
2011 Oct 20	2011.800	Gemini-S/NICI	0.455 ± 0.003	211.9 ± 0.4	[–0.240 ± 0.003]	[–0.386 ± 0.003]	Nielsen et al. (2014
2011 Oct 20	2011.800	Gemini-S/NICI	0.452 ± 0.005	211.6 ± 0.6	[–0.237 ± 0.005]	[–0.385 ± 0.005]	Nielsen et al. (2014
2011 Dec 11	2011.942	VLT/NaCo	0.441 ± 0.003	212.9 ± 0.3	[–0.240 ± 0.003]	[–0.370 ± 0.003]	Milli et al. (2014)
2012 Mar 29	2012.341	Gemini-S/NICI	0.447 ± 0.003	210.8 ± 0.4	[–0.229 ± 0.003]	[–0.384 ± 0.003]	Nielsen et al. (2014
2012 Mar 29	2012.341	Gemini-S/NICI	0.448 ± 0.005	211.8 ± 0.6	[–0.236 ± 0.005]	[–0.381 ± 0.005]	Nielsen et al. (2014
2012 Nov 01	2012.835	VLT/NaCo	0.456 ± 0.011	211.9 ± 2.3	–0.241 ± 0.013	–0.387 ± 0.014	Bonnefoy et al. (201
2012 Dec 04	2012.925	Magellan/MagAO	0.470 ± 0.010	212.0 ± 1.2	[–0.249 ± 0.010]	[–0.399 ± 0.010]	Males et al. (2014
2012 Dec 01–07	2012.92	Magellan/MagAO	0.461 ± 0.014	211.9 ± 1.2	[–0.244 ± 0.011]	[–0.391 ± 0.013]	Morzinski et al. (20
2012 Dec 16	2012.958	VLT/NaCo	0.449 ± 0.006	211.6 ± 0.7	[–0.235 ± 0.006]	[–0.382 ± 0.006]	Milli et al. (2014)
2013 Jan 31	2013.082	VLT/NaCo+AGPM	0.452 ± 0.010	211.2 ± 1.3	[–0.234 ± 0.010]	[–0.387 ± 0.010]	Absil et al. (2013)
2013 Jan 31[a]	2013.082	VLT/NaCo+AGPM	0.448 ± 0.004	212.3 ± 0.3	[–0.239 ± 0.003]	[–0.379 ± 0.004]	Milli et al. (2014)
2013 Nov 16	2013.873	Gemini-S/GPI	0.430 ± 0.003	212.3 ± 0.4	[–0.230 ± 0.003]	[–0.363 ± 0.003]	Millar-Blanchaer et al.
2013 Nov 16	2013.873	Gemini-S/GPI	0.426 ± 0.003	212.8 ± 0.4	[–0.231 ± 0.003]	[–0.358 ± 0.003]	Millar-Blanchaer et al.
2013 Nov 18	2013.879	Gemini-S/GPI	0.434 ± 0.006	211.8 ± 0.5	[–0.229 ± 0.005]	[–0.369 ± 0.005]	Macintosh et al. (20
2013 Nov 18[a]	2013.879	Gemini-S/GPI	0.428 ± 0.003	212.2 ± 0.4	[–0.228 ± 0.003]	[–0.362 ± 0.003]	Millar-Blanchaer et al.
2013 Dec 10	2013.939	Gemini-S/GPI	0.430 ± 0.010	211.6 ± 1.3	[–0.225 ± 0.010]	[–0.366 ± 0.010]	Bonnefoy et al. (201
2013 Dec 10[a]	2013.939	Gemini-S/GPI	0.419 ± 0.006	212.2 ± 0.8	[–0.223 ± 0.006]	[–0.355 ± 0.006]	Millar-Blanchaer et al.
2013 Dec 10	2013.939	Gemini-S/GPI	0.419 ± 0.004	212.6 ± 0.5	[–0.226 ± 0.004]	[–0.353 ± 0.004]	Millar-Blanchaer et al.
2013 Dec 11	2013.939	Gemini-S/GPI	0.419 ± 0.005	212.3 ± 0.7	[–0.224 ± 0.005]	[–0.354 ± 0.005]	Millar-Blanchaer et al.
2013 Dec 12	2013.945	Gemini-S/GPI	0.427 ± 0.007	211.8 ± 0.7	[–0.225 ± 0.006]	[–0.363 ± 0.007]	Millar-Blanchaer et al.
2014 Mar 23	2014.222	Gemini-S/GPI	0.413 ± 0.003	212.1 ± 0.4	[–0.219 ± 0.003]	[–0.350 ± 0.003]	Millar-Blanchaer et al.
2014 Nov 08	2014.852	Gemini-S/GPI	0.363 ± 0.004	212.2 ± 0.7	[–0.193 ± 0.004]	[–0.307 ± 0.004]	Millar-Blanchaer et al.
2015 Jan 24	2015.063	Gemini-S/GPI	0.348 ± 0.005	212.2 ± 0.7	[–0.185 ± 0.004]	[–0.294 ± 0.005]	Millar-Blanchaer et al.

NOTE. — Astrometry listed in brackets either in ρ and θ or ΔR.A. and ΔDec is inferred from published measurements.

[a] Re-reduction of published data.

[b] Konopacky et al. (2016) note that this epoch of astrometry for HR 8799 d may be biased because the primary is positioned near the edge of the coronagraph.

[c] Sum of observations taken on 2009 Nov 24, Nov 25, and Dec 17.

[d] Bonnefoy et al. (2011) report astrometry using two reduction procedures for each data set. Values listed here are the weighted average of both methods.